ANALYSIS OF BABU AND ODEH'S MODEL

A Thesis

by

ESTEBAN ALBERTO GRASSI

Submitted to the Office of Graduate and Professional Studies of
Texas A&M University
in partial fulfillment of the requirements for the degree of

MASTER OF SCIENCE

Chair of Committee,	Rahid Hasan
Co-Chair of Committee,	Ding Zhu
Committee Member,	Maria Barrufet
Head of Department,	A. Dan Hill

August 2015

Major Subject: Petroleum Engineering

ABSTRACT

In this work, Babu and Odeh's model for estimating flow rate from partially penetrating systems is studied. A VBA code is written in order to simulate the model and its results are compared against simulations using Eclipse Software. Sensitivity to different parameters is analyzed and an increasing-decreasing behavior as the reservoir's length is increased is specifically addressed and analyzed.

After simulating different scenarios it is observed that Babu and Odeh's model predicts that there will be a specific reservoir's length for which a maximum flow rate will be predicted. An explicit analytical expression is obtained for one of the cases considered in the model.

The results obtained are compared against Eclipse runs, it is observed that the model is reasonably accurate, and that the reservoir's length at which the maximum flow rate onsets is similar in both cases.

It is concluded that the model is accurate within its simplistic assumptions, but it is in these same assumptions that it might yield very different results than reality itself.

ACKNOWLEDGEMENTS

I would like to thank Dr. Hasan and Dr. Zhu for their guidance and support throughout the course of this research.

Thanks also go to my friends and colleagues and the department faculty and staff for making my time at Texas A&M University a great experience.

TABLE OF CONTENTS

LIST OF FIGURES

Page

LIST OF TABLES

Page

CHAPTER I

INTRODUCTION AND LITERATURE REVIEW

I.1. Introduction

This work will address the well-known model developed by Babu and Odeh (Babu and Odeh, 1989) to predict the productivity of partially penetrating horizontal wellbores in pseudo steady state.

Even though this model was developed more than 20 years ago, its results are still used today by many authors in technical papers.

In their work, the authors proposed a new skin factor, which they named S_R and is added to account for the decrease in the productivity inherent from a partial penetration, yielding the following inflow equation:

$$q = \frac{\sqrt{k_H k_V}\, b(\bar{p} - p_{wf})}{141.2 B_o \mu \left\{ ln\left(\frac{\sqrt{A}}{r_w}\right) + ln(C_H) - 0.75 + S_R + s \right\}} \qquad \text{Eq. I.1}$$

The details of the formulas and calculations required to obtaine S_R are summarized in Appendix A

It has been observed that in some cases, the model presents a particular behavior, and even when all the restrictions and assumptions proposed by Babu and Odeh (B&O) are

obeyed, the model would sometimes predict a decrease in productivity as the reservoir length is increased while the rest of the parameters kept constant.

In this work I will first show how, for different scenarios, this behavior can be observed, plotting the predicted flow rate in each case as the reservoir length is increased using one set scenario as parameter.

In order to do so, a simple code in VBA is developed, which can compute the results of different scenarios once the variables and the different values one want to consider for each one are input. It then runs all the possible combinations and displays the results. The scenarios are analyzed, and then they will be compared against results obtained using Eclipse software.

The accuracy of B&O's model with respect to Eclipse's results will be analyzed as well.

I.2. Problem statement and simulation results

The problem addressed in this work is the fact that Babu and Odeh's model can predict a decline in the flow rate of a partially penetrating horizontal well when the reservoir's length is increased keeping everything constant. If it is assumed that this prediction is accurate, this could be used to define an optimum well length for a certain reservoir length.

Also, B&O's model's accuracy with respect to Eclipse's results will be assessed by running different scenarios on a VBA code developed for this purpose. The code considers only single phase, since the purpose is to analyze the model itself this measure was taken in order to minimize any kind of "noise" that could be introduced for other factors than the solution proposed by Babu and Odeh.

Each parameter is addressed individually, using a rather stable set of values for which the sensitivity of all of them can be appreciated.

In this Chapter I will discuss the results obtained for the simulation of different scenarios, which illustrate the behavior observed.

The VBA code developed has the following input:

Parameter	Initial	Steps	Increase
Wellbore length, L (ft)	**3100**	0	0
Thickness, h(ft)	**200**	0	0
Horizontal permeability, kx (md)	**75**	0	0
Horizontal permeability, ky (md)	**75**	0	0
Vertical permeability, kz (md)	**25**	0	0
Wellbore radius, rw(ft)	**0.25**	0	0
Reservoir width, a(ft)	**4000**	0	0
Reservoir length, b(ft)	**3300**	10	30
Well heel location in x, x1(ft)	**100**	0	0
Well toe location in x, x2(ft)	**3200**	0	0
Well location in y, y0(ft)	**2900**	0	0
Well location in z, z0(ft)	**120**	0	0
Average pressure, pave (PSI)	**3800**	0	0
Bottomhole pressure, pwf (PSI)	**3000**	0	0
Viscosity, μ (cp)	**1.05**	0	0
Volume factor, B	**1.1**	0	0
Skin, s	**-1**	1	2
Center wellbore? 1=yes	**1**		

Figure I.1: Sample input data for VBA Code

In Figure 1 some data has already been entered. The program reads the first value (column “Initial”) and then increases each of them a number of times set by the “Steps” column, by an amount set by the “Increase” column. One variable is changed at the time, and once all the steps for that variable have been evaluated, that variable is reset and a new value for another variable is set. In this example, it will first run the simulation for 11 different values of reservoir length, then the skin will be increased from -1 to 1 and the same 11 values of reservoir length will be evaluated again. The reservoir length will be the primary variable.

The plots will display 3 curves each, one will correspond to the ratio of L/b (secondary y-axis), since one of the restrictions of B&O's model is that when the wellbore length is shorter than 70% of the reservoir length, it loses accuracy. In this work I will limit the scenarios to cases that comply with the condition that *L/b* always remains >0.7. Another curve will be the flow rate predicted by Babu and Odeh's model (primary y-axis), and the third one will show the flow rate of a "short" system (primary y-axis), that is, the productivity for a fully penetrated system with the length of the wellbore. This last one is included as a reference parameter. The x-axis will show the different wellbore lengths considered.

The effect of the different parameters was analyzed. For each parameter different scenarios are provided that keep all other variables constant, the data used and the results are included in Appendix B. Following, two sets taken from Appendix B are shown, corresponding to two different reservoir thicknesses:

Reservoir thickness (h)

- First set of values:

Parameter	Initial	Steps	Increase
Wellbore length, L (ft)	**3000**	0	0
Thickness, h(ft)	**200**	0	0
Horizontal permeability, kx (md)	**5**	0	0
Horizontal permeability, ky (md)	**5**	0	0
Vertical permeability, kz (md)	**1**	0	0
Wellbore radius, rw(ft)	**0.25**	0	0
Reservoir width, a(ft)	**1500**	0	0
Reservoir length, b(ft)	**3300**	175	3
Well heel location in x, x1(ft)	**150**	0	0
Well toe location in x, x2(ft)	**3150**	0	0
Well location in y, y0(ft)	**750**	0	0
Well location in z, z0(ft)	**100**	0	0
Average pressure, pave (PSI)	**3600**	0	0
Bottomhole pressure, pwf (PSI)	**3000**	0	0
Viscosity, μ (cp)	**1.05**	0	0
Volume factor, B	**1.1**	0	0
Skin, s	**10**	0	0.0
Center wellbore? 1=yes	**1**		

Table I.1: Reservoir thickness, first set of values

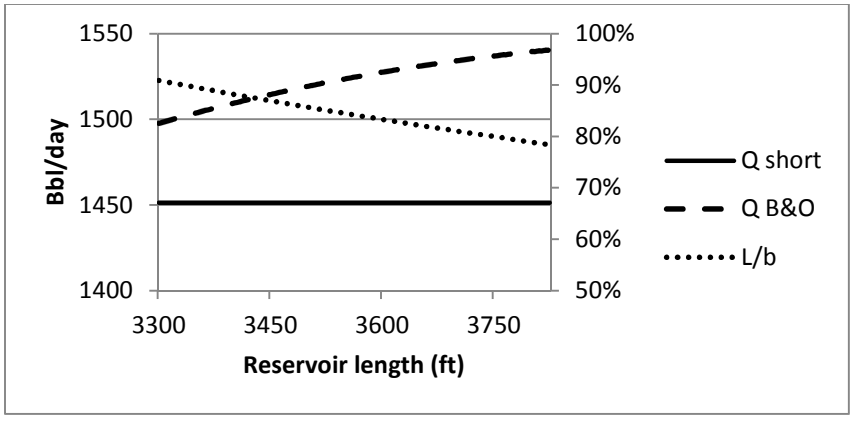

Figure I.2: Reservoir thickness, simulation results for first set of values

Second set of values:

Parameter	Initial	Steps	Increase
Wellbore length, L (ft)	**3000**	0	0
Thickness, h(ft)	**100**	0	0
Horizontal permeability, kx (md)	**5**	0	0
Horizontal permeability, ky (md)	**5**	0	0
Vertical permeability, kz (md)	**1**	0	0
Wellbore radius, rw(ft)	**0.25**	0	0
Reservoir width, a(ft)	**1500**	0	0
Reservoir length, b(ft)	**3300**	175	3
Well heel location in x, x1(ft)	**150**	0	0
Well toe location in x, x2(ft)	**3150**	0	0
Well location in y, y0(ft)	**750**	0	0
Well location in z, z0(ft)	**50**	0	0
Average pressure, pave (PSI)	**3600**	0	0
Bottomhole pressure, pwf (PSI)	**3000**	0	0
Viscosity, μ (cp)	**1.05**	0	0
Volume factor, B	**1.1**	0	0
Skin, s	**10**	0	0.0
Center wellbore? 1=yes	**1**		

Table I.2: Reservoir thickness, second set of values

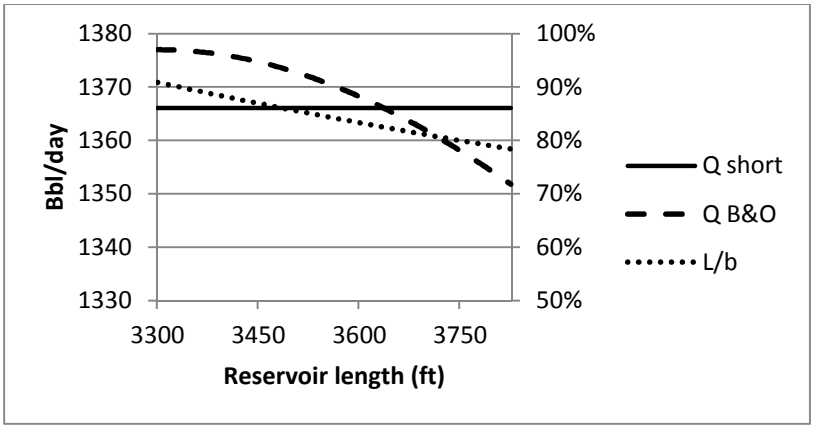

Figure I.3: Reservoir thickness, simulation results for second set of values

Different conclusions and observations can be drawn from the results presented: first of all, it is important to mention that some variables were not simulated, these variables are the oil formation volume factor, oil viscosity, oil density, pressure drawdown and wellbore radius. This is due to the fact that all these variables, except for r_w, do not affect the addressed phenomena, since they do not have any effect over the terms present in the brackets in equation I.1, so the behavior (i.e.: increasing or decreasing) of the flow rate will not change: the curve will only be displaced upward or downward, maintaining its shape. This does not apply to the wellbore radius, which is present inside the brackets; the reason to not simulate different values for the wellbore radius is that this is a relatively constant parameter, and the value of 0.25 ft. was taken as constant for it.
We can also observe that changing the value of any of the variables presented can determine whether the predicted flow rate decreases or not along with the reservoir length.

It has been observed that, even when the behavior displayed is that of an increasing productivity with reservoir length, the flow rate will eventually start decreasing, but this point will not always occur within the model's geometric restrictions ($L/b > 0.7$).

If the productivity is treated just as a function of b, where b is non-negative, then the resulting plot is always going to start in zero, increase until a maximum value is reached, which will happen when *b* reaches a value that will be called "*b critical*" (b_{crit}), and then it will start decreasing. The following figure depicts this observation:

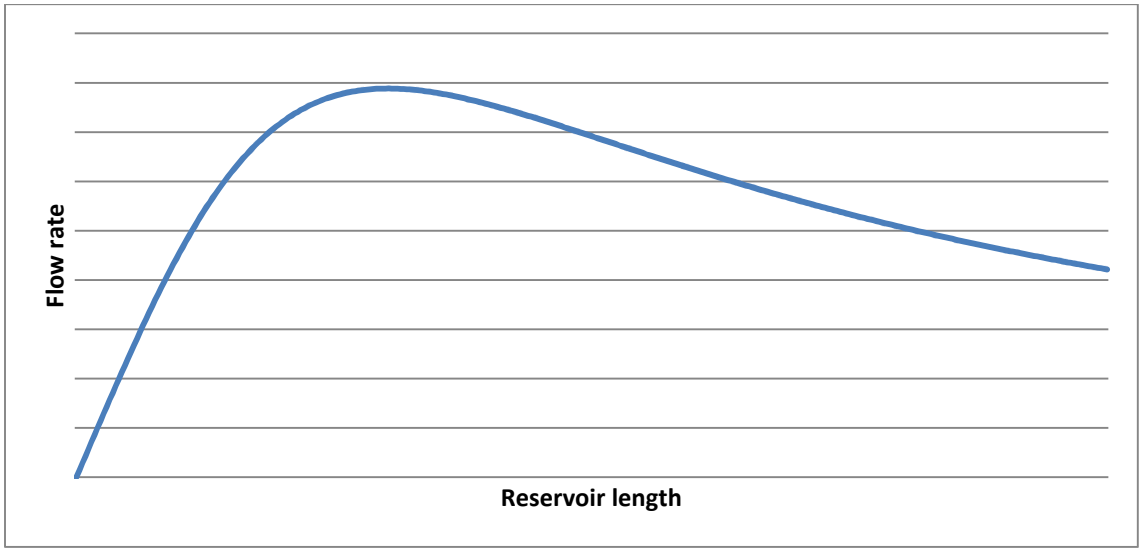

Figure I.4: General behavior of flow rate vs reservoir length

Figure I.4 presents flow rate (y-axis) vs reservoir's length (x-axis). The axes do not show values because the plot only intends to depict the general shape of the curve. While small values of *b* will never take place in the real world (that is, the reservoir will be

always at least as long as the wellbore), it is useful to consider b as non-negative to better understand the general behavior. According to the rest of the parameters, either the increasing or the decreasing sections of the plot can be more or less steep. The set of variables analyzed (h, k_x, k_y, etc..) will determine what section of the plot will describe the flow rate behavior for the reservoir's lengths considered and how steep it will be.

I.3. Literature review

I.3.1. Babu and Odeh's model

In this Chapter I will go through the basics of Babu and Odeh's model, without delving on the calculations, which are available in Appendix A, or the derivations, which can be found on their paper(Babu and Odeh 1989).

I will also discuss how the model is still contemporary and why it is relevant to analyze it.

Babu and Odeh developed a general solution to predict the flow rate of a horizontal well placed in a box-shaped reservoir. The constrains used were no flow boundaries (all along the reservoir limits) and uniform flux along the wellbore, although they stated that their results apply to both uniform flux and uniform wellbore pressure.

The well can be located anywhere within the reservoir, but it must be parallel to one of the coordinate axes. It can also be of any length, but in their paper they state that for well lengths shorter than 70% of the reservoir's length in the wellbore's direction, the model's accuracy is highly compromised.

The reservoir must be homogeneous, with constant porosity, although it might be anisotropic.

In this work, the pressure along the wellbore will be assumed to be uniform, and no frictional pressure loss will be included in the calculations.

Today the industry has more and more computational power available to apply numerical simulations, thus relying less on analytical or semi analytical models. Still, many investigators use this model's results in different ways to pursue further research. Following some recent works that have done so are summarized, for reference:

- Thomas, Todd, Evans and Pierson in 1996(Thomas, Todd, Evans and Pierson 1996) presented calculations of near-wellbore skin and non-Darcy flow for horizontal wells based on how these wells were drilled and completed, and they presented a modification of Babu and Odeh's equation for productivity by adding a laminar/turbulent skin term (leaving the rest of the model as is).

- Dietrich and Kuo, in 1996(Dietrich and Kuo 1996), presented and analyzed an explicit modelling technique to predict horizontal well productivity, and used Babu and Odeh's results for validation purposes.
- Helmy and Wattenbarger in 1998(Helmy and Wattenbarger1998) developed a new model to calculate the productivity of wells producing at constant rate or constant wellbore pressure using numerical simulation to calculate the shape factor and partial penetration skin factor, and they compared their results with Babu and Odeh's model.
- Kamkom and Zhu in 2005(Kamkom and Zhu 2005) developed a method to predict two phase multilateral well deliverability, treating each lateral as a horizontal well and using Vogel's correlation and Babu and Odeh's model for this purpose.
- Yuan and Zhou, in 2010(Yuan and Zhou 2010), presented a new model to predict fractured horizontal wells productivity that can be used in horizontal wells without fractures and compared their results with other models, including Babu and Odeh's.
- Zarea and Zhu, in 2011(Zarea and Zhu 2011), presented an analysis of multilateral well productivity prediction taking into account the effect of ICVs, in this analysis they computed the flow in different laterals (or segments of them) using Babu and Odeh's model.

- Lin and Zhu, in 2012(Lin and Zhu 2012), proposed a new approach to distribute the partial penetration skin introduced by Babu and Odeh when accounting for frictional pressure loss in partially penetrating horizontal wells.

The list could go on, but as it is it serves the purpose of proving that Babu and Odeh's model is still contemporary to our time, and thus it is worth of being critically analyzed.

I.3.2. Pressure transient analysis

In this Chapter, the basics of pressure transient applied to this work will be covered. The relevancy of this subject relies on the fact that Babu and Odeh's model applies when the flow has reached pseudo steady state.

The results obtained from the analysis of the model will be compared with simulations run using Eclipse software, thus the importance of identifying when Eclipse's simulations have reached the pseudo steady state. Establishing the time to reach pseudo steady state can be done using pressure transient analysis.

The estimation of a horizontal well's productivity and the interpretation of well-test data are more complicated than those of a vertical well. The biggest issue is the 3D geometry of the flow.

Also, wellbore storage effects are more significant than in vertical wells, and the partial penetration introduces even more complications to the analysis.

A pressure transient test in a horizontal well can involve five distinct flow regimes, but this does not necessarily mean that all of them will be observed in each horizontal well test.

Samandarli, Valbuena and Ehlig-Economides developed an analysis of long term data that uses Rate Normalized Pressure (*RNP*) and is focused in production data (Samandarli, Valbuena and Ehlig-Economides 2012).

Horner and Lee and Spivey (Horner 1967, Lee and Spivey 2003) presented a way to apply time superposition, known as material time balance, which is applicable when the production rates vary smoothly.

These two techniques were summarized by Samandarli, Valbuena and Ehlig-Economides(Samandarli, Valbuena and Ehlig-Economides 2012) and applied them to unconventional reservoirs analysis. In this work, I will use this same approach to determine the onset of Pseudo Steady State flow.

For each scenario, the Rate Normalized Pressure (*RNP*), its derivative and the material time balance, t_e, are computed as follows:

$$RNP = \frac{p_i - p_{wf}}{q_{(t)}} \qquad \text{Eq. I.2}$$

$$RNP' = \frac{RNP_{j+1} - RNP_j}{\ln(\frac{t_{e_{j+1}}}{t_{e_j}})} \qquad \text{Eq. I.3}$$

$$t_e = \frac{Q_{(t)}}{q_{(t)}} \qquad \text{Eq. I.4}$$

RNP and its derivative are plotted against t_e and once the plot develops a slope of 1, it is assumed that pseudo steady state flow is reached, the following sample diagnostic plot depicts this behavior:

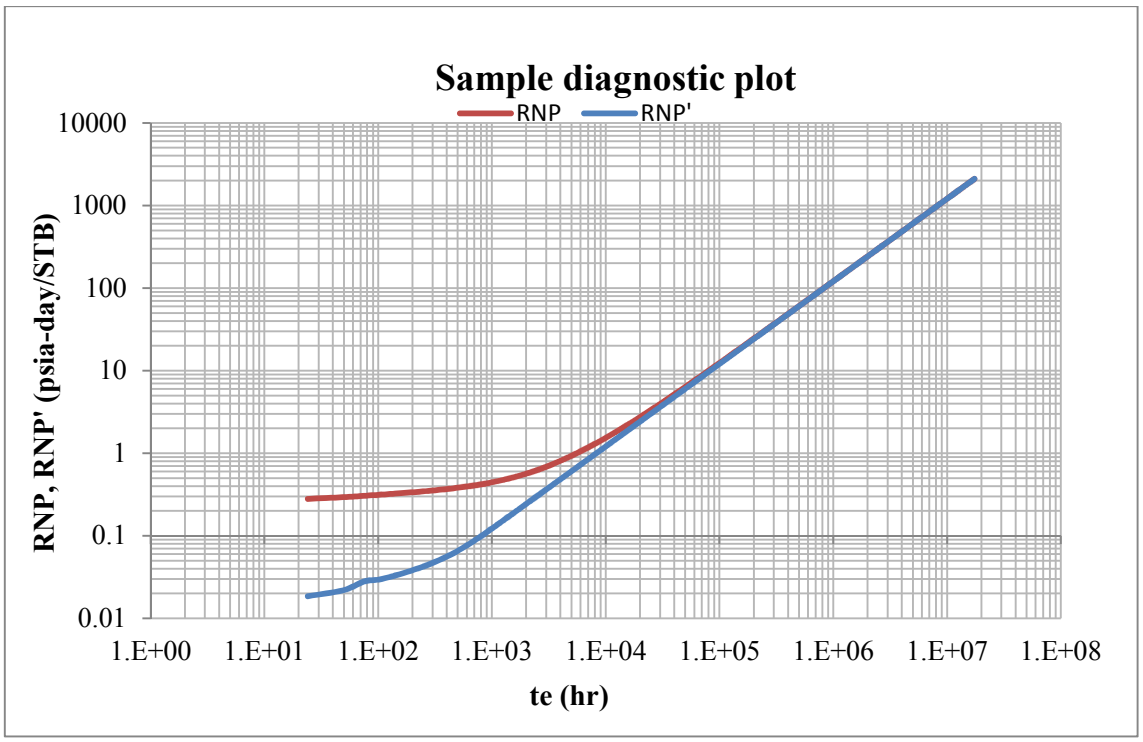

Figure I.5: Sample diagnostic plot

Fig I.5 shows how, for this specific case, PSS is reached approximately at $t_e = 50{,}000\ hr$. Plots like the one showed in fig I.5 were developed for each scenario run in Eclipse to determine the time of the onset of the PSS.

Note that t_e does not represent the actual time of the onset of pseudo steady state flow, the way to obtain the time is explained in Chapter II.

I.4. Objectives of study

According to the problem presented, this work will intend to:

- Derive an analytical expression for b_{crit} in order to determine, when using Babu and Odeh's model, if we are on the decreasing or increasing side of the curve obtained for *flow rate* vs *b*.
- Compare the results obtained with simulations run with Eclipse software, in order to obtain conclusions regarding the accuracy of the model not only in the prediction of flow rate, but also regarding b_{crit}.
- Propose further research recommendations.

CHAPTER II

RESULTS AND ANALYSIS

II.1 Introduction

Our approach to solving the problem would require the use of a "critical length" of b, termed b_{crit}, which is observed when the increasing (with b) flow rate reaches a maximum and starts to decline. This maximum is observed when the reservoir's length, is equal to b_{crit}.

The derivation of such an expression is presented later in this Chapter, and the complete derivation is compiled in Appendixes C and D.

The second part of the approach is to validate the results obtained in the problem statement and b_{crit} derivation. In order to do so Eclipse software is used to run the same scenarios.

Eclipse's result, being it a state of the art simulation tool widely used by the industry, are assumed to be accurate, thus considered benchmarking values.

II.2 Derivation of b_{crit}

In order to derive an expression of bcrit the approach followed consists of obtaining an

expression of the productivity as a function of b, that is:

$$q = f_{(b)} \qquad \text{Eq. II.1}$$

Once this expression is obtained, it can be differentiated and presented as a homogeneous equation:

$$\frac{\partial f_{(b)}}{\partial b} = 0 \qquad \text{Eq. II.2}$$

After solving Eq. II.2 for b, the expression obtained will be b_{crit}, and:

$$\max f = f_{(b_{crit})} \qquad \text{Eq. II.3}$$

The derivation is described thoroughly on Appendixes C and D.

In order to derive these expressions, 4 different scenarios were used; first, the model itself presents two cases (case 1 and case 2) as explained in Appendix A, which correspond to a long and wide scenario. The conditions for each case are described by equations A-1 and A-7.

Both cases include the position of the wellbore on its calculations, so I decided to consider two subcases in each one. One where the wellbore position does not vary with *b*, and another one when the wellbore's position is itself a function of *b*, that is, the wellbore remains centered as *b* varies.

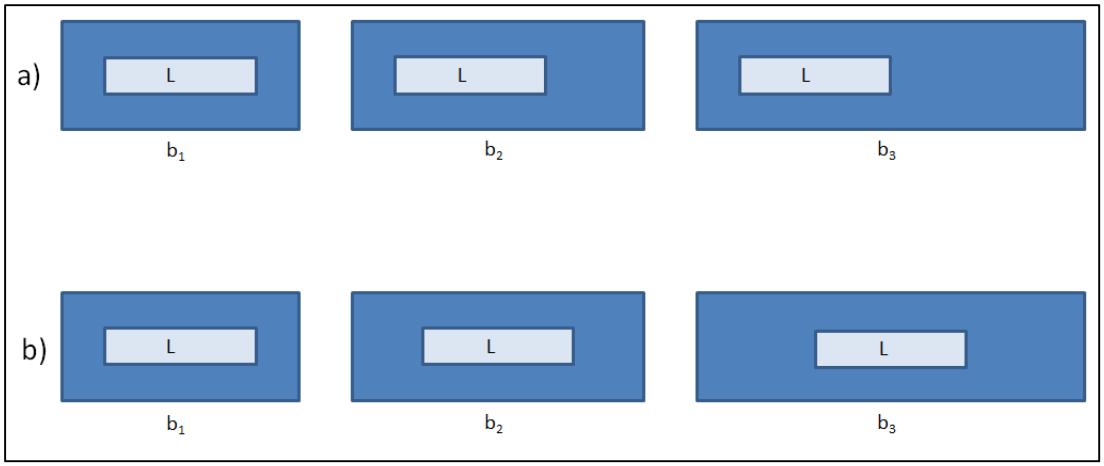

Figure II.1: a) Shows the wellbore's position fixed and not as a function of b. b) Shows the case when the wellbore is centered, with its position varying with b.

Figure II.1 shows the two subcases considered for this analysis.

Considering both subcases, it was possible to obtain an expression for b_{crit} for case 2 (equation A-7). For case 1 (equation A-1) it was not possible to solve the problem analytically with Mathematica or Wolfram Alpha.

The procedure to find an explicit expression for b_{crit} followed in Appendixes C and D was:

1. Analyze each of the terms that are used to compute S_R individually, get an explicit expression for them as functions of b and differentiate them with respect to b.
2. Obtain explicit expressions for S_R as a function of b and its derivative.
3. Obtain explicit expressions for flow rate for each case as a function of b.

4. Differentiate each expression respect to b and attempt to solve for its roots.
5. Check that the solutions obtained verify the conditions for b_{crit} using Ms. Excel.

The summary of the results obtained is the following: for case 2, explicit solutions were obtained, and they were validated simulating different scenarios, the expressions for b_{crit} are shown in equation II.4 for the case when y_{mid} is kept constant, and equation II.5 for the case when y_{mid} is kept at the center of the wellbore:

$$b_{crit} = SQRT\left[\left[\frac{3}{\frac{6.28}{ah}\frac{\sqrt{k_x k_z}}{k_y}}\left[\left[ln\left(\frac{\sqrt{A}}{r_w}\right) + ln(C_H) - 0.75 + s\right]\right.\right.\right.$$
$$\left. - \left[ln\frac{h}{r_w} + 0.25ln\frac{k_x}{k_z} - ln\left(sin\frac{180°z}{h}\right) - 1.84\right]\right. \quad \text{Eq. II.4}$$
$$\left.\left. + \frac{6.28}{ah}\frac{\sqrt{k_x k_z}}{k_y}\left(\frac{L^2 + 24y_{mid}^2}{24}\right) - \left(\frac{6.28a}{hL}\sqrt{\frac{k_z}{k_x}}\right)\left(\frac{1}{3} - \frac{x_0}{a} + \frac{x_0^2}{a^2}\right)\right]\right]$$

$$b_{crit} = SQRT\left[\left[\frac{12}{\frac{6.28}{ah}\frac{\sqrt{k_x k_z}}{k_y}}\left(ln\left(\frac{\sqrt{A}}{r_w}\right) + ln(C_H) - 0.75 + s\right.\right.\right.$$
$$\left. - \left[ln\frac{h}{r_w} + 0.25ln\frac{k_x}{k_z} - ln\left(sin\frac{180°z}{h}\right) - 1.84\right] + \frac{\frac{6.28}{ah}\frac{\sqrt{k_x k_z}}{k_y}L^2}{24}\right. \quad \text{Eq. II.5}$$
$$\left.\left. - \left(\frac{6.28a}{hL}\sqrt{\frac{k_z}{k_x}}\right)\left(\frac{1}{3} - \frac{x_0}{a} + \frac{x_0^2}{a^2}\right)\right)\right]$$

For case 1, the final equations obtained proved to be too complicated to be solved analytically, the final expressions are listed in Appendix D as equations D-16 and D-17.

II.3. Verification using Eclipse

Only case 2 scenarios will be considered, since the expression for b_{crit} has only been obtained for this case.

The expression of b_{crit} is not to be verified in this Chapter, for it is an analytical solution for a mathematical problem. What will be approached here is the accuracy of Babu and Odeh's model using reservoir lengths in the vicinity of b_{crit} and meeting the geometric restrictions required by the authors.

For this verification, Eclipse software will be used.

The reservoir will be modelled following a common approach suggested by many authors, such as Peaceman (Peaceman 1991) and Aziz (Aziz 1993) , which consists of refining the grid in whichever zone is of especial interest or requires more accuracy, in this case the vicinity of the wellbore.

Since the non-penetrated sector of the reservoir is of special interest, this area of the grid will be refined as well.

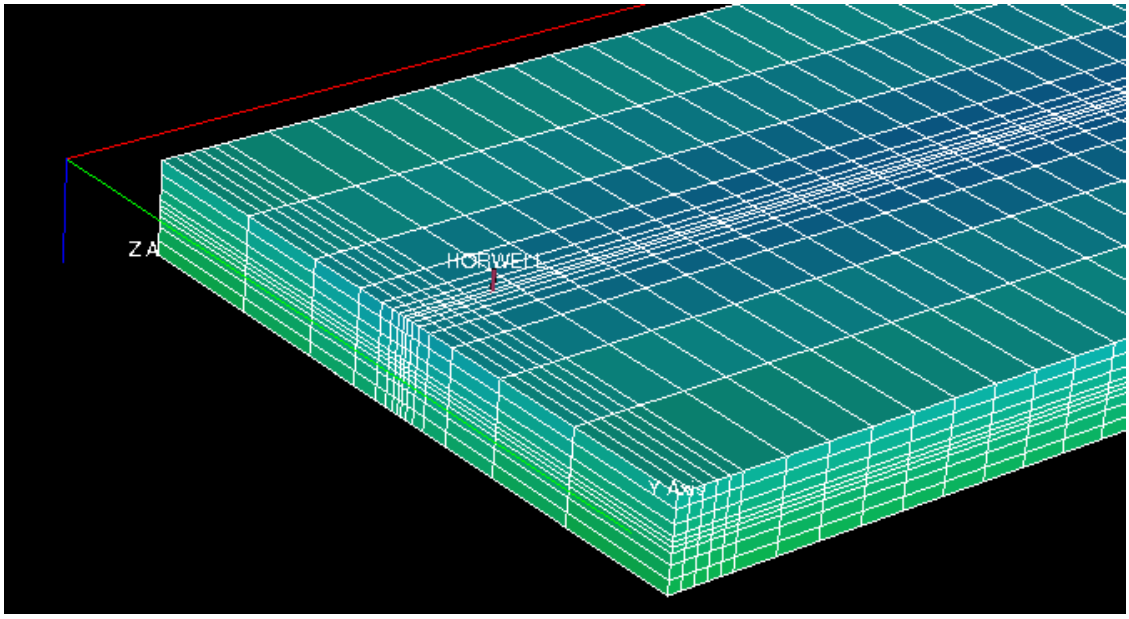

Figure II.2: Reservoir grid design – Eclipse software

Figure II.2 shows a portion of a reservoir grid designed in this fashion using Eclipse. In order to verify the results obtained with Babu and Odeh against those obtained with Eclipse, a particular procedure had to be developed, since the software only simulates over time.

The procedure followed was:

A. For each set of values presented on Appendix B, a set of 6 Eclipse deck files was written and run, with the purpose of obtaining 6 points to plot for each set of values. A list of all the scenarios is compiled in Appendix H.

B. Each deck file (all the keywords used to write them are explained in Appendix F, as well as an example) was written with a different reservoir length, these lengths are shown on the list provided on Appendix H. The length of each reservoir is obtained by modifying the length of the grids in the x direction for the non-penetrated zone of the reservoir.

C. The deck files were written in such a fashion so that they will yield an RSM report including the reservoir's average pressure and the average daily production rate.

D. It is important to notice that, in order to generate a pseudo steady state solution to compare with, we need to follow the procedure described in the literature review:

    1. For each scenario, the information obtained from its RSM file (time, production per day and average reservoir pressure) is copied into an Excel spreadsheet.
    2. The spreadsheet computes and plots the *NRP* (Normalized Rate Pressure) and its derivative, *NRP'* vs t_e (material balance time).
    3. The material balance time from which a unit slope onsets is identified.
    4. For this material balance time, its corresponding average reservoir pressure is registered.
    5. The procedure is repeated for the 6 scenarios included in the set, and the lower average reservoir pressure is taken as reference. Since the average reservoir pressure follows a decline curve, whenever the rest of the scenarios with a higher average reservoir pressure at the onset of the

pseudo steady state reachs this lower average reservoir pressure, they will be as well already in pseudo steady state.

6. An average reservoir pressure smaller than the previous value is taken as datum pressure.
7. In order to serve comparative purposes, for most scenarios the same average reservoir pressure is taken as reference (as long as they verify PSS for such pressure).

E. The average reservoir pressure taken as reference for each set of scenarios is searched in each RSM report file. Since it is unlikely that the report will have one value matching exactly such pressure, two are taken and their respective flow rates are interpolated linearly. Since small time steps have been used to run Eclipse, the variation in flow rate from one time step to the following is small as well, thus the linear interpolation yields a good approximation.

F. The process is repeated for each set of 6 scenarios.

G. Each set of values presented on Appendix B is rerun, modifying the pressure drawdown in each case to match those obtained in the previous step and used as reference to read Eclipse's flow rate estimation.

H. For each set of 6 scenarios, the information obtained is compiled in one plot of predicted flow rate vs reservoir's length, each plot including Babu and Odeh's and Eclipse's results. These plots are provided in Appendix G.

The simulation data and the results obtained are summarized in table H.1, provided in Appendix H.

The results obtained for the first list of scenarios showed a significant difference between Babu and Odeh's predictions and Eclipse's. But also, a relationship can be observed when we consider the different drawdowns used.

In the case of the smallest drawdowns used (10 psia) the ratio of Babu and Odeh's rate predictions to Eclipse's is higher, this ratio gets lower for the highest drawdowns (80 psia).

This might indicate that as the drawdown is increased, the ratio would be reduced and that, for some average reservoir pressures the results obtained would be closer to Eclipse's. Also, for all cases, Eclipse predicted a higher flow rate than B&O.

An explanation for this difference could be the fact that the viscosity and oil formation volume factor used for B&O are the ones used in Eclipse for a reference pressure of 3900, and Eclipse computes the variation of both properties with pressure. In order to estimate the changes in these parameters, Ecrin software was used, and the result was that this might lead to an error of an overestimation of around 4.3% using Eclipse. Even when this is a small difference, it is important to notice that Eclipse's reservoir pressure is the average, meaning that there will be points within the reservoir with higher and

lower pressures than such value, so this might be contributing to a higher error than the one estimated with this simplistic approach.

Another possible factor that could yield error is that the procedure described, in point B, mentions that the reservoir's length is increased by increasing the length of the non-penetrated grids. Some authors prefer to keep the grid geometry constant and add new grids when running this kind of analysis. Considering this observation both approaches were compared using the set of scenarios 109 to 114. The results obtained were compared with a new set of runs that added new grids instead of increasing the length of the existing ones. The difference was less than 0.5%, so the contribution of this factor to the error in estimations was discarded.

Considering previous observations, and in order to minimize the possible contribution of the different pressures affecting the fluid properties, the procedure described before is repeated for all scenarios, changing the initial reservoir pressure to simulate with Eclipse from 4,000 psia to 20,000 psia, in order to be able to analyze higher flow rates and use an average reservoir pressure closer to the reference pressure used.

The average reservoir pressure used for this second set of runs was 3900 psia, oil formation volume factor and viscosity were input on Eclipse's deck files at a reference pressure of 3800 psia, and this same values were used to run B&O. This should

minimize any already small impact on the results, considering that the fluid used is dead oil and that the difference from reference pressure and the pressure used is only 100psia.

The results obtained are summarized and compared with the previous ones in table H.I, found in Appendix H.

The following plot shows the different ratios between Eclipse's and B&O's estimations obtained for this second run, for each set of 6 scenarios:

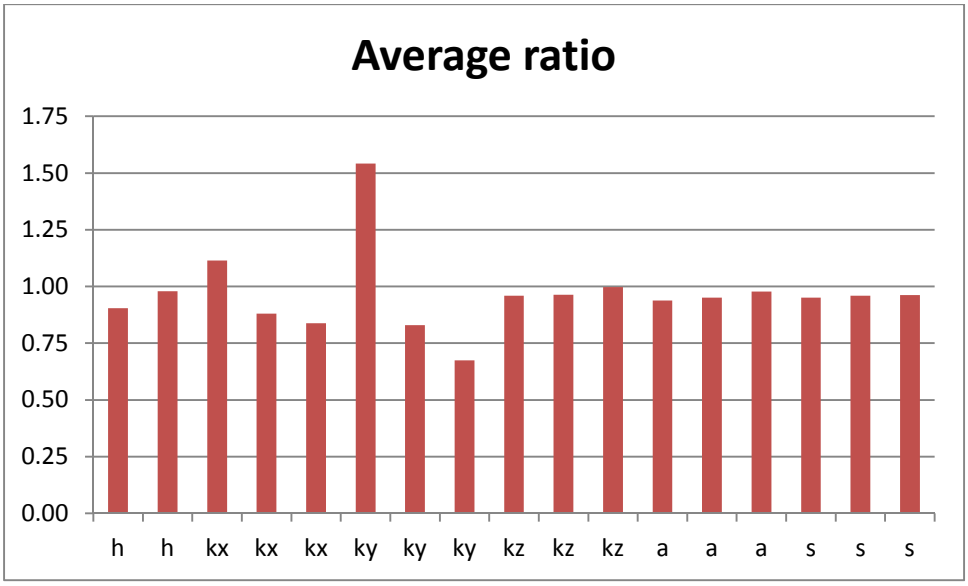

Figure II.3: Average ratio of Eclipse to B&O estimation for each set of 6 scenarios. X-axis depict which parameter is being evaluated in each case.

Figure II.3. is included only to present one observation: in most scenarios, the B&O's model yields results reasonably close to those obtained with eclipse. Each bar represents the average ratio for one set of 6 scenarios, and the x axis tags which parameter was analyzed, this means that, for instance, the only difference between the first two bars tagged with "h", is effectively the payzone, same applies for the following three bars tagged with "kx", this means that the only difference between them is the permeability value used in the "x" direction.

Figure II.3. is not so useful to evaluate the impact of each parameter. In order to be able to do so, the variation from one scenario to the other was normalized based on the incremental change respective to the parameter being evaluated. This normalized change was used to obtain the impact on the ratio. The following plot illustrates the results obtained:

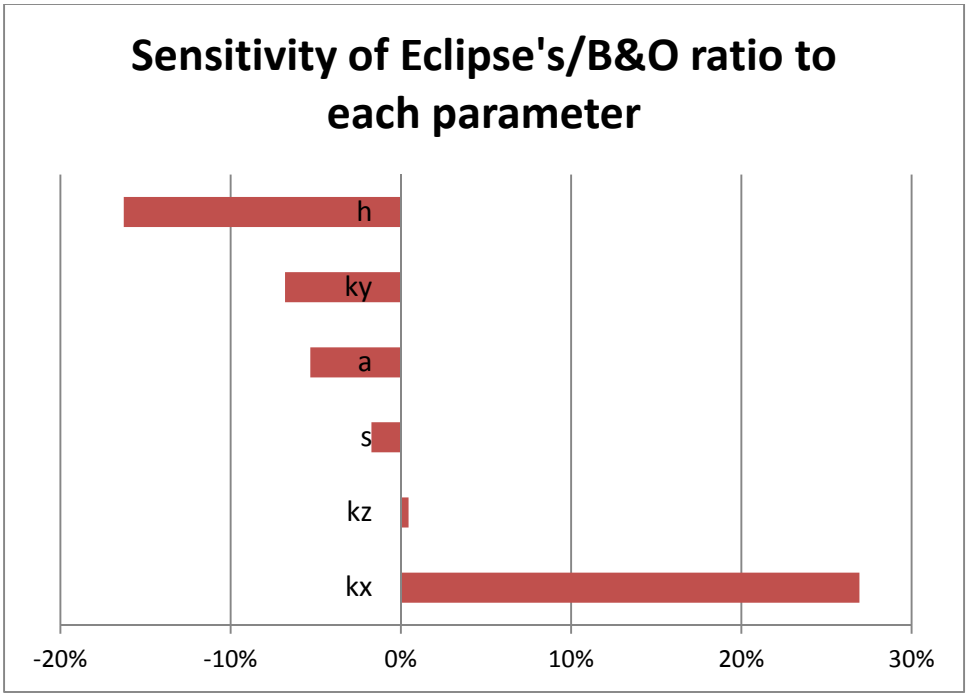

Figure II.4: Sensitivity analysis of the ratio between Eclipse's and B&O estimations

Figure II.4 presents, for the cases considered, in which percentage the ratio of Eclipse's to B&O's estimations change for a change in 100% for each parameter. In the case of negative values this means an inverse relationship (increasing the value of the parameter would decrease the ratio).

The primary conclusion from these results is that the reservoir height and the permeability in the direction of the wellbore are the two most sensitive parameters, these need special attention.

Further observations can be made when analyzing each set of 6 scenarios in detail.

The set of scenarios 61 to 66 deserve particular attention, for this is the only group in which we can observe that in the first three scenarios, Eclipse's results are lower and then in the following three scenarios they grow higher than B&O's.

The following figures show this observation:

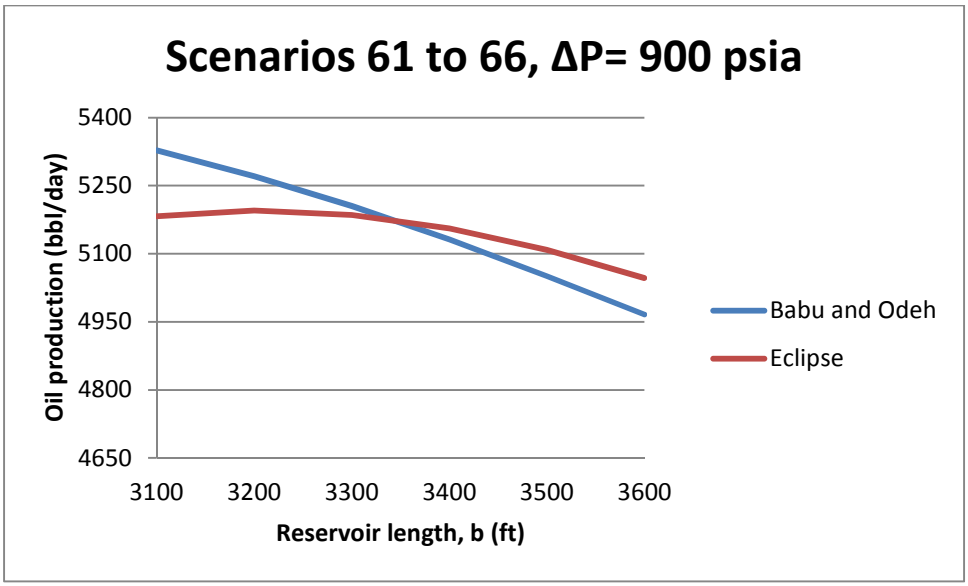

Figure II.5: Flow rates estimation for scenarios 61 to 66, in the second run considering ΔP = 900 psia

Figures II.5 show the flow rates estimations for scenarios 61 to 66 obtained using a drawdown of 900 psia. Similar plots for all sets of scenarios are provided in Appendix G.

This last observation, together with the plots in appendix G and table H.I from appendix H, can lead to a hypothesis regarding b_{crit}. Analysis of the columns Var-B&O and Var-Eclipse from this table and the plots show that in most cases, b_{crit} is essentially the same for both B&O and Eclipse, but in some other cases, the phase shift is bigger.

Appendix G also shows that, in some cases, the differences between B&O's and Eclipse's estimations increase. Figure II.6 shows the flow rate estimation for scenarios 7 to 12 in the second run, using a drawdown of 900 psia, and illustrates this point:

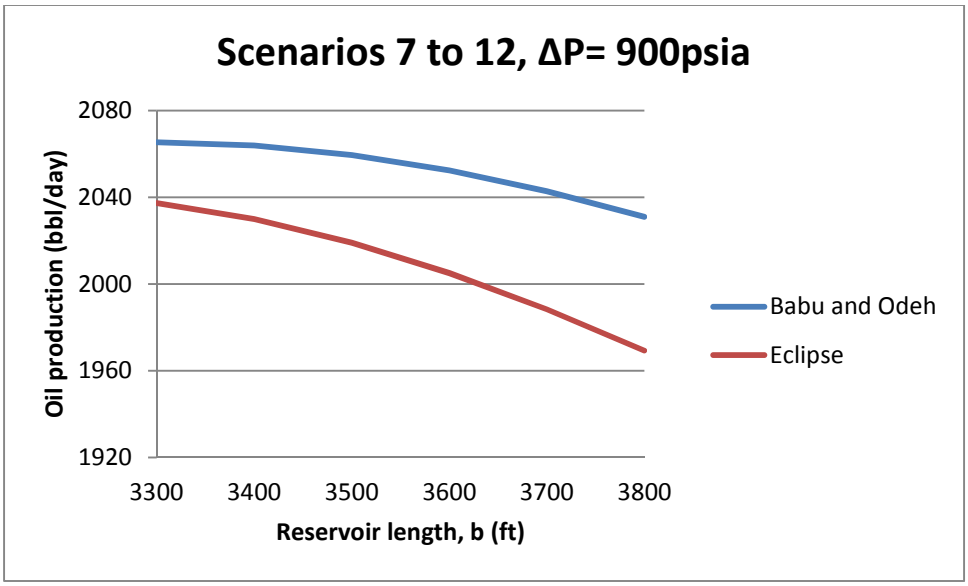

Figure II.6: Flow rates estimation for scenarios 7 to 12, in the second run considering ΔP = 900 psia

On the other hand, in other cases, the exact opposite can be observed. Such is the case of figure II.7, that shows the flow rate estimation for scenarios 13 to 18 in the second run, using a drawdown of 900 psia, and illustrates this point:

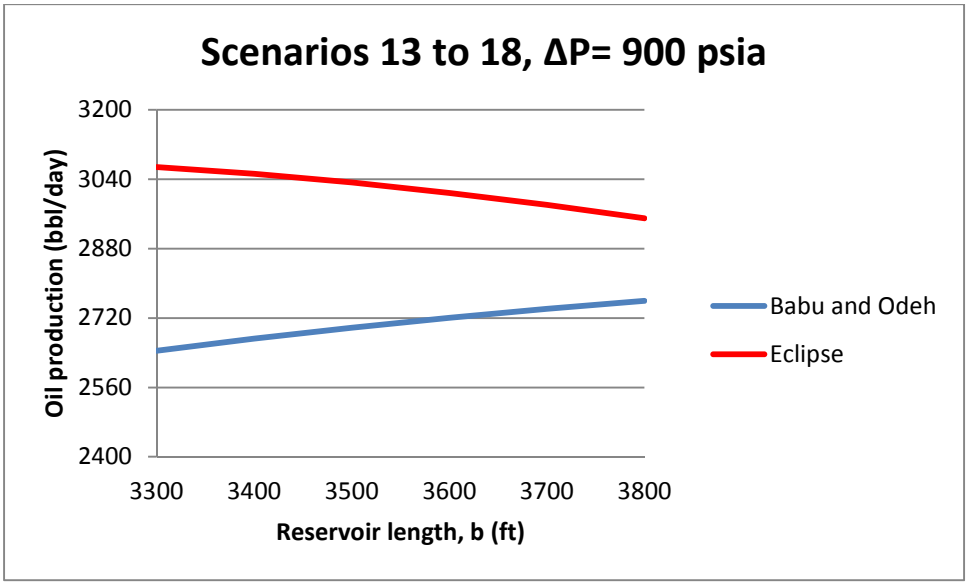

Figure II.7: Flow rates estimation for scenarios 13 to 18, in the second run considering ΔP = 900 psia

A hypothesis might be formulated from this observations: B&O and Eclipse might yield two different solutions similar to the one presented in Fig 1.22, they might have different slopes, different maximum values and this maximums might occur at different values of b, meaning that there would only be certain ranges of reservoir lengths when B&O's approximations will be rather accurate. This would require further investigation.

CHAPTER III

CONCLUSIONS AND RECOMMENDATIONS

A detailed comparison between Babu and Odeh's model and Eclipse's results was developed.

B&O's results turned out to be within an acceptable range of those obtained with Eclipse, but as the reservoir's length is increased in most cases it can be observed that the accuracy is compromised. This is consistent with the concept introduced by the authors that for a certain ratio between wellbore and reservoir's lengths, the model begins to lose accuracy, although it has been observed that assuming 70% as a cut off value might not be accurate, for this depends largely on other parameters, which means that, in some cases, the accuracy can be compromised much earlier.

The results obtained for lower average pressures were not accurate, this might be attributed to the fact that in the simulation of Babu and Odeh the properties of the fluid were kept constant. Also, in the reservoir and while using Eclipse, an average pressure is being used, which means that in some points it will be higher, and in others, lower. The change of the values of viscosity and oil formation volume factor was taken into account and mentioned, but only considering this average pressure, which can be highly inaccurate if the pressure goes under the bubble point pressure, for these properties will vary much more significantly after that point. This observation shows how significant

the impact of assumptions of these nature can be when using B&O's model to estimate flow rate.

The most (h and k_x) and least (k_z, s and a) sensitive parameters were identified in the simulations, running more simulations with different base cases and longer reservoirs is recommended to further validate this results.

The skin factor deserves a special mention: as we can see in the term between brackets from the inflow equation (Eq. I.1.) this is the only term completely independent from the geometry. That is, if the reservoir's length change, the skin will remain the same unless otherwise noticed. So, if we look at very damaged wells, with high skin values (s>200), this might mask the effect of partial penetration, and the flow rate estimation would barely change with an increasing reservoir's length.

An analytical explicit expression for b_{crit} was obtained for one of the geometry cases presented by Babu and Odeh in their paper. This expression might be used to obtain an optimum wellbore length for a determined reservoir length, for b_{crit} in B&O's and Eclipse's result has proven to be very close. This result might be used to fracture analysis, for the way in which the flow is modeled in Babu and Odeh's work is similar to the way in which it is sometimes modeled for fractures (ellipsoidal flow lines), further investigation should be conducted to determine if it applies. It is important to remind that

the geometry of the reservoirs required by Babu and Odeh is very different than the geometries present in a fractured reservoir.

NOMENCLATURE

a, reservoir width (ft)

A, drainage area (ft^2)

b, reservoir length (ft)

B_o, oil formation volume factor (res bbl/scf)

C_H, shape factor

h, payzone height (ft)

$k_{x,}$ permeability in x direction (mD)

$k_{y,}$ permeability in y direction (mD)

k_z, permeability in z direction (mD)

L, wellbore length (ft)

$\bar{p}$, average reservoir pressure (psia)

p_{wf}, bottomhole pressure (psia)

r_w, wellbore radius (ft)

s, skin factor

μ, oil viscosity (cp)

ρ , fluid density (lb/ft^3)

b_{crit}, critical reservoir length (ft)

S_R, partial penetration skin factor

REFERENCES

Aziz, K. (1993). "Reservoir Simulation Grids: Opportunities and Problems." SPE 25233.

Babu, D. K., and Odeh, A. S. (1989). "Productivity of a Horizontal Well (includes associated papers 20306, 20307, 20394, 20403, 20799, 21307, 21610, 21611, 21623, 21624, 25295, 25408, 26262, 26281, 31025, and 31035)." SPE 19117.

Yuan, H., and Zhou, D. (2010). "A New Model for Predicting Inflow Performance of Fractured Horizontal Wells." SPE 133610.

Horner, D. R. (1967). "Pressure Buildup in wells." WPC 4135.

Dietrich, J.K, and Kuo, S. S.(1996). "Predicting Horizontal Well Productivity." PETSOC-96-06-04.

Lin, J., and Zhu, D. (2012). "A New Approach of Applying Analytical Inflow Model for Horizontal Well Performance of Non-Fully Penetrated Wells." SPE 157483.

Lee, J., and Spivey, J. (2003). "Pressure Transient Testing" SPE Textbook Series, Vol. 9, Chapters 3, 4, 7, 8, 9, 10, 11.

Thomas, L. K., Todd, B. J., Evans, C.E., and Pierson, R. G. (1996). "Horizontal Well IPR Calculations." SPE 36753.

Zarea, M., and Zhu, D. (2011). "An Integrated Performance Model for Multilateral Wells Equipped with Inflow Control Valves." SPE 142373.

Samandarli, O., Valbuena, E., and Ehlig-Economides, C. (2012). "Production Data Analysis in Unconventional Reservoirs with Rate-Normalized Pressure (RNP): Theory, Methodology, and Applications." SPE 155614.

Peaceman, D. W. (1991). "Representation of a Horizontal Well in Numerical Reservoir Simulation." SPE 21217.

Kamkom, R., and Zhu, D. (2005). "Two-Phase Correlation for Multilateral Well Deliverability." SPE 95652.

Helmy, M. W., and Wattenbarger, R. A. (1998). "Simplified Productivity Equations for Horizontal Wells Producing at Constant Rate and Constant Pressure." SPE 49090.

APPENDIX A: SUMMARY OF BABU AND ODEH'S MODEL

This Appendix will provide the formulas required to obtain the partial penetration skin factor introduced by Babu and Odeh:

Case 1: Wide reservoir

If

$$\frac{a}{\sqrt{k_x}} \geq \frac{0.75b}{\sqrt{k_y}} \geq \frac{0.75h}{\sqrt{k_z}} \qquad \text{Eq. A-1}$$

$$S_R = P_{xyz} + P'_{xy} \qquad \text{Eq. A-2}$$

$$P_{xyz} = \left(\frac{b}{L} - 1\right)\left[ln\left(\frac{h}{r_w}\right) + 0.25ln\left(\frac{k_x}{k_z}\right) - \ln\left(sin\left(\frac{\pi z}{h}\right)\right) - 1.84\right] \qquad \text{Eq. A-3}$$

$$P'_{xy} = \frac{2b^2}{Lh}\sqrt{\frac{k_z}{k_x}}\left\{F\left(\frac{L}{2b}\right) + 0.5\left[F\left(\frac{4x_{mid} + L}{2b}\right) - F\left(\frac{4x_{mid} - L}{2b}\right)\right]\right\} \qquad \text{Eq. A-4}$$

$F(x)$ is different depending on the value of the argument:

If $x \leq 1$, then:

$$F_{(x)}(x) = -x[0.145 + \ln(x) - 0.137x^2] \qquad \text{Eq. A-5}$$

If $x > 1$, then:

$$F_{(x)} = (2-x)[0.145 + ln(2-x) - 0.137(2-x)^2] \quad \text{Eq. A-6}$$

Case 2: Long reservoir

If

$$\frac{b}{\sqrt{k_y}} \geq \frac{1.33a}{\sqrt{k_x}} \geq \frac{h}{\sqrt{k_z}} \quad \text{Eq. A-7}$$

$$S_R = P_{xyz} + P_{xy} + P_y \quad \text{Eq. A-8}$$

$$P_y = \frac{6.28b^2}{ah}\frac{\sqrt{k_z k_x}}{k_y}\left[\frac{1}{3} - \frac{x_{mid}}{b} + \frac{x_{mid}^2}{b^2} + \frac{L}{24b}\left(\frac{L}{b} - 3\right)\right] \quad \text{Eq. A-9}$$

$$P_{xy} = \left(\frac{b}{L} - 1\right)\left[\left(\frac{6.28a}{h}\right)\sqrt{\frac{k_z}{k_x}}\right]\left(\frac{1}{3} - \frac{y_0}{a} + \frac{y_0^2}{a^2}\right) \quad \text{Eq. A-10}$$

P_{xyz} is computed with equation A-3.

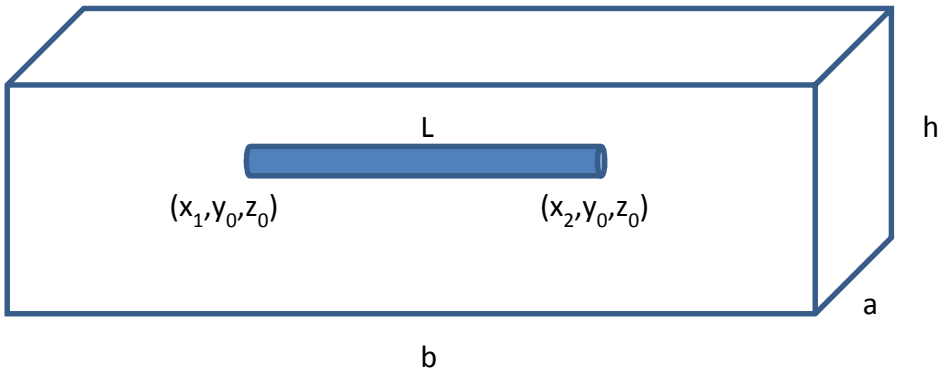

Figure A.1: Geometry model for Babu and Odeh's model

APPENDIX B: SIMULATED SCENARIOS

Reservoir thickness (h)

- First set of values:

Parameter	Initial	Steps	Increase
Wellbore length, L (ft)	**3000**	0	0
Thickness, h(ft)	**200**	0	0
Horizontal permeability, kx (md)	**5**	0	0
Horizontal permeability, ky (md)	**5**	0	0
Vertical permeability, kz (md)	**1**	0	0
Wellbore radius, rw(ft)	**0.25**	0	0
Reservoir width, a(ft)	**1500**	0	0
Reservoir length, b(ft)	**3300**	175	3
Well heel location in x, x1(ft)	**150**	0	0
Well toe location in x, x2(ft)	**3150**	0	0
Well location in y, y0(ft)	**750**	0	0
Well location in z, z0(ft)	**100**	0	0
Average pressure, pave (PSI)	**3600**	0	0
Bottomhole pressure, pwf (PSI)	**3000**	0	0
Viscosity, μ (cp)	**1.05**	0	0
Volume factor, B	**1.1**	0	0
Skin, s	**10**	0	0.0
Center wellbore? 1=yes	**1**		

Table B.1: Reservoir thickness, first set of values

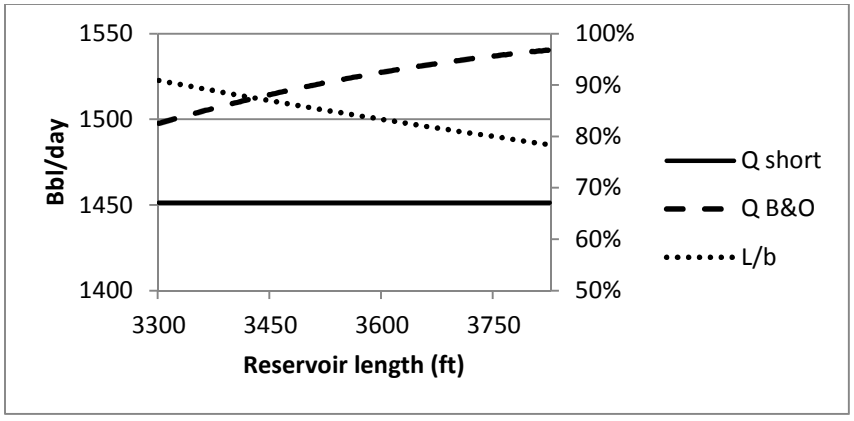

Figure B.1: Reservoir thickness, simulation results for first set of values

- Second set of values:

Parameter	Initial	Steps	Increase
Wellbore length, L (ft)	**3000**	0	0
Thickness, h(ft)	**100**	0	0
Horizontal permeability, kx (md)	**5**	0	0
Horizontal permeability, ky (md)	**5**	0	0
Vertical permeability, kz (md)	**1**	0	0
Wellbore radius, rw(ft)	**0.25**	0	0
Reservoir width, a(ft)	**1500**	0	0
Reservoir length, b(ft)	**3300**	175	3
Well heel location in x, x1(ft)	**150**	0	0
Well toe location in x, x2(ft)	**3150**	0	0
Well location in y, y0(ft)	**750**	0	0
Well location in z, z0(ft)	**50**	0	0
Average pressure, pave (PSI)	**3600**	0	0
Bottomhole pressure, pwf (PSI)	**3000**	0	0
Viscosity, μ (cp)	**1.05**	0	0
Volume factor, B	**1.1**	0	0
Skin, s	**10**	0	0.0
Center wellbore? 1=yes	**1**		

Table B.2: Reservoir thickness, second set of values

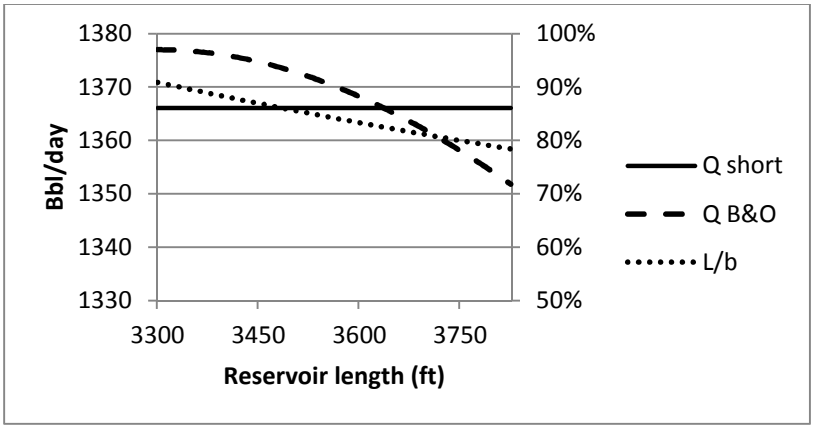

Figure B.2: Reservoir thickness, simulation results for second set of values

Horizontal permeability (k_x)

- First set of values

Parameter	Initial	Steps	Increase
Wellbore length, L (ft)	**3000**	0	0
Thickness, h(ft)	**150**	0	0
Horizontal permeability, kx (md)	**10**	0	0.0
Horizontal permeability, ky (md)	**5**	0	0
Vertical permeability, kz (md)	**1**	0	0
Wellbore radius, rw(ft)	**0.25**	0	0
Reservoir width, a(ft)	**1500**	0	0
Reservoir length, b(ft)	**3300**	175	3
Well heel location in x, x1(ft)	**150**	0	0
Well toe location in x, x2(ft)	**3150**	0	0
Well location in y, y0(ft)	**750**	0	0
Well location in z, z0(ft)	**75**	0	0
Average pressure, pave (PSI)	**3600**	0	0
Bottomhole pressure, pwf (PSI)	**3000**	0	0
Viscosity, μ (cp)	**1.05**	0	0
Volume factor, B	**1.1**	0	0
Skin, s	**10**	0	0.0
Center wellbore? 1=yes	**1**		

Table B.3: Horizontal permeability (k_x), first set of values

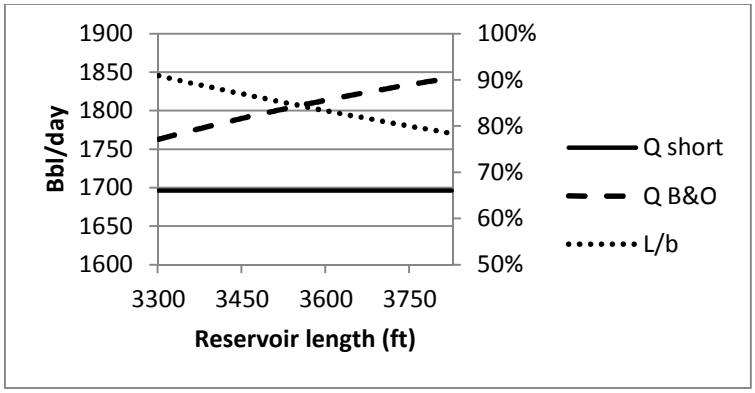

Figure B.3: Horizontal permeability (k_x), simulation results for first set of values

- Second set of values

Parameter	Initial	Steps	Increase
Wellbore length, L (ft)	**3000**	0	0
Thickness, h(ft)	**150**	0	0
Horizontal permeability, kx (md)	**4**	0	0.0
Horizontal permeability, ky (md)	**5**	0	0
Vertical permeability, kz (md)	**1**	0	0
Wellbore radius, rw(ft)	**0.25**	0	0
Reservoir width, a(ft)	**1500**	0	0
Reservoir length, b(ft)	**3300**	175	3
Well heel location in x, x1(ft)	**150**	0	0
Well toe location in x, x2(ft)	**3150**	0	0
Well location in y, y0(ft)	**750**	0	0
Well location in z, z0(ft)	**75**	0	0
Average pressure, pave (PSI)	**3600**	0	0
Bottomhole pressure, pwf (PSI)	**3000**	0	0
Viscosity, μ (cp)	**1.05**	0	0
Volume factor, B	**1.1**	0	0
Skin, s	**10**	0	0.0
Center wellbore? 1=yes	**1**		

Table B.4: Horizontal permeability (k_x), second set of values

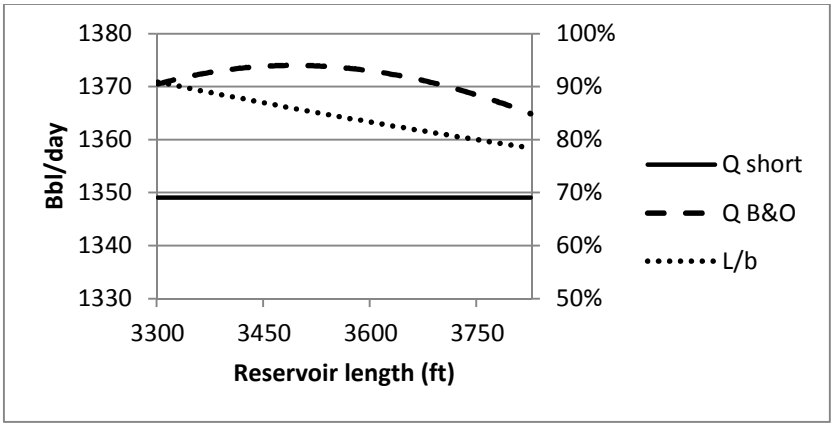

Figure B.4: Horizontal permeability (k_x), simulation results for second set of values

- Third set of values

Parameter	Initial	Steps	Increase
Wellbore length, L (ft)	**3000**	0	0
Thickness, h(ft)	**150**	0	0
Horizontal permeability, kx (md)	**3**	0	0.0
Horizontal permeability, ky (md)	**5**	0	0
Vertical permeability, kz (md)	**1**	0	0
Wellbore radius, rw(ft)	**0.25**	0	0
Reservoir width, a(ft)	**1500**	0	0
Reservoir length, b(ft)	**3300**	175	3
Well heel location in x, x1(ft)	**150**	0	0
Well toe location in x, x2(ft)	**3150**	0	0
Well location in y, y0(ft)	**750**	0	0
Well location in z, z0(ft)	**75**	0	0
Average pressure, pave (PSI)	**3600**	0	0
Bottomhole pressure, pwf (PSI)	**3000**	0	0
Viscosity, μ (cp)	**1.05**	0	0
Volume factor, B	**1.1**	0	0
Skin, s	**10**	0	0.0
Center wellbore? 1=yes	**0**		

Table B.5: Horizontal permeability (k_x), third set of values

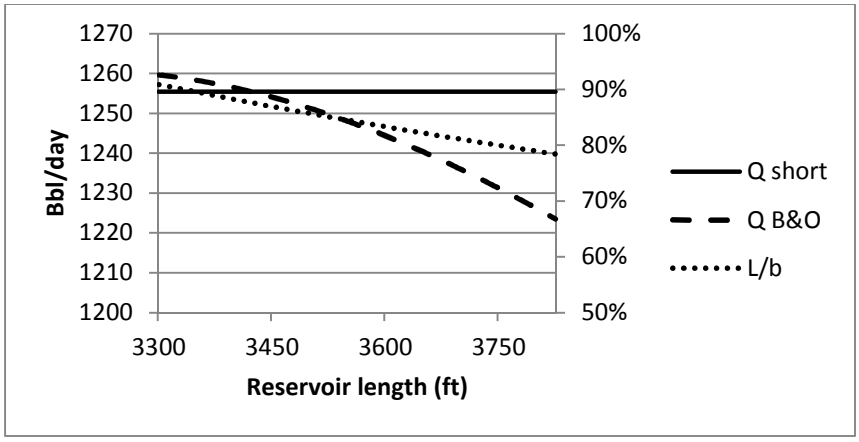

Figure B.5: Horizontal permeability (k_x), simulation results for third set of values

Horizontal permeability (k_y)

- First set of values

Parameter	Initial	Steps	Increase
Wellbore length, L (ft)	**3000**	0	0
Thickness, h(ft)	**150**	0	0
Horizontal permeability, kx (md)	**5**	0	0.0
Horizontal permeability, ky (md)	**1**	0	0.0
Vertical permeability, kz (md)	**1**	0	0
Wellbore radius, rw(ft)	**0.25**	0	0.00
Reservoir width, a(ft)	**1500**	0	0
Reservoir length, b(ft)	**3100**	175	5
Well heel location in x, x1(ft)	**50**	0	0
Well toe location in x, x2(ft)	**3050**	0	0
Well location in y, y0(ft)	**750**	0	0
Well location in z, z0(ft)	**75**	0	0
Average pressure, pave (PSI)	**3600**	0	0
Bottomhole pressure, pwf (PSI)	**3000**	0	0
Viscosity, μ (cp)	**1.05**	0	0
Volume factor, B	**1.1**	0	0
Skin, s	**10**	0	0.0
Center wellbore? 1=yes	**1**		

Table B.6: Horizontal permeability (k_y), first set of values

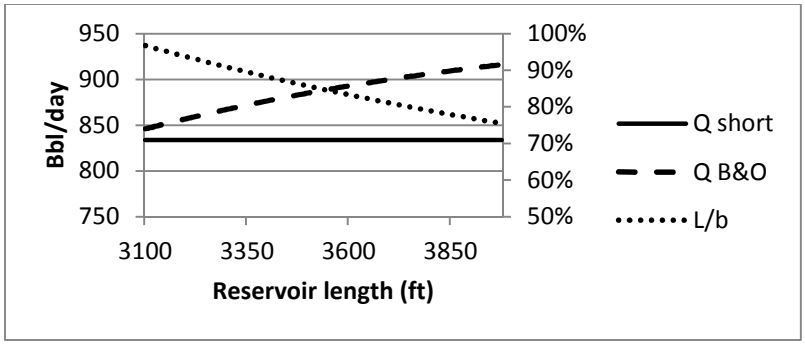

Figure B.6: Horizontal permeability (k_y), simulation results for first set of values

- Second set of values

Parameter	Initial	Steps	Increase
Wellbore length, L (ft)	**3000**	0	0
Thickness, h(ft)	**150**	0	0
Horizontal permeability, kx (md)	**5**	0	0.0
Horizontal permeability, ky (md)	**8.5**	0	0.0
Vertical permeability, kz (md)	**1**	0	0
Wellbore radius, rw(ft)	**0.25**	0	0
Reservoir width, a(ft)	**1500**	0	0
Reservoir length, b(ft)	**3100**	175	5
Well heel location in x, x1(ft)	**50**	0	0
Well toe location in x, x2(ft)	**3050**	0	0
Well location in y, y0(ft)	**750**	0	0
Well location in z, z0(ft)	**75**	0	0
Average pressure, pave (PSI)	**3600**	0	0
Bottomhole pressure, pwf (PSI)	**3000**	0	0
Viscosity, μ (cp)	**1.05**	0	0
Volume factor, B	**1.1**	0	0
Skin, s	**10**	0	0.0
Center wellbore? 1=yes	**1**		

Table B.7: Horizontal permeability (k_y), second set of values

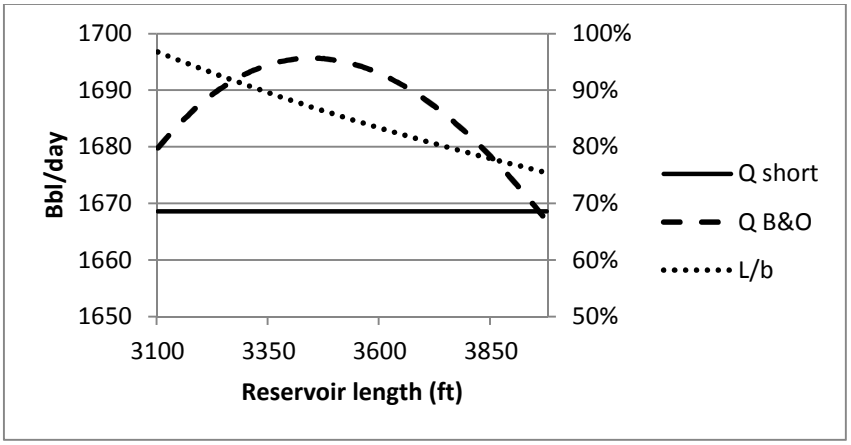

Figure B.7: Horizontal permeability (k_y), simulation results for second set of values

- Third set of values

Parameter	Initial	Steps	Increase
Wellbore length, L (ft)	**3000**	0	0
Thickness, h(ft)	**150**	0	0
Horizontal permeability, kx (md)	**5**	0	0.0
Horizontal permeability, ky (md)	**20**	0	0.0
Vertical permeability, kz (md)	**1**	0	0
Wellbore radius, rw(ft)	**0.25**	0	0.00
Reservoir width, a(ft)	**1500**	0	0
Reservoir length, b(ft)	**3100**	175	5
Well heel location in x, x1(ft)	**50**	0	0
Well toe location in x, x2(ft)	**3050**	0	0
Well location in y, y0(ft)	**750**	0	0
Well location in z, z0(ft)	**75**	0	0
Average pressure, pave (PSI)	**3600**	0	0
Bottomhole pressure, pwf (PSI)	**3000**	0	0
Viscosity, μ (cp)	**1.05**	0	0
Volume factor, B	**1.1**	0	0
Skin, s	**10**	0	0.0
Center wellbore? 1=yes	**1**		

Table B.8: Horizontal permeability (k_y) , third set of values

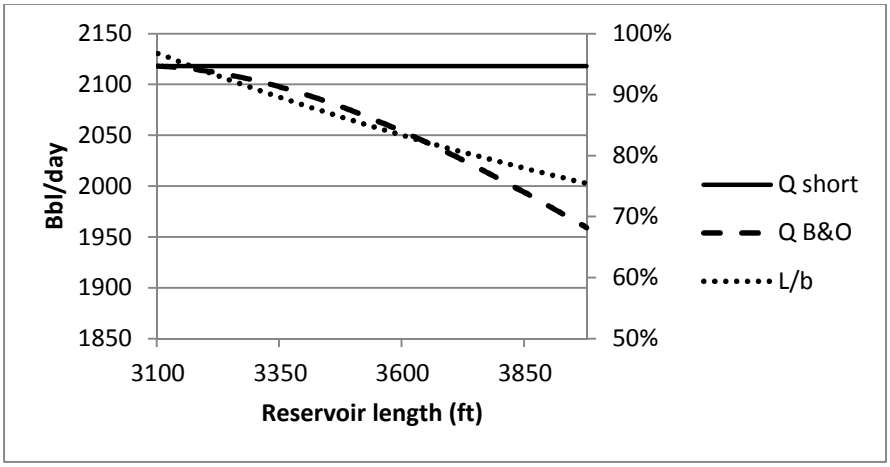

Figure B.8: Horizontal permeability (k_y), simulation results for third set of values

Vertical permeability

- First set of values

Parameter	Initial	Steps	Increase
Wellbore length, L (ft)	**3000**	0	0
Thickness, h(ft)	**150**	0	0
Horizontal permeability, kx (md)	**5**	0	0.0
Horizontal permeability, ky (md)	**5**	0	0.0
Vertical permeability, kz (md)	**0.01**	0	0
Wellbore radius, rw(ft)	**0.25**	0	0.00
Reservoir width, a(ft)	**1500**	0	0
Reservoir length, b(ft)	**3100**	175	3
Well heel location in x, x1(ft)	**50**	0	0
Well toe location in x, x2(ft)	**3050**	0	0
Well location in y, y0(ft)	**750**	0	0
Well location in z, z0(ft)	**75**	0	0
Average pressure, pave (PSI)	**3600**	0	0
Bottomhole pressure, pwf (PSI)	**3000**	0	0
Viscosity, μ (cp)	**1.05**	0	0
Volume factor, B	**1.1**	0	0
Skin, s	**10**	0	0.0
Center wellbore? 1=yes	**1**		

Table B.9: Vertical permeability, first set of values

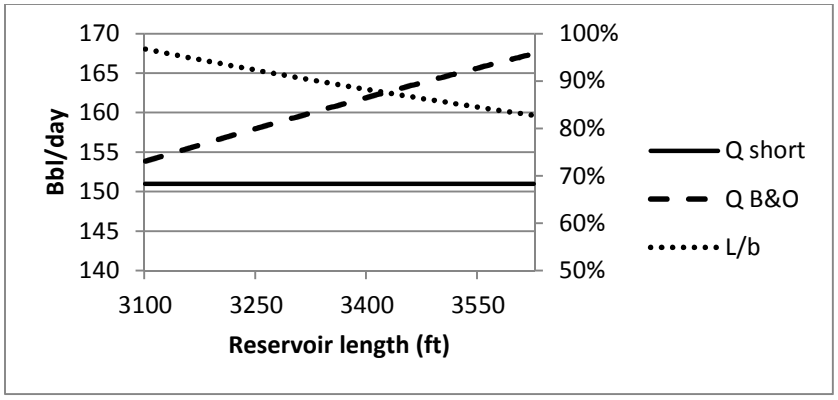

Figure B.9: Vertical permeability, simulation results for first set of values

- Second set of values

Parameter	Initial	Steps	Increase
Wellbore length, L (ft)	**3000**	0	0
Thickness, h(ft)	**150**	0	0
Horizontal permeability, kx (md)	**5**	0	0.0
Horizontal permeability, ky (md)	**5**	0	0.0
Vertical permeability, kz (md)	**2**	0	0
Wellbore radius, rw(ft)	**0.25**	0	0
Reservoir width, a(ft)	**1500**	0	0
Reservoir length, b(ft)	**3100**	175	3
Well heel location in x, x1(ft)	**50**	0	0
Well toe location in x, x2(ft)	**3050**	0	0
Well location in y, y0(ft)	**750**	0	0
Well location in z, z0(ft)	**75**	0	0
Average pressure, pave (PSI)	**3600**	0	0
Bottomhole pressure, pwf (PSI)	**3000**	0	0
Viscosity, μ (cp)	**1.05**	0	0
Volume factor, B	**1.1**	0	0
Skin, s	**10**	0	0.0
Center wellbore? 1=yes	**1**		

Table B.10: Vertical permeability, first set of values

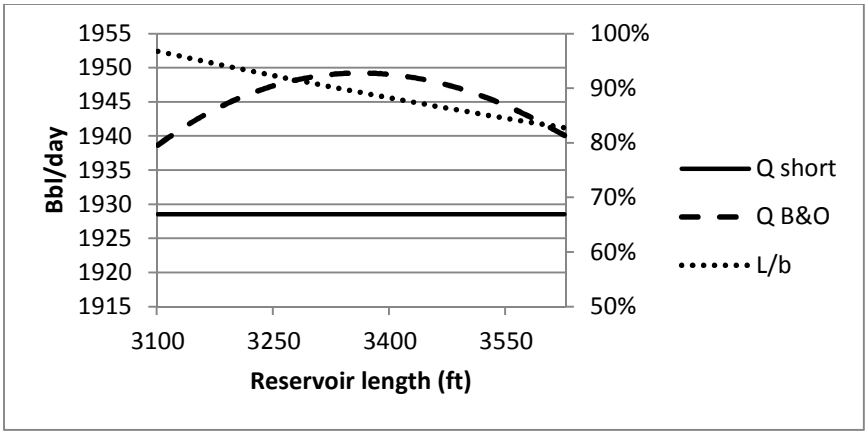

Figure B.10: Vertical permeability, simulation results for first set of values

- Third set of values

Parameter	Initial	Steps	Increase
Wellbore length, L (ft)	**3000**	0	0
Thickness, h(ft)	**150**	0	0
Horizontal permeability, kx (md)	**5**	0	0.0
Horizontal permeability, ky (md)	**5**	0	0.0
Vertical permeability, kz (md)	**10**	0	0
Wellbore radius, rw(ft)	**0.25**	0	0.00
Reservoir width, a(ft)	**1500**	0	0
Reservoir length, b(ft)	**3100**	175	3
Well heel location in x, x1(ft)	**50**	0	0
Well toe location in x, x2(ft)	**3050**	0	0
Well location in y, y0(ft)	**750**	0	0
Well location in z, z0(ft)	**75**	0	0
Average pressure, pave (PSI)	**3600**	0	0
Bottomhole pressure, pwf (PSI)	**3000**	0	0
Viscosity, μ (cp)	**1.05**	0	0
Volume factor, B	**1.1**	0	0
Skin, s	**10**	0	0.0
Center wellbore? 1=yes	**1**		

Table B.11: Vertical permeability, third set of values

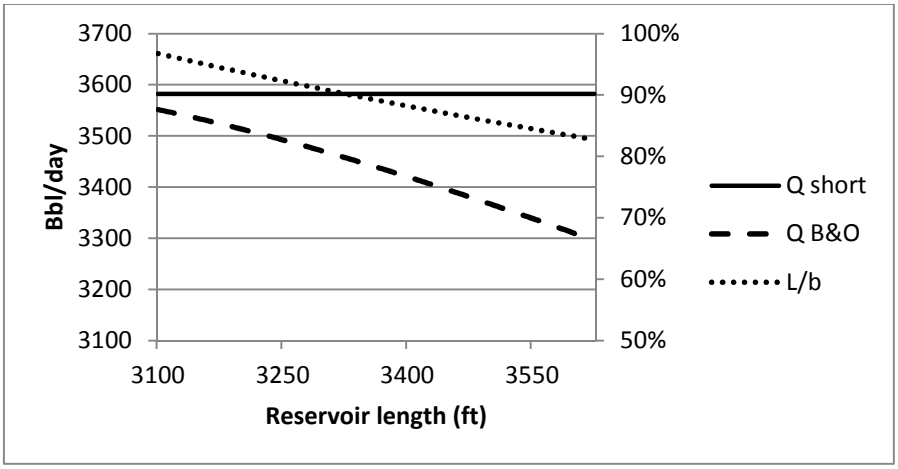

Figure B.11: Vertical permeability, simulation results for third set of values

Reservoir width

- First set of values

Parameter	Initial	Steps	Increase
Wellbore length, L (ft)	**3000**	0	0
Thickness, h(ft)	**150**	0	0
Horizontal permeability, kx (md)	**5**	0	0.0
Horizontal permeability, ky (md)	**5**	0	0.0
Vertical permeability, kz (md)	**1**	0	0
Wellbore radius, rw(ft)	**0.25**	0	0.00
Reservoir width, a(ft)	**2000**	0	0
Reservoir length, b(ft)	**3100**	175	5
Well heel location in x, x1(ft)	**50**	0	0
Well toe location in x, x2(ft)	**3050**	0	0
Well location in y, y0(ft)	**1000**	0	0
Well location in z, z0(ft)	**75**	0	0
Average pressure, pave (PSI)	**3600**	0	0
Bottomhole pressure, pwf (PSI)	**3000**	0	0
Viscosity, μ (cp)	**1.05**	0	0
Volume factor, B	**1.1**	0	0
Skin, s	**10**	0	0.0
Center wellbore? 1=yes	**1**		

Table B.12: Reservoir width, first set of values

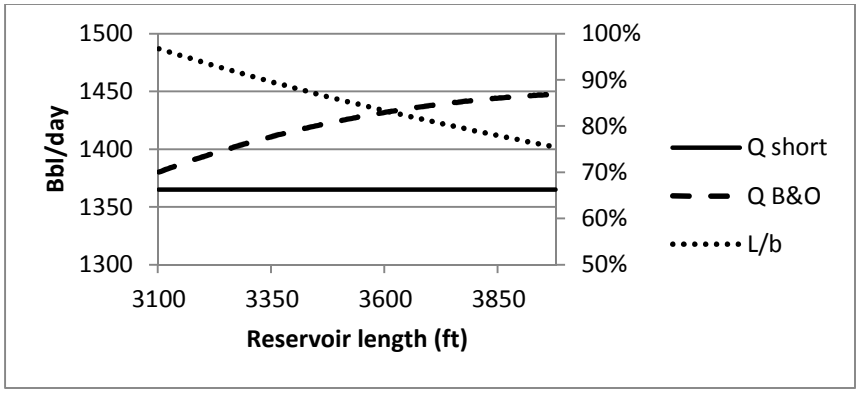

Figure B.12: Reservoir width, simulation results for first set of values

- Second set of values

Parameter	Initial	Steps	Increase
Wellbore length, L (ft)	**3000**	0	0
Thickness, h(ft)	**150**	0	0
Horizontal permeability, kx (md)	**5**	0	0.0
Horizontal permeability, ky (md)	**5**	0	0.0
Vertical permeability, kz (md)	**1**	0	0
Wellbore radius, rw(ft)	**0.25**	0	0.00
Reservoir width, a(ft)	**1200**	0	0
Reservoir length, b(ft)	**3100**	175	5
Well heel location in x, x1(ft)	**50**	0	0
Well toe location in x, x2(ft)	**3050**	0	0
Well location in y, y0(ft)	**600**	0	0
Well location in z, z0(ft)	**75**	0	0
Average pressure, pave (PSI)	**3600**	0	0
Bottomhole pressure, pwf (PSI)	**3000**	0	0
Viscosity, μ (cp)	**1.05**	0	0
Volume factor, B	**1.1**	0	0
Skin, s	**10**	0	0.0
Center wellbore? 1=yes	**1**		

Table B.13: Reservoir width, second set of values

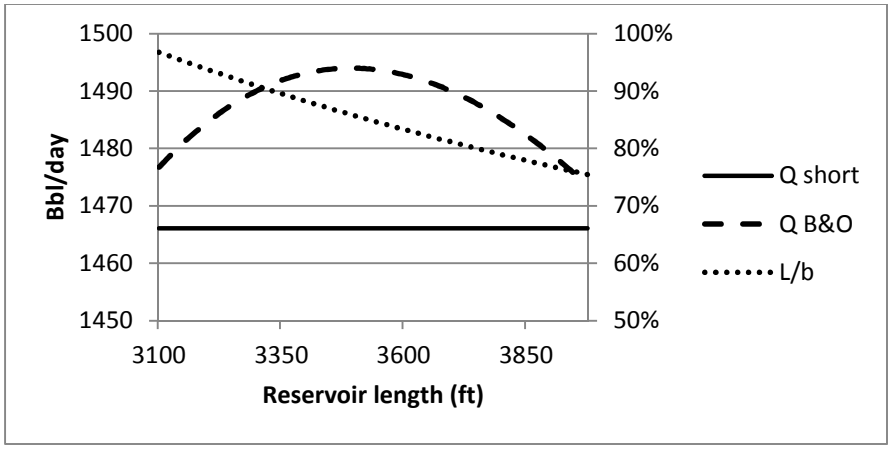

Figure B.13: Reservoir width, simulation results for second set of values

- Third set of values

Parameter	Initial	Steps	Increase
Wellbore length, L (ft)	**3000**	0	0
Thickness, h(ft)	**150**	0	0
Horizontal permeability, kx (md)	**5**	0	0.0
Horizontal permeability, ky (md)	**5**	0	0.0
Vertical permeability, kz (md)	**1**	0	0
Wellbore radius, rw(ft)	**0.25**	0	0.00
Reservoir width, a(ft)	**750**	0	0
Reservoir length, b(ft)	**3100**	175	5
Well heel location in x, x1(ft)	**50**	0	0
Well toe location in x, x2(ft)	**3050**	0	0
Well location in y, y0(ft)	**375**	0	0
Well location in z, z0(ft)	**75**	0	0
Average pressure, pave (PSI)	**3600**	0	0
Bottomhole pressure, pwf (PSI)	**3000**	0	0
Viscosity, μ (cp)	**1.05**	0	0
Volume factor, B	**1.1**	0	0
Skin, s	**10**	0	0.0
Center wellbore? 1=yes	**1**		

Table B.14: Reservoir width, third set of values

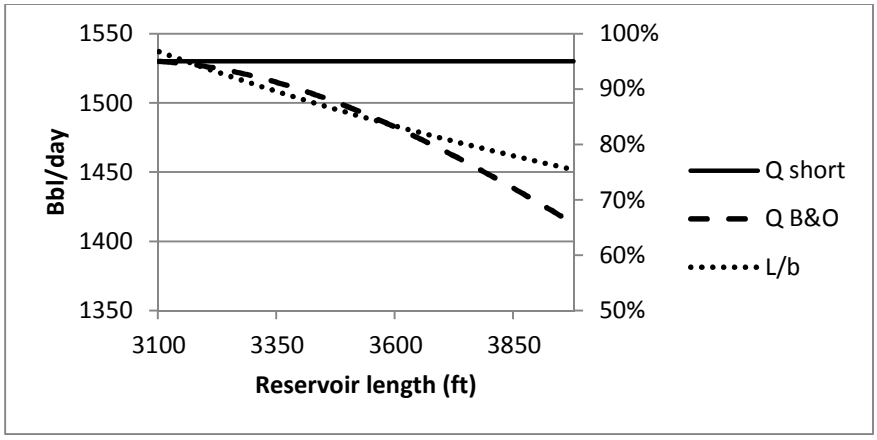

Figure B.14: Reservoir width, simulation results for third set of values

Skin

- First set of values

Parameter	Initial	Steps	Increase
Wellbore length, L (ft)	**3000**	0	0
Thickness, h(ft)	**150**	0	0
Horizontal permeability, kx (md)	**5**	0	0.0
Horizontal permeability, ky (md)	**5**	0	0.0
Vertical permeability, kz (md)	**1**	0	0
Wellbore radius, rw(ft)	**0.25**	0	0.00
Reservoir width, a(ft)	**1500**	0	0
Reservoir length, b(ft)	**3100**	175	3
Well heel location in x, x1(ft)	**50**	0	0
Well toe location in x, x2(ft)	**3050**	0	0
Well location in y, y0(ft)	**750**	0	0
Well location in z, z0(ft)	**75**	0	0
Average pressure, pave (PSI)	**3600**	0	0
Bottomhole pressure, pwf (PSI)	**3000**	0	0
Viscosity, μ (cp)	**1.05**	0	0
Volume factor, B	**1.1**	0	0
Skin, s	**15**	0	0.0
Center wellbore? 1=yes	**1**		

Table B.15: Skin, first set of values

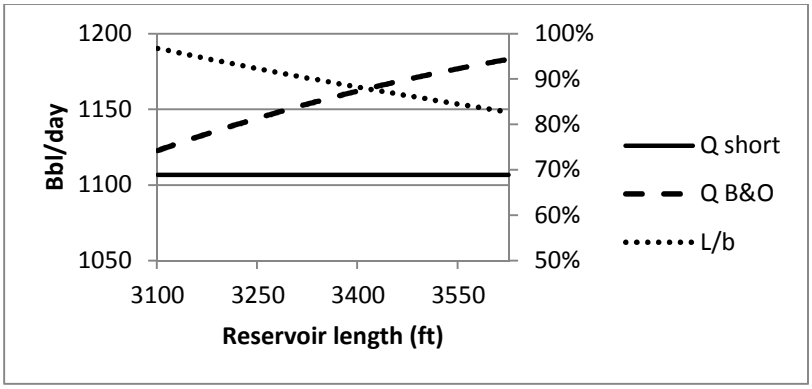

Figure B.15: Skin, simulation results for first set of values

- Second set of values

Parameter	Initial	Steps	Increase
Wellbore length, L (ft)	**3000**	0	0
Thickness, h(ft)	**150**	0	0
Horizontal permeability, kx (md)	**5**	0	0.0
Horizontal permeability, ky (md)	**5**	0	0.0
Vertical permeability, kz (md)	**1**	0	0
Wellbore radius, rw(ft)	**0.25**	0	0.00
Reservoir width, a(ft)	**1500**	0	0
Reservoir length, b(ft)	**3100**	175	3
Well heel location in x, x1(ft)	**50**	0	0
Well toe location in x, x2(ft)	**3050**	0	0
Well location in y, y0(ft)	**750**	0	0
Well location in z, z0(ft)	**75**	0	0
Average pressure, pave (PSI)	**3600**	0	0
Bottomhole pressure, pwf (PSI)	**3000**	0	0
Viscosity, μ (cp)	**1.05**	0	0
Volume factor, B	**1.1**	0	0
Skin, s	**8**	0	0.0
Center wellbore? 1=yes	**1**		

Table B.16: Skin, second set of values

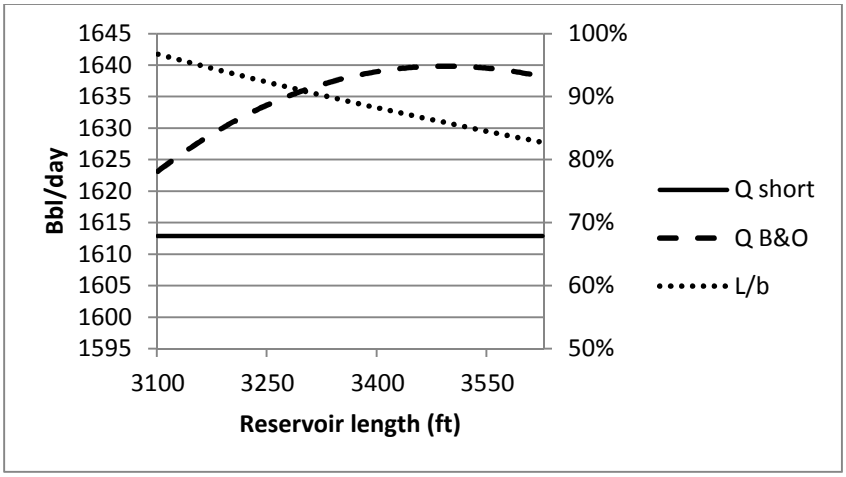

Figure B.16: Skin simulation results for, second set of values

- Third set of values

Parameter	Initial	Steps	Increase
Wellbore length, L (ft)	**3000**	0	0
Thickness, h(ft)	**150**	0	0
Horizontal permeability, kx (md)	**5**	0	0.0
Horizontal permeability, ky (md)	**5**	0	0.0
Vertical permeability, kz (md)	**1**	0	0
Wellbore radius, rw(ft)	**0.25**	0	0.00
Reservoir width, a(ft)	**1500**	0	0
Reservoir length, b(ft)	**3100**	175	3
Well heel location in x, x1(ft)	**50**	0	0
Well toe location in x, x2(ft)	**3050**	0	0
Well location in y, y0(ft)	**750**	0	0
Well location in z, z0(ft)	**75**	0	0
Average pressure, pave (PSI)	**3600**	0	0
Bottomhole pressure, pwf (PSI)	**3000**	0	0
Viscosity, μ (cp)	**1.05**	0	0
Volume factor, B	**1.1**	0	0
Skin, s	**6**	0	0.0
Center wellbore? 1=yes	**1**		

Table B.17: Skin, third set of values

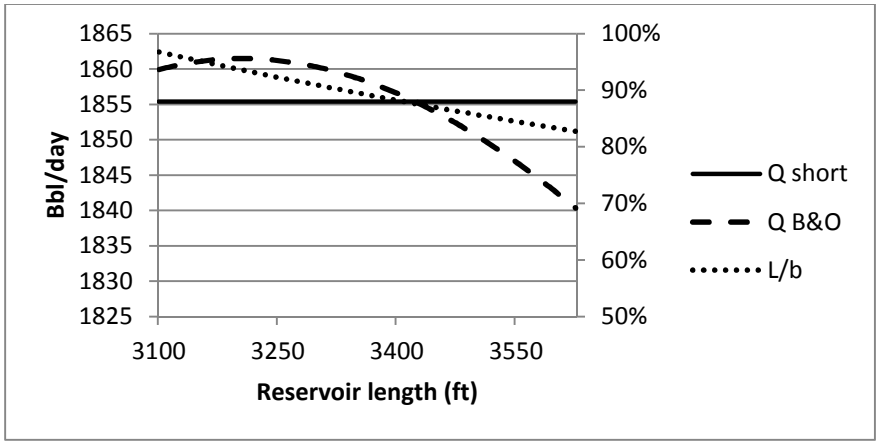

Figure B.17: Skin, simulation results for third set of values

APPENDIX C: ANALYTICAL ANALYSIS OF SR

In order to obtain an expression for the reservoir length after which the model starts predicting a decreasing productivity, b_{crit} (b critical) we should obtain a general expression for it, applying the model and without replacing any values, differentiate the expression, ask for it to be zero and obtain it's value.

The approach will be to try to obtain polynomial expressions on *b*.

The equations to be used are presented on the Appendix, I will cover first Case 2, which corresponds to the "Long reservoir" and one would expect to be the situation in most cases:

Analysis of Case 2:

Case 2 happens when:

$$\frac{b}{\sqrt{k_y}} > \frac{1.33a}{\sqrt{k_x}} \geq \frac{h}{\sqrt{k_z}} \qquad \text{Eq. C-1}$$

In case 2, the model computes the partial penetration skin factor as:

$$S_R = P_{xyz} + P_y + P_{xy} \qquad \text{Eq. C-2}$$

$$\frac{dS_R}{db} = \frac{dP_{xyz}}{db} + \frac{dP_y}{db} + \frac{dP_{xy}}{db} \qquad \text{Eq. C-3}$$

$$P_{xyz} = \left(\frac{b}{L} - 1\right)\left[ln\frac{h}{r_w} + 0.25ln\frac{k_x}{k_z} - ln\left(sin\frac{180°z}{h}\right) - 1.84\right] \qquad \text{Eq. C-4}$$

Let

$$\beta_2 = ln\frac{h}{r_w} + 0.25ln\frac{k_x}{k_z} - ln\left(sin\frac{180°z}{h}\right) - 1.84 \quad \text{Eq. C-5}$$

So

$$P_{xyz} = b\frac{\beta_2}{L} - \beta_2 \quad \text{Eq. C-6}$$

$$\frac{dP_{xyz}}{db} = \frac{\beta_2}{L} \quad \text{Eq. C-7}$$

$$P_y = \frac{6.28b^2}{ah}\frac{\sqrt{k_x k_z}}{k_y}\left[\left(\frac{1}{3} - \frac{y_{mid}}{b} + \frac{y_{mid}^2}{b^2}\right) + \frac{L}{24b}\left(\frac{L}{b} - 3\right)\right] \quad \text{Eq. C-8}$$

Let:

$$\beta_1 = \frac{6.28}{ah}\frac{\sqrt{k_x k_z}}{k_y} \quad \text{Eq. C-9}$$

At this point, I will assume that the wellbore position does not change with the reservoir's length, that is, y_{mid} is constant and not a function of b. The case for the centered wellbore will be addressed later. As well, whenever the parameter y is used, I am referring to y_{mid}.

$$P_y = \beta_1 b^2\left(\frac{1}{3} - \frac{y_{mid}}{b} + \frac{y_{mid}^2}{b^2} + \frac{L^2}{24b^2} - \frac{3L}{24b}\right) \quad \text{Eq. C-10}$$

$$= \beta_1\left(\frac{b^2}{3} - y_{mid}b + y_{mid}^2 + \frac{L^2}{24} - \frac{3Lb}{24}\right)$$

$$P_y = \beta_1\left(\frac{L^2 + 24y^2}{24}\right) - \beta_1 b\left(\frac{L + 8y}{8}\right) + \beta_1\frac{b^2}{3} \quad \text{Eq. C-11}$$

$$\frac{dP_y}{db} = -\beta_1\left(\frac{L + 8y}{8}\right) + \beta_1\frac{2b}{3} \quad \text{Eq. C-12}$$

$$P_{xy} = \left(\frac{b}{L} - 1\right)\left(\frac{6.28a}{h}\sqrt{\frac{k_z}{k_x}}\right)\left(\frac{1}{3} - \frac{x_0}{a} + \frac{x_0^2}{a^2}\right) \quad \text{Eq. C-13}$$

Let:

$$\beta_3 = \left(\frac{6.28a}{hL}\sqrt{\frac{k_z}{k_x}}\right)\left(\frac{1}{3} - \frac{x_0}{a} + \frac{x_0^2}{a^2}\right) \quad \text{Eq. C-14}$$

$$P_{xy} = b\beta_3 - \beta_3 \quad \text{Eq. C-15}$$

$$\frac{dP_{xy}}{db} = \beta_3 \quad \text{Eq. C-16}$$

So we obtained, from equations C-2, C-6, C-11 and C-15:

$$S_R = b\frac{\beta_2}{L} - \beta_2 + \beta_1\left(\frac{L^2 + 24y_{mid}^2}{24}\right) - \beta_1 b\left(\frac{L + 8y_{mid}}{8}\right) + \beta_1\frac{b^2}{3} + b\beta_3 - \beta_3 \quad \text{Eq. C-17}$$

And from equations C-3, C-7, C-12 and C-16:

$$\frac{dS_R}{db} = \frac{\beta_2}{L} - \beta_1\left(\frac{L + 8y_{mid}}{8}\right) + \beta_1\frac{2b}{3} + \beta_3 \quad \text{Eq. C-18}$$

Now I will consider the situation when the wellbore is always centered as the reservoir's length increases, that is:

$$y_{mid} = \frac{b}{2} \quad \text{Eq. C-19}$$

The results obtained for P_{xyz} and P_{xy} in equations C-6 and C-13 are still valid, but P_y has to be analyzed again, replacing equation C-19 in equation C-11:

$$P_y = \beta_1 b^2\left(\frac{1}{3} - \frac{\frac{b}{2}}{b} + \frac{\left(\frac{b}{2}\right)^2}{b^2} + \frac{L^2}{24b^2} - \frac{3L}{24b}\right) = \beta_1 b^2\left(\frac{1}{12} + \frac{L^2}{24b^2} - \frac{L}{8b}\right) \quad \text{Eq. C-20}$$

$$P_y = b^2\frac{\beta_1}{12} - b\frac{\beta_1 L}{8} + \frac{\beta_1 L^2}{24} \quad \text{Eq. C-21}$$

$$\frac{dP_y}{db} = b\frac{\beta_1}{6} - \frac{\beta_1 L}{8} \quad \text{Eq. C-22}$$

And now rewriting equations C-17 and C-18 using this new results for P_y:

$$S_R = b\frac{\beta_2}{L} - \beta_2 + b^2\frac{\beta_1}{12} - b\frac{\beta_1 L}{8} + \frac{\beta_1 L^2}{24} + b\beta_3 - \beta_3 \qquad \text{Eq. C-23}$$

$$\frac{dS_R}{db} = \frac{\beta_2}{L} + b\frac{\beta_1}{6} - \frac{\beta_1 L}{8} + \beta_3 \qquad \text{Eq. C-24}$$

Analysis of case 1

Case 1 happens when:

$$a/\sqrt{k_x} \geq 0.75b/\sqrt{k_y} \geq 0.75h/\sqrt{k_z} \qquad \text{Eq. C-25}$$

In case 1 the model computes the partial penetration skin factor as:

$$S_R = P_{xyz} + P'_{xy} \qquad \text{Eq. C-26}$$

$$\frac{dS_R}{db} = \frac{dP_{xyz}}{db} + \frac{dP'_{xy}}{db} \qquad \text{Eq. C-27}$$

P_{xyz} is computed in the same way for both cases, so the results obtained in Eq C-6 for case 2 apply.

$$P'_{xy} = \frac{2b^2}{Lh}\sqrt{\frac{k_z}{k_y}}\left\{F\left(\frac{L}{2b}\right) + 0.5\left[F\left(\frac{4y_{mid}+L}{2b}\right) - F\left(\frac{4y_{mid}-L}{2b}\right)\right]\right\} \qquad \text{Eq. C-28}$$

As it was done before for case 2, first I will consider that y_{mid} is fixed, and does not change with the reservoir's length

The results obtained in Appendix E, equations E-13, E-18 and E-20, are used here for the expressions of the 3 F functions present in equation C-28.

I am first considering that the position of the wellbore remains constant, that is, y_{mid} is not a function of the reservoir's length.

$$P'_{xy} = \frac{2b^2}{Lh}\sqrt{\frac{k_z}{k_y}}\left\{\left[0.137\left(\frac{L}{2}\right)^3 b^{-3} - b^{-1}\frac{L}{2}\left[0.145 + \ln\left(\frac{L}{2}\right)\right] + \frac{L}{2}b^{-1}\ln(b)\right]\right.$$

$$+ 0.5\left[b^{-3}0.017125(4y_{mid} + L)^3 - b^{-2}0.2055(4y_{mid} + L)^2\right.$$

$$+ b^{-1}0.2015(4y_{mid} + L) + \left(\frac{2.192y_{mid}}{L} - 0.258\right)$$

$$+ \left(2 - \frac{4y_{mid} + L}{2b}\right)ln\left(2 - \frac{4y_{mid} + L}{2b}\right)$$

$$- b^{-3}0.03425(4y_{mid} - L)^3 + b^{-1}0.0725(4y_{mid} - L)$$

$$\left.\left. + \left(\frac{4y_{mid} - L}{2b}\right)ln\left(\frac{4y_{mid} - L}{2b}\right)\right]\right\}$$

Eq. C-29

$$P'_{xy} = \frac{2b^2}{Lh}\sqrt{\frac{k_z}{k_y}}\left\{b^{-3}[0.017125L^3 + 0.008563(4y_{mid} + L)^3\right.$$

$$- 0.017125(4y_{mid} - L)^3] + b^{-2}[-0.10275(4y_{mid} + L)^2]$$

$$+ b^{-1}\left[-0.0725L - 0.5Lln\left(\frac{L}{2}\right) + 0.10075(4y_{mid} + L)\right.$$

$$\left. + 0.03625(4y_{mid} - L)\right] + \left[\frac{1.096y_{mid}}{L} - 0.129\right] + b^{-1}\frac{L}{2}\ln(b)$$

$$+ \left(1 - \frac{4y_{mid} + L}{4b}\right)ln\left(2 - \frac{4y_{mid} + L}{2b}\right)$$

$$\left. + \left(\frac{4y_{mid} - L}{4b}\right)ln\left(\frac{4y_{mid} - L}{2b}\right)\right\}$$

Eq. C-30

$$P'_{xy} = \frac{2}{Lh}\sqrt{\frac{k_z}{k_y}}\Big\{b^{-1}[0.017125L^3 + 0.008563(4y_{mid} + L)^3 - 0.017125(4y_{mid} - L)^3] + [-0.10275(4y_{mid} + L)^2] + b\left[-0.0725L - 0.5Lln\left(\frac{L}{2}\right) + 0.10075(4y_{mid} + L) + 0.03625(4y_{mid} - L)\right] + b^2\left[\frac{1.096y_{mid}}{L} - 0.129\right] + b\frac{L}{2}\ln(b) + b^2\left(1 - \frac{4y_{mid} + L}{4b}\right)ln\left(2 - \frac{4y_{mid} + L}{2b}\right) + b\left(\frac{4y_{mid} - L}{4}\right)ln\left(\frac{4y_{mid} - L}{2b}\right)\Big\} \quad \text{Eq. C-31}$$

Let:

$$\beta_6 = \frac{2}{Lh}\sqrt{\frac{k_z}{k_y}} \quad \text{Eq. C-32}$$

$$\beta_7 = 0.017125L^3 + 0.008563(4y_{mid} + L)^3 - 0.017125(4y_{mid} - L)^3 \quad \text{Eq. C-33}$$

$$\beta_8 = [-0.10275(4y_{mid} + L)^2] \quad \text{Eq. C-34}$$

$$\beta_9 = -0.0725L - 0.5Lln\left(\frac{L}{2}\right) + 0.10075(4y_{mid} + L) + 0.03625(4y_{mid} - L) \quad \text{Eq. C-35}$$

$$\beta_{10} = \frac{1.096y_{mid}}{L} - 0.129 \quad \text{Eq. C-36}$$

We can replace equations C-32, C-33, C-34, C-35 and C-36 in equation C-31:

$$P'_{xy} = \beta_6\left[b^{-1}\beta_7 + \beta_8 + b\beta_9 + b^2\beta_{10} + b\frac{L}{2}\ln(b) + b^2\left(1 - \frac{4y_{mid} + L}{4b}\right)ln\left(2 - \frac{4y_{mid} + L}{2b}\right) + b\left(\frac{4y_{mid} - L}{4}\right)ln\left(\frac{4y_{mid} - L}{2b}\right)\right] \quad \text{Eq. C-37}$$

So, replacing equations C-6 and C-37 in equation C-26 we can obtain the new expression for S_R for the first case:

$$S_R = \beta_6 \left[b^{-1}\beta_7 + \beta_8 - \frac{\beta_2}{\beta_6} + b\left(\beta_9 + \frac{\beta_2}{L\beta_6}\right) + b^2\beta_{10} + b\frac{L}{2}\ln(b) + b^2\left(1 - \frac{4y_{mid} + L}{4b}\right) ln\left(2 - \frac{4y_{mid} + L}{2b}\right) + b\left(\frac{4y_{mid} - L}{4}\right) ln\left(\frac{4y_{mid} - L}{2b}\right)\right] \quad \text{Eq. C-38}$$

And differentiating equation C-38 with respect to b we obtain:

$$\frac{dS_R}{db} = \beta_6 \left\{ -b^{-2}\beta_7 + \beta_9 + \frac{\beta_2}{L\beta_6} + 2b\beta_{10} + \frac{L}{2} + \frac{L}{2}\ln(b) + \frac{1}{4}\left[(8b - L - 4y_{mid}) ln\left(2 - \frac{4y_{mid} + L}{2b}\right)\right] + b\left(\frac{4y_{mid} - L}{4}\right) ln\left(\frac{4y_{mid} - L}{2b}\right) + L + 4y_{mid} + \left(y_{mid} - \frac{L}{4}\right)\left[ln\left(\frac{4y_{mid} - L}{2b}\right) - 1\right]\right\} \quad \text{Eq. C-39}$$

The derivative of the last term of S_R was obtained reminding that all the variables have positive values, for they are all lengths.

The fourth case correspond to case 1 when the wellbore remains centered as the reservoir's length increases, that is:

$$y_{mid} = \frac{b}{2} \quad \text{Eq. C-40}$$

We can rewrite equation C-37 using equation C-40:

$$P'_{xy} = \beta_6 \left[b^{-1}\beta_7 + \beta_8 + b\beta_9 + b^2\beta_{10} + b\frac{L}{2}\ln(b) + b^2\left(1 - \frac{2b+L}{4b}\right) ln\left(2 - \frac{2b+L}{2b}\right) + b\left(\frac{2b-L}{4}\right) ln\left(\frac{2b-L}{2b}\right)\right] \quad \text{Eq. C-41}$$

$$P'_{xy} = \beta_6 \left[b^{-1}\beta_7 + \beta_8 + b\beta_9 + b^2\beta_{10} + b\frac{L}{2}\ln(b) + b^2\left(\frac{1}{2} - \frac{L}{4b}\right) ln\left(1 - \frac{L}{2b}\right) + b\left(\frac{2b-L}{4}\right) ln\left(1 - \frac{L}{2b}\right)\right] \quad \text{Eq. C-42}$$

$$\frac{dP'_{xy}}{db} = \beta_6 \left[-b^{-2}\beta_7 + \beta_9 + 2b\beta_{10} + \frac{L}{2}\ln(b) + \left(2b - \frac{L}{2}\right) ln\left(1 - \frac{L}{2b}\right) + L\right] \quad \text{Eq. C-43}$$

So we have:

$$S_R = b\frac{\beta_2}{L} - \beta_2 + \beta_6 \left[b^{-1}\beta_7 + \beta_8 + b\beta_9 + b^2\beta_{10} + b\frac{L}{2}\ln(b) + b^2\left(\frac{1}{2} - \frac{L}{4b}\right) ln\left(1 - \frac{L}{2b}\right) + b\left(\frac{2b-L}{4}\right) ln\left(1 - \frac{L}{2b}\right)\right] \quad \text{Eq. C-44}$$

$$\frac{dS_R}{db} = \frac{\beta_2}{L} + \beta_6 \left[-b^{-2}\beta_7 + \beta_9 + 2b\beta_{10} + \frac{L}{2}\ln(b) + \left(2b - \frac{L}{2}\right) ln\left(1 - \frac{L}{2b}\right) + L\right] \quad \text{Eq. C-45}$$

We can compile the results obtained replacing equations C-5, C-32, C-33, C-34, C-35 and C-36 in equations C-44, C-45, C-23 and C-22:

Case 1:

$$a/\sqrt{k_x} \geq 0.75b/\sqrt{k_y} \geq 0.75h/\sqrt{k_z} \qquad \text{Eq. C-46}$$

$$\begin{aligned} S_R = \frac{2}{Lh}\sqrt{\frac{k_z}{k_y}}\Bigg[& b^{-1}[0.017125L^3 + 0.008563(4y_{mid}+L)^3 \\ & - 0.017125(4y_{mid}-L)^3] + [-0.10275(4y_{mid}+L)^2] \\ & - \frac{Lh}{2}\sqrt{\frac{k_y}{k_z}}\left[ln\frac{h}{r_w} + 0.25ln\frac{k_x}{k_z} - ln\left(sin\frac{180°z}{h}\right) - 1.84\right] \\ & + b\Bigg\{\Big[-0.0725L - 0.5Lln\left(\frac{L}{2}\right) + 0.10075(4y_{mid}+L) \\ & + 0.03625(4y_{mid}-L)\Big] \\ & + \frac{h}{2}\sqrt{\frac{k_y}{k_z}}\left[ln\frac{h}{r_w} + 0.25ln\frac{k_x}{k_z} - ln\left(sin\frac{180°z}{h}\right) - 1.84\right]\Bigg\} \\ & + b^2\left[\frac{1.096y_{mid}}{L} - 0.129\right] + b\frac{L}{2}\ln(b) \\ & + b^2 ln\left(2 - \frac{4y_{mid}+L}{2b}\right) + b\left(\frac{4y_{mid}+L}{4}\right) ln\left(2 - \frac{4y_{mid}+L}{2b}\right) \\ & + b\left(\frac{4y_{mid}-L}{4}\right) ln\left(\frac{4y_{mid}-L}{2b}\right)\Bigg] \end{aligned} \qquad \text{Eq. C-47}$$

$$\frac{dS_R}{db} = \frac{2}{Lh}\sqrt{\frac{k_z}{k_y}}\Bigg[-b^{-2}[0.017125L^3 + 0.008563(4y_{mid} + L)^3$$

$$- 0.017125(4y_{mid} - L)^3]$$

$$+ \left\{\left[-0.0725L - 0.5Lln\left(\frac{L}{2}\right) + 0.10075(4y_{mid} + L)\right.\right.$$

$$\left.+ 0.03625(4y_{mid} - L)\right]$$

$$\left.+ \frac{h}{2}\sqrt{\frac{k_y}{k_z}}\left[ln\frac{h}{r_w} + 0.25ln\frac{k_x}{k_z} - ln\left(sin\frac{180°z}{h}\right) - 1.84\right]\right\}$$

$$+ 2b\left[\frac{1.096y_{mid}}{L} - 0.129\right] + \frac{L}{2} + \frac{L}{2}\ln(b)$$

$$+ 2bln\left(2 - \frac{4y_{mid} + L}{2b}\right) + \frac{(4y_{mid} + L)}{4 - \left(\frac{4y_{mid} + L}{b}\right)}$$

$$+ \frac{(L + 4y_{mid})^2}{8b\left(2 - \frac{L + 4y_{mid}}{2b}\right)} + 0.25(4y_{mid} + L)ln\left(2 - \frac{4y_{mid} + L}{2b}\right)$$

$$+ \frac{1}{4}(L - 4y_{mid})\ln(b)$$

$$\left.+ \frac{1}{4}(L - 4y_{mid})\big(1 + \ln(2) - \ln(4y_{mid} - L)\big)\right]\Bigg]$$

Eq. C-48

Case 2:

$$b\Big/\sqrt{k_y} > 1.33a\Big/\sqrt{k_x} \geq h\Big/\sqrt{k_z}$$

Eq. C-1

$$S_R = b\left\{\frac{1}{L}\left[ln\frac{h}{r_w} + 0.25ln\frac{k_x}{k_z} - ln\left(sin\frac{180°z}{h}\right) - 1.84\right]\right\}$$
$$- \left[ln\frac{h}{r_w} + 0.25ln\frac{k_x}{k_z} - ln\left(sin\frac{180°z}{h}\right) - 1.84\right]$$
$$+ \beta_1\left[\left(\frac{L^2 + 24{y_{mid}}^2}{24}\right) - b\left(\frac{L + 8y_{mid}}{8}\right) + \frac{b^2}{3}\right]$$
$$+ b\left(\frac{6.28a}{hL}\sqrt{\frac{k_z}{k_x}}\right)\left(\frac{1}{3} - \frac{x_0}{a} + \frac{x_0^2}{a^2}\right)$$
$$- \left(\frac{6.28a}{h}\sqrt{\frac{k_z}{k_x}}\right)\left(\frac{1}{3} - \frac{x_0}{a} + \frac{x_0^2}{a^2}\right)$$

Eq. C-49

$$\frac{dS_R}{db} = \frac{1}{L}\left[ln\frac{h}{r_w} + 0.25ln\frac{k_x}{k_z} - ln\left(sin\frac{180°z}{h}\right) - 1.84\right]$$
$$+ \left(\frac{6.28}{ah}\frac{\sqrt{k_x k_z}}{k_y}\right)\left[-\left(\frac{L + 8y_{mid}}{8}\right) + \frac{2b}{3}\right]$$
$$+ \left(\frac{6.28a}{hL}\sqrt{\frac{k_z}{k_x}}\right)\left(\frac{1}{3} - \frac{x_0}{a} + \frac{x_0^2}{a^2}\right)$$

Eq. C-50

APPENDIX D: DERIVATION OF b_{crit}

Using the results for each case obtained in Apendix B, we can now apply it for the productivity equation, which in oilfield units is:

$$q = \frac{\sqrt{k_H k_V}\, b(\bar{p} - p_{wf})}{141.2 B_o \mu \left\{ ln\left(\frac{\sqrt{A}}{r_w}\right) + ln(C_H) - 0.75 + S_R + s \right\}} \qquad \text{Eq. D-1}$$

The productivity is being addressed as a function of the reservoir length, b, in order to obtain the value of b that makes the derivative equal to zero. Since S_R is a function of b and it is, as it has been shown, different for each case, both cases will be addressed here as well.

$$q_{(b)} = \frac{\sqrt{k_H k_V}\, b(\bar{p} - p_{wf})}{141.2 B_o \mu \left\{ ln\left(\frac{\sqrt{A}}{r_w}\right) + ln(C_H) - 0.75 + S_{R(b)} + s \right\}} \qquad \text{Eq. D-2}$$

Let:

$$\beta_4 = \frac{\sqrt{k_H k_V}(\bar{p} - p_{wf})}{141.2 B_o \mu} \qquad \text{Eq. D-3}$$

$$\beta_5 = ln\left(\frac{\sqrt{A}}{r_w}\right) + ln(C_H) - 0.75 + s \qquad \text{Eq. D-4}$$

So we have:

$$q_{(b)} = \beta_4 \frac{b}{\{\beta_5 + S_{R(b)}\}} \qquad \text{Eq. D-5}$$

and:

$$\frac{dq_{(b)}}{db}\frac{1}{\beta_4} = \frac{\{\beta_5 + S_{R(b)} - bS'_{R(b)}\}}{\{\beta_5 + S_{R(b)}\}^2} \qquad \text{Eq. D-6}$$

Now I will attempt to obtain the root for the derivative of $q_{(b)}$, which will be named b_{crit} and should verify:

$$\beta_5 + S_{R(b_{crit})} - bS'_{R(b_{crit})} = 0 \qquad \text{Eq. D-7}$$

Since β_4 can't be zero, it is moved to the left term, the right term is the one that can be zero in order to obtain b_{crit}.

Analyzing first for **case 2**, when the wellbore's position is fixed and does not change with the reservoir's length, I rewrite the expressions for $S_{R(b)}$ and $S_{R\,(b)}$ 'obtained in Appendix B (equations C-23 and C-24) and then replace them in equation D-7:

$$\beta_5 - \beta_2 + \beta_1\left(\frac{L^2 + 24y_{mid}^2}{24}\right) - \beta_3 - b_{crit}^2\frac{\beta_1}{3} = 0 \qquad \text{Eq. D-8}$$

Thus:

$$b_{crit} = \sqrt{\frac{3\left[\beta_5 - \beta_2 + \beta_1\left(\frac{L^2 + 24y_{mid}^2}{24}\right) - \beta_3\right]}{\beta_1}} \qquad \text{Eq. D-9}$$

Which turns out to be, replacing back the expressions C-9, C-5, C-14 and D-4 in equation D-9:

$$b_{crit} = SQRT\left\{\frac{3}{\frac{6.28}{ah}\frac{\sqrt{k_x k_z}}{k_y}}\left[\left[ln\left(\frac{\sqrt{A}}{r_w}\right) + ln(C_H) - 0.75 + s\right]\right.\right.$$
$$\left. - \left[ln\frac{h}{r_w} + 0.25ln\frac{k_x}{k_z} - ln\left(sin\frac{180°z}{h}\right) - 1.84\right]\right. \qquad \text{Eq.D-10}$$
$$\left.\left. + \frac{6.28}{ah}\frac{\sqrt{k_x k_z}}{k_y}\left(\frac{L^2 + 24y_{mid}^2}{24}\right) - \left(\frac{6.28a}{hL}\sqrt{\frac{k_z}{k_x}}\right)\left(\frac{1}{3} - \frac{x_0}{a} + \frac{x_0^2}{a^2}\right)\right]\right\}$$

Equation D-10 shows the analytical expression for b_{crit} for the case 2 when y_{mid} is kept fixed as the reservoir's length increases.

Now, again for case 2, but for the case when the position of the wellbore is always centered, the procedure is the same as before, in equation D-8 we replace y_{mid} with $b_{crit}/2$, and we obtain:

$$\beta_5 - \beta_2 + \frac{\beta_1 L^2}{24} - \beta_3 - b_{crit}^2 \frac{\beta_1}{12} = 0 \qquad \text{Eq.D-11}$$

So:

$$b_{crit} = \sqrt{\frac{12\left(\beta_5 - \beta_2 + \frac{\beta_1 L^2}{24} - \beta_3\right)}{\beta_1}} \qquad \text{Eq.D-12}$$

Replacing back the expressions C-9, C-5, C-14 and D-4 in equation D-12 we obtain:

$$b_{crit} = SQRT\left\{\frac{12}{\frac{6.28}{ah}\frac{\sqrt{k_x k_z}}{k_y}}\left(ln\left(\frac{\sqrt{A}}{r_w}\right) + ln(C_H) - 0.75 + s - \left[ln\frac{h}{r_w} + 0.25ln\frac{k_x}{k_z} - ln\left(sin\frac{180°z}{h}\right) - 1.84\right] + \frac{\beta_1 L^2}{24} - \beta_3\right)\right\} \qquad \text{Eq.D-13}$$

Equation D-13 shows the analytical expression for b_{crit} for the case 2 when y_{mid} is kept in the center of the reservoir.

Analyzing now for the case 1, again, the procedure is the same, I will rewrite the expressions for $S_{R(b)}$ and $S_{R\,(b)}$ ' previously obtained (equations C-44 and C-45) for the case when the wellbore's position is fixed and does not change with the reservoir's length and then replace them in equation D-6:

$$S_R = \beta_6 \left[b^{-1}\beta_7 + \beta_8 - \frac{\beta_2}{\beta_6} + b\left(\beta_9 + \frac{\beta_2}{L\beta_6}\right) + b^2\beta_{10} + b\frac{L}{2}\ln(b) \right.$$
$$+ b^2\left(1 - \frac{4y_{mid} + L}{4b}\right) ln\left(2 - \frac{4y_{mid} + L}{2b}\right) \qquad \text{Eq.C-44}$$
$$\left. + b\left(\frac{4y_{mid} - L}{4}\right) ln\left(\frac{4y_{mid} - L}{2b}\right)\right]$$

$$\frac{dS_R}{db} = \beta_6 \left\{ -b^{-2}\beta_7 + \beta_9 + \frac{\beta_2}{L\beta_6} + 2b\beta_{10} + \frac{L}{2} + \frac{L}{2}\ln(b) \right.$$
$$+ \frac{1}{4}\left[(8b - L - 4y_{mid}) ln\left(2 - \frac{4y_{mid} + L}{2b}\right)\right]$$
$$+ b\left(\frac{4y_{mid} - L}{4}\right) ln\left(\frac{4y_{mid} - L}{2b}\right) + L + 4y_{mid} \qquad \text{Eq.C-45}$$
$$\left. + \left(y_{mid} - \frac{L}{4}\right)\left[ln\left(\frac{4y_{mid} - L}{2b}\right) - 1\right]\right\}$$

$$\frac{dq_{(b)}}{db}\frac{1}{\beta_4} = \left\{ \beta_5 + \beta_6 \left[b^{-1}\beta_7 + \beta_8 - \frac{\beta_2}{\beta_6} + b\left(\beta_9 + \frac{\beta_2}{L\beta_6}\right) + b^2\beta_{10} + b\frac{L}{2}\ln(b) \right.\right.$$
$$+ b^2\left(1 - \frac{4y_{mid} + L}{4b}\right) ln\left(2 - \frac{4y_{mid} + L}{2b}\right)$$
$$\left. + b\left(\frac{4y_{mid} - L}{4}\right) ln\left(\frac{4y_{mid} - L}{2b}\right)\right]$$
$$- b\beta_6 \left\{ -b^{-2}\beta_7 + \beta_9 + \frac{\beta_2}{L\beta_6} + 2b\beta_{10} + \frac{L}{2} + \frac{L}{2}\ln(b) \right. \qquad \text{Eq.D-14}$$
$$+ \frac{1}{4}\left[(8b - L - 4y_{mid}) ln\left(2 - \frac{4y_{mid} + L}{2b}\right)\right]$$
$$+ b\left(\frac{4y_{mid} - L}{4}\right) ln\left(\frac{4y_{mid} - L}{2b}\right) + L + 4y_{mid}$$
$$\left.\left. + \left(y_{mid} - \frac{L}{4}\right)\left[ln\left(\frac{4y_{mid} - L}{2b}\right) - 1\right]\right\}\right\} \frac{1}{\left\{\beta_5 + S_{R(b)}\right\}^2}$$

Again, it is necessary to solve for the numerator to obtain b_{crit}:

$$2\beta_7 b_{crit}^{-1} + (\beta_8 - \beta_2 + \beta_5) + b_{crit}\left(\frac{\beta_2}{L} - \frac{\beta_2}{L\beta_6} - \frac{3L}{2} - 4y_{mid}\right)$$
$$- b_{crit}^2\beta_{10}$$
$$+ b_{crit}^2\left(1 - \frac{4y_{mid} + L}{4b_{crit}}\right) ln\left(2 - \frac{4y_{mid} + L}{2b_{crit}}\right)$$
$$+ b_{crit}\left(\frac{4y_{mid} - L}{4}\right) ln\left(\frac{4y_{mid} - L}{2b_{crit}}\right)$$
$$- \frac{b_{crit}}{4}\left[(8b_{crit} - L - 4y_{mid}) ln\left(2\right.\right.$$
$$\left.\left. - \frac{4y_{mid} + L}{2b_{crit}}\right)\right]$$
$$- b_{crit}^2\left(\frac{4y_{mid} - L}{4}\right) ln\left(\frac{4y_{mid} - L}{2b_{crit}}\right)$$
$$- b_{crit}\left(\frac{4y_{mid} - L}{4}\right)\left[ln\left(\frac{4y_{mid} - L}{2b_{crit}}\right) - 1\right] = 0$$

Eq.D-15

Equation D-15 was attempted to be solved using Wolfram Alpha and Mathematica, but this software could not obtain an explicit analytical solution.

Finally, for the case 1 when the wellbore is kept in the middle of the reservoir, we repeat the previous procedure replacing y_{mid} with $b_{crit}/2$, and obtain:

$$\beta_5 + b_{crit}\frac{\beta_2}{L} - \beta_2$$
$$+ \beta_6\left[b_{crit}^{-1}\beta_7 + \beta_8 + b_{crit}\beta_9 + b_{crit}^2\beta_{10} + b_{crit}\frac{L}{2}\ln(b_{crit})\right.$$
$$+ b_{crit}^2\left(\frac{1}{2} - \frac{L}{4b_{crit}}\right)ln\left(1 - \frac{L}{2b_{crit}}\right)$$
$$\left.+ b\left(\frac{2b_{crit} - L}{4}\right)ln\left(1 - \frac{L}{2b_{crit}}\right)\right] \qquad \text{Eq.D-16}$$
$$- b_{crit}\left\{\frac{\beta_2}{L}\right.$$
$$+ \beta_6\left[-b_{crit}^{-2}\beta_7 + \beta_9 + 2b_{crit}\beta_{10} + \frac{L}{2}\ln(b_{crit})\right.$$
$$\left.\left.+ \left(2b_{crit} - \frac{L}{2}\right)ln\left(1 - \frac{L}{2b_{crit}}\right) + L\right]\right\} = 0$$

Rearranging:

$$b_{crit}^{-1}(2\beta_6\beta_7) + (\beta_5 - \beta_2 + \beta_6\beta_8) + b_{crit}(-L\beta_6) + b_{crit}^2(-\beta_6\beta_{10})$$
$$+ \frac{\beta_6 b_{crit}L}{2}\ln(b_{crit}) + b_{crit}^2\beta_6\left(\frac{1}{2} - \frac{L}{4b_{crit}}\right)ln\left(1 - \frac{L}{2b_{crit}}\right)$$
$$+ b_{crit}\left(\frac{2b_{crit} - L}{4}\right)ln\left(1 - \frac{L}{2b_{crit}}\right) - \frac{b_{crit}L}{2}\ln(b_{crit}) \qquad \text{Eq.D-17}$$
$$- b_{crit}\beta_6\left(2b_{crit} - \frac{L}{2}\right)ln\left(1 - \frac{L}{2b_{crit}}\right) = 0$$

Again, equation D-17 was attempted to be solved using Wolfram Alpha and Mathematica, but this software could not obtain an explicit analytical solution.

APPENDIX E: ANALYSIS OF F FUNCTION

In this Appendix an analysis of $F_{(x)}$ function, introduced by Babu & Odeh in their model, is presented, the conclusions are applied to the analytical analysis of the partial penetration skin factor.

The function F(x) is defined in Babu and Odeh's model as follows:

$$F(x) = \begin{cases} -x[0.145 + ln(x) - 0.137x^2] & if\ \ x \leq 1 \\ (2-x)[0.145 + ln(2-x) - 0.137(2-x)^2] & if\ \ x > 1 \end{cases} \qquad \text{Eq. E-1}$$

We can see that this function appears three times in the equation B-28. The first time with an argument that is always smaller than one, but the other two cases similar conclusions are not straight forward, and the formula is even presented in a way that may lead us to believe that either (argument bigger or smaller than 1) can happen indistinctively for each case.

We will assume that the following geometric restriction applies, since it is required by the authors for the model to remain accurate:

$$L > 0.7b \qquad \text{Eq. E-2}$$

Now, when we have:

$$\frac{4y_{mid} + L}{2b} \qquad \text{Eq. E-3}$$

We know that:

$$0.35b < y_{mid} < 0.65b \quad and \quad 0.7b < L < b \qquad \text{Eq. E-4}$$

The minimum and maximum values for y_{mid} occur when L=0.7b and the wellbore is located on the ends of the reservoir.

This argument will be minimum when L=0.7b and y_{mid}=0.35b, and it will yield:

$$\frac{4 * 0.35 * b + 0.7b}{2b} = 1.05 \qquad \text{Eq. E-5}$$

We can see then that

$$\frac{4y_{mid} + L}{2b} > 1 \qquad \text{Eq. E-6}$$

So:

$$F\left(\frac{4y_{mid} + L}{2b}\right) = \left(2 - \left(\frac{4y_{mid} + L}{2b}\right)\right)\left[0.145 + ln\left(2 - \left(\frac{4y_{mid} + L}{2b}\right)\right) - 0.137\left(2 - \left(\frac{4y_{mid} + L}{2b}\right)\right)^2\right] \qquad \text{Eq. E-7}$$

A similar analysis can be done for the other argument, which is:

$$\frac{4y_{mid} - L}{2b} \qquad \text{Eq. E-8}$$

In this case, we will look for its maximum value, which will be obtained when y_{mid} is maximum and L minimum, thus:

$$\frac{4 * 0.65 * b - 0.7b}{2b} = 0.95 \qquad \text{Eq. E-9}$$

And it can be seen then that:

$$\frac{4y_{mid} - L}{2b} < 1 \qquad \text{Eq. E-10}$$

So:

$$F\left(\frac{4y_{mid} - L}{2b}\right) = -\left(\frac{4y_{mid} - L}{2b}\right)\left[0.145 + ln\left(\frac{4y_{mid} - L}{2b}\right) - 0.137\left(\frac{4y_{mid} - L}{2b}\right)^2\right] \qquad \text{Eq. E-11}$$

With the results obtained in equations E-7 and E-11, we can now proceed to analyze P'_{xy}, in order to do so, first the results for each of the 3 "F" functions involved will be analyzed:

$$F\left(\frac{L}{2b}\right) = -\left(\frac{L}{2b}\right)\left[0.145 + ln\left(\frac{L}{2b}\right) - 0.137\left(\frac{L}{2b}\right)^2\right] \quad \text{Eq. E-12}$$

$$F\left(\frac{L}{2b}\right) = 0.137\left(\frac{L}{2}\right)^3 b^{-3} - b^{-1}\frac{L}{2}\left[0.145 + \ln\left(\frac{L}{2}\right)\right] + \frac{L}{2}b^{-1}\ln(b) \quad \text{Eq. E-13}$$

$$F\left(\frac{4y_{mid}+L}{2b}\right) = \left(2 - \left(\frac{4y_{mid}+L}{2b}\right)\right)\left[0.145 + ln\left(2 - \left(\frac{4y_{mid}+L}{2b}\right)\right) - 0.137\left(2 - \left(\frac{4y_{mid}+L}{2b}\right)\right)^2\right] \quad \text{Eq. E-14}$$

$$F\left(\frac{4y_{mid}+L}{2b}\right) = 0.29 + 2ln\left(2 - \left(\frac{4y_{mid}+L}{2b}\right)\right) - 0.274\left(2 - \left(\frac{4y_{mid}+L}{2b}\right)\right)^2 - 0.145\left(\frac{4y_{mid}+L}{2b}\right) - \left(\frac{4y_{mid}+L}{2b}\right) ln\left(2 - \frac{4y_{mid}+L}{2b}\right) + 0.137\left(\frac{4y_{mid}+L}{2b}\right)\left(2 - \left(\frac{4y_{mid}+L}{2b}\right)\right)^2 \quad \text{Eq. E-15}$$

$$F\left(\frac{4y_{mid}+L}{2b}\right) = 0.29 + 2ln\left(2-\left(\frac{4y_{mid}+L}{2b}\right)\right) - 0.274\left[4-\left(\frac{8y_{mid}+2L}{b}\right)+\frac{(4y+L)^2}{4b^2}\right] - 0.145\left(\frac{4y_{mid}+L}{2b}\right)-\left(\frac{4y_{mid}+L}{2b}\right)ln\left(2-\frac{4y_{mid}+L}{2b}\right) + 0.137\left(\frac{4y_{mid}+L}{2b}\right)\left[4-\left(\frac{8y_{mid}+2L}{b}\right)+\frac{(4y+L)^2}{4b^2}\right]$$ Eq. E-16

$$F\left(\frac{4y_{mid}+L}{2b}\right) = 0.29 + 2ln\left(2-\left(\frac{4y_{mid}+L}{2b}\right)\right) - 1.096 + 0.274\frac{(8y_{mid}+2L)}{L} - 0.274\frac{(4y_{mid}+L)^2}{4b^2} - 0.145\left(\frac{4y_{mid}+L}{2b}\right) - \left(\frac{4y_{mid}+L}{2b}\right)ln\left(2-\frac{4y_{mid}+L}{2b}\right) + 0.548\left(\frac{4y_{mid}+L}{2b}\right) - 0.137\frac{(4y_{mid}+L)^2}{b^2} + 0.137\frac{(4y_{mid}+L)^3}{8b^3}$$ Eq. E-17

$$F\left(\frac{4y_{mid}+L}{2b}\right) = b^{-3}0.017125(4y_{mid}+L)^3 - b^{-2}0.2055(4y_{mid}+L)^2 + b^{-1}0.2015(4y_{mid}+L) + \left(\frac{2.192y_{mid}}{L}-0.258\right) + \left(2-\frac{4y_{mid}+L}{2b}\right)ln\left(2-\frac{4y_{mid}+L}{2b}\right)$$ Eq. E-18

$$F\left(\frac{4y_{mid}-L}{2b}\right)=-\left(\frac{4y_{mid}-L}{2b}\right)\left[0.145+ln\left(\frac{4y_{mid}-L}{2b}\right)-0.137\left(\frac{4y_{mid}-L}{2b}\right)^{2}\right] \quad \text{Eq. E-19}$$

$$F\left(\frac{4y_{mid}-L}{2b}\right)=b^{-3}0.03425(4y_{mid}-L)^{3}-b^{-1}0.0725(4y_{mid}-L)-\left(\frac{4y_{mid}-L}{2b}\right)ln\left(\frac{4y_{mid}-L}{2b}\right) \quad \text{Eq. E-20}$$

Eq. E-18 and Eq E-20 are a valuable result, for they enable the analysis of S_R (Appendix B) to be reduced to 4 cases, for if the F function could take different expressions, more cases should be considered.

APPENDIX F: ECLIPSE DECK FILE

In this Appendix the keywords which were used in the deck files for Eclipse will be described.

To run the Eclipse simulations in this work I have used Eclipse 100, which corresponds to deal oil simulations.

The explanation for each keyword is taken from Eclipse's manual, and they are listed in the order in which they appear on the deck file, and they are grouped according to the different sections in the deck file

RUNSPEC

- DIMENS: this keyword defines the basic size of the simulation grid. It is followed by three integers, specifying the number of cells in the x, y and z directions respectively.
- FIELD: indicates that field units are to be used.
- OIL: indicates that a run contains an oil phase.
- START: specifies the date in which the simulation starts running.
- WELLDIMS: this keyword may include many items, in this case, it indicates the maximum number of wells (1), the maximum number of connections per well (80), the maximum number of groups in the model (1) and the maximum number of wells in any one group (1).
- UNIFOUT: unifies reports in one single file.

GRID

- GRIDFILE: controls the grid file outputs, in this case the integer 2 indicates that the GRID file produced contains extended data, and by default, an extensible file (EGRID) is generated as well.
- DXV, DYV: This two keywords indicate the number of divisions in the X and Y directions, and their length.
- DZ: this keyword specifies the size of the cells in the Z-direction.
- TOPS: specifies the depth at the top of the gridblock.
- EQUALS: is used to specify the porosity and permeabilities along the reservoir.
- INIT: generates a file with reported input data.

PROPS

- PVCDO: dead oil properties with constant compressibility, includes the reference pressure (3800), the oil formation volume factor (1.1), the oil compressibility (1.6e-5), oil viscosity (1.05) and oil viscosibility.
- GRAVITY: oil API gravity, water specific gravity and gas gravity.
- ROCK: reference pressure and rock compressibility.

SOLUTION

- EQUIL: sets the contacts and pressures for conventional hydrostatic equilibrium, includes datum depth, pressure at such depth, contact depth, capillary pressure at contact (ignored for single phase), depth of gas-oil contact (ignored for single phase), gas-oil capillary pressure at the gas-oil contact (ignored for single phase),

integer that affects gas concentration in undersaturated oil (ignored for dead oil), integer ignored for deal oil.

- DATUM: indicates the datum depth.
- RPTSOL: output of initial grid block pressures (POIL), output of initial oil pressures (PRES), current fluids in place and phase potentials in each grid cell are written to the restart files (RESTART=2), initial fluids in place are reported for the whole field (FIP=1)

SUMMARY

- RUNSUM: requests that the data in the SUMMARY files should be tabulated in the print file at the end of the run.
- EXCEL: this keyword requests that the run summary output, generated by using the RUNSUM keyword, should be written in a format that can be easily imported into Excel.
- FOPR: field oil production rate.
- FPR: field average pressure.
- WBHP: wellbore pressure.

SCHEDULE

- WELSPECS: introduces a new well, defining its name (HorWell), group (WellGrp), I -location of the well head or heel, J – location of the well head or heel, reference depth for bottom hole pressure (7150), preferred phase (OIL), drainage radius for productivity index calculation (default = the pressure

equivalent radius of the grid blocks containing the well connections is used), flag for use of a special inflow equation (STD= standard inflow equation is used), instructions for automatic shut-in (STOP=stop well above formation), crossflow ability flag (YES = crossflow allowed in the well), pressure table number for wellbore fluid properties (default: pressure table number is set equal to the PVT region number of the lowest grid block in which the well is completed), type of density calculation for the wellbore hydrostatic head (SEG: segmented density calculation).

- COMPDAT: this keyword specifies the position and properties of one or more well completions, well name (HorWell), I – location of connecting grid block, J – location of connecting grid block, K – location of upper connecting block, K – location of lower connecting block, open/shut flag of connection (open to flow), saturation table number for connection relative permeabilities (default: relative permeabilities are calculated using the same saturation table as the grid block containing the connection), transmissibility factor for the connection (default: the connection transmissibility factor is calculated using the remaining items of data in this record), wellbore diameter at the connection, effective permeability times thickness value of the connection (default: calculated from grid block data), skin factor, D – factor for handling non Darcy flow of free gas (disregarded), direction in which the well penetrates the grid block (X direction).
- WCONPROD: well name (HorWell), open/shut flag for the well (open), control mode (BHP: controlled by wellbore pressure), oil rate target or upper limit

(default: no target or limit), water rate target or upper limit (default: no target or limit), gas rate target or upper limit (default: no target or limit), liquid rate target or upper limit (default: no target or limit), reservoir fluid volume rate target or upper limit (default: no target or limit), BHP target or lower limit, THP target or lower limit (default: 0), production well VFP table number (default: no THP calculation are required), artificial lift quantity (default: 0).

- RPTSCHED: controls output from schedule section
- TSTEP: sets the number of time steps to run the simulation and the number of days in each time step.

Following, one sample deck file is provided:

RUNSPEC

TITLE

TEST HORIZONTAL WELL FOR THESIS

DIMENS

40 15 9

/

FIELD

OIL

START

1 'JAN' 1990 /

WELLDIMS

1   80   1   1 /

-- Unifies reports in one single file

UNIFOUT

--

--

GRID

GRIDFILE

2 /

DXV

* 5*30 30*100 5*30*

/

DYV

275 205 135 65 30 20 15 10 15 20 30 65 135 205 275

/

DZ

*600*22 600*22 600*14 600*12*

*600*10 600*12 600*14 600*22 600*22*

/

TOPS

*600*7000*

/

-- Overwrites some data provided by other sections.

EQUALS

'PORO' 0.25 /

'PERMX' 1 /

'PERMY' 5 /

'PERMZ' 1 /

/

-- Use to write a data file with reported inpu data

INIT

--

--

PROPS

PVCDO

3800 1.1 1.6e-5 1.05 0.0 /

GRAVITY

7.0000 1.00960 0.75000 /

ROCK

3214.70 0.40E-05 /

RPTPROPS

'PVTO' 'PVDO' 'DENSITY' 'GRAVITY' 'SDENSITY' 'TRACER'

/

SOLUTION

EQUIL

7150.00 20000.00 7200.00 0.00000 7100.00 0.00000 1 0 10 /

DATUM

7000.000 /

-- Initialisation Print Output

-- POIL = Initial Gridblock Pressures

-- PRES = Initial oil pressures

RPTSOL

'POIL' 'PRES' 'RESTART=2' 'FIP=1' /

--

SUMMARY

RUNSUM

EXCEL

FOPR

/

FPR

/

WBHP

/

--

--

SCHEDULE

WELSPECS

'HorWell ','WellGrp ', 6, 1,7150.00,'OIL'

1 ,'STD','STOP','YES',1* ,'SEG', /*

/

-- Well name, location of connecting gridblocks (x, y, upper connecting block in z, lower connecting block in z)

-- 'OPEN'

-- 5 connection relative permeabilities, default is calculated using tables provided

-- 1 transmissibility factor for the connection: default calculates using the remaining items in data on this record*

-- 1.0200 wellbore diameter at the connection

-- 1 default for permeability x thickness, calculated from grid block data*

-- 1 SKIN FACTOR*

-- 1 D factor for handling the effect of non Darcy flow.*

-- 'X' direction in which the well penetrates the grid block

COMPDAT

'HorWell ' 6 8 5 5 'OPEN' 1 1* 0.2500*

1 10 1* 'X' /*

'HorWell ' 7 8 5 5 'OPEN' 1 1* 0.2500*

1 10 1* 'X' /*

'HorWell ' 8 8 5 5 'OPEN' 1 1* 0.2500*

1 10 1* 'X' /*

'HorWell ' 9 8 5 5 'OPEN' 1 1* 0.2500*

1 10 1* 'X' /*

'HorWell ' 10 8 5 5 'OPEN' 1 1* 0.2500*

1 10 1* 'X' /*

'HorWell ' 11 8 5 5 'OPEN' 1 1* 0.2500*

1 10 1* 'X' /*

'HorWell ' 12 8 5 5 'OPEN' 1 1* 0.2500*

1 10 1* 'X' /*

'HorWell ' 13 8 5 5 'OPEN' 1 1* 0.2500*

1 10 1* 'X' /*

'HorWell ' 14 8 5 5 'OPEN' 1 1* 0.2500*

1 10 1* 'X' /*

'HorWell ' 15 8 5 5 'OPEN' 1 1* 0.2500*

1 10 1* 'X' /*

'HorWell ' 16 8 5 5 'OPEN' 1 1* 0.2500*

1 10 1* 'X' /*

'HorWell ' 17 8 5 5 'OPEN' 1 1* 0.2500*

1 10 1* 'X' /*

'HorWell ' 18 8 5 5 'OPEN' 1 1* 0.2500*

1 10 1* 'X' /*

'HorWell ' 19 8 5 5 'OPEN' 1 1* 0.2500*

1 10 1* 'X' /*

'HorWell ' 20 8 5 5 'OPEN' 1 1* 0.2500*

1 10 1* 'X' /*

'HorWell ' 21 8 5 5 'OPEN' 1 1* 0.2500*

1 10 1* 'X' /*

'HorWell ' 22 8 5 5 'OPEN' 1 1* 0.2500*

1 10 1* 'X' /*

'HorWell ' 23 8 5 5 'OPEN' 1 1* 0.2500*

1 10 1* 'X' /*

'HorWell ' 24 8 5 5 'OPEN' 1 1* 0.2500*

1 10 1* 'X' /*

'HorWell ' 25 8 5 5 'OPEN' 1 1* 0.2500*

1 10 1* 'X' /*

'HorWell ' 26 8 5 5 'OPEN' 1 1* 0.2500*

1 10 1* 'X' /*

'HorWell ' 27 8 5 5 'OPEN' 1 1* 0.2500*

1 10 1* 'X' /*

'HorWell ' 28 8 5 5 'OPEN' 1 1* 0.2500*

1 10 1* 'X' /*

'HorWell ' 29 8 5 5 'OPEN' 1 1* 0.2500*

1 10 1* 'X' /*

'HorWell ' 30 8 5 5 'OPEN' 1 1* 0.2500*

1 10 1* 'X' /*

'HorWell ' 31 8 5 5 'OPEN' 1 1* 0.2500*

1 10 1* 'X' /*

'HorWell ' 32 8 5 5 'OPEN' 1 1* 0.2500*

1 10 1* 'X' /*

'HorWell ' 33 8 5 5 'OPEN' 1 1* 0.2500*

1 10 1* 'X' /*

'HorWell ' 34 8 5 5 'OPEN' 1 1* 0.2500*

1 10 1* 'X' /*

'HorWell ' 35 8 5 5 'OPEN' 1 1* 0.2500*

1 10 1* 'X' /*

/

-- 'OPEN': well open for production

-- 'BHP': controlled by BHP target (other options could be ORAT for oil rate instead of BHP)

-- 1 oil rate target or upper limit. Default is no target limit*

-- 1 water rate target or upper limit. Default is no limit.*

-- 1 gas rate target or upper limit. Default is no limit.*

-- 1 liquid rate target or upper limit. Default is no limit.*

-- 2000 reservoir fluid volume rate target or upper limit.

-- 3000 BHP target or lower limit

*-- 1*THP target or lower limit*

-- 1 production well VFP table number. Default is 0*

-- Artificial lift quantity. Default is 0

WCONPROD

'HorWell ','OPEN','BHP' 1 1* 1**

1 1* 3000.000 1* 1* 1* /*

/

-- Controls the output of SCHEDULE section data to the print file

-- Restart=2 means restart files are created at every report time until this switch is reset, and all are kept

-- FIP=2 fluids in place are reported for the whole field and in addition, a balance sheet is produced for each fluid in place region. Shows cumulative flows to wells and other regions and material balance errors

-- WELLS= 1 gives a report of well flows

-- SEUMMARY=1 report is sent to print file

-- CPU=2 report is sent to print file and in addition a copy is sent to the short form output.

-- WELSPECS means output of connection, well and group keyboard data from the SCHEDULE section

-- NEWTON=1 Outpus of a summary of the convergence of the Newton iteration, report is sent to print file

RPTSCHED

'RESTART=2' 'FIP=1' 'WELLS=1' 'SUMMARY=1' 'CPU=2' 'WELSPECS' 'NEWTON=1'

/

-- The keyword should be followed by up to 1000 real numbers, each of which is a time interval through

-- which the simulator is to be advanced.

TSTEP

*1000*4*

/

END

APPENDIX G: BABU AND ODEH'S AND ECLIPSE'S RESULTS

In this Appendix, the plots for all scenarios comparing B&O's and Eclipse's results are provided. The input used for each scenario will not be provided for simplicity, but they can be obtained from table H.1, in Appendix H. In this plots, the scenarios will be labeled with their number.

On the left, the plots obtained using the lower drawdown will be displayed, on the right, their match with higher drawdown.

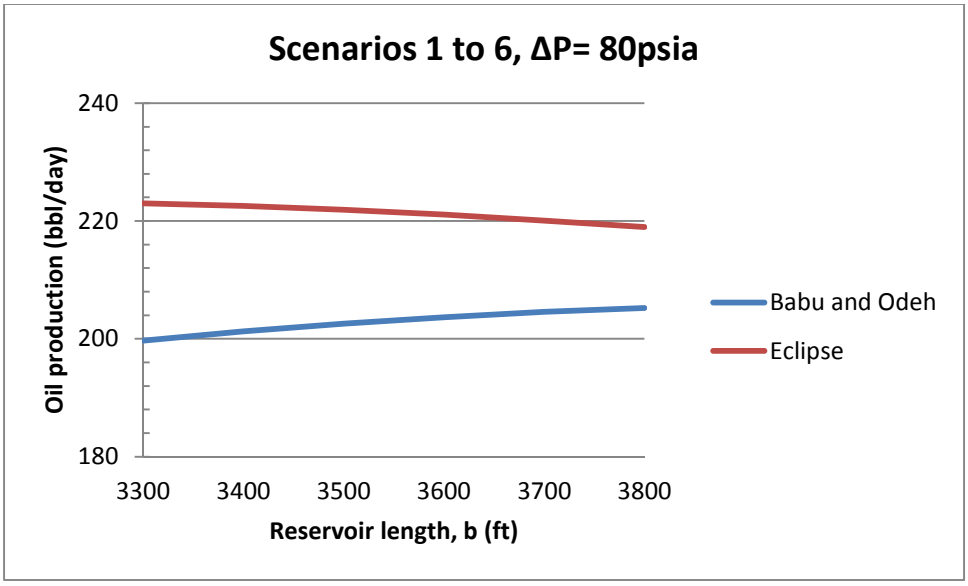

Figure G.1: Flow rates estimation for scenarios 1 to 6 with ΔP = 80 psi

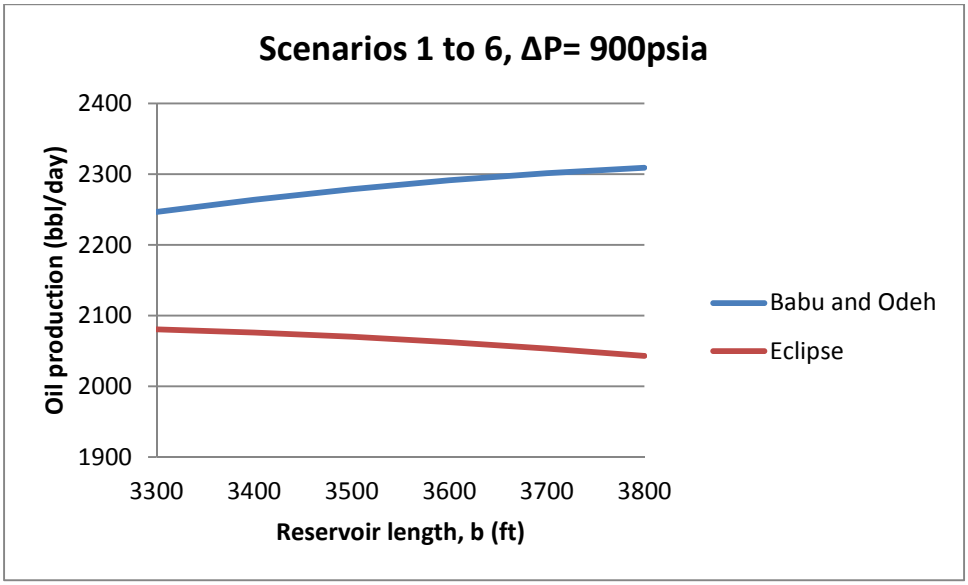

Figure G.2: Flow rates estimation for scenarios 1 to 6 with ΔP = 900 psi

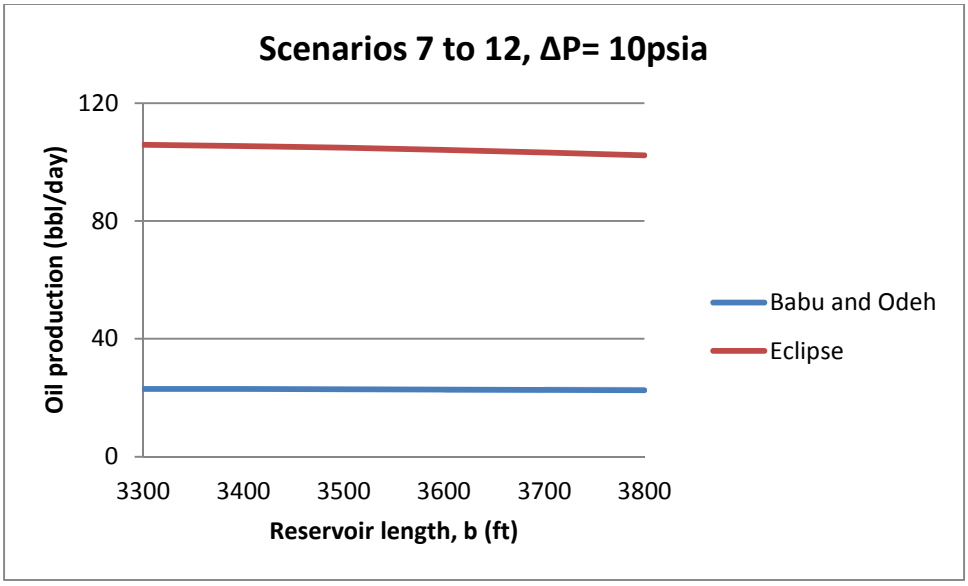

Figure G.3: Flow rates estimation for scenarios 7 to 12 with ΔP = 10 psi

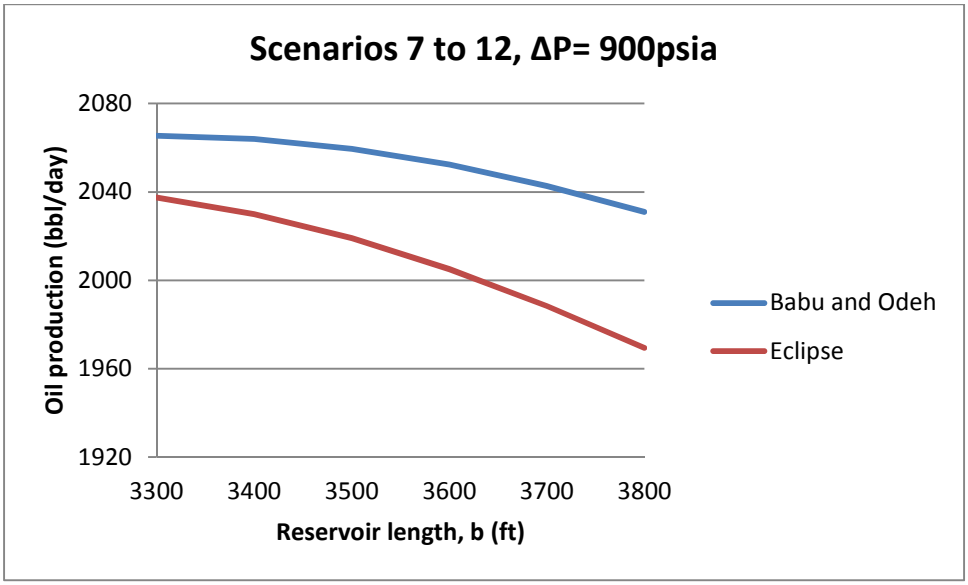

Figure G.4: Flow rates estimation for scenarios 7 to 12 with ΔP = 900 psi

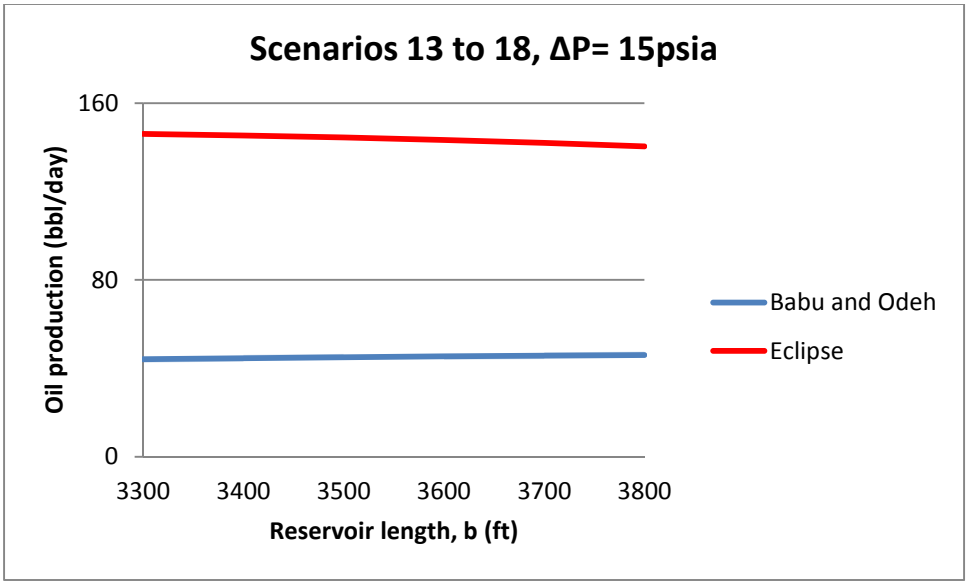

Figure G.5: Flow rates estimation for scenarios 13 to 18 with ΔP = 15 psi

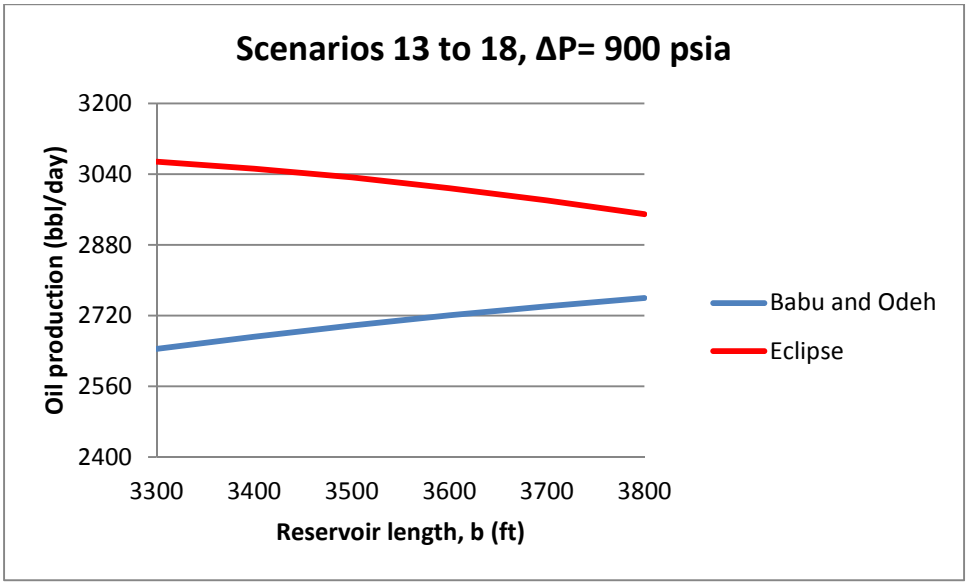

Figure G.6: Flow rates estimation for scenarios 13 to 18 with ΔP = 900 psi

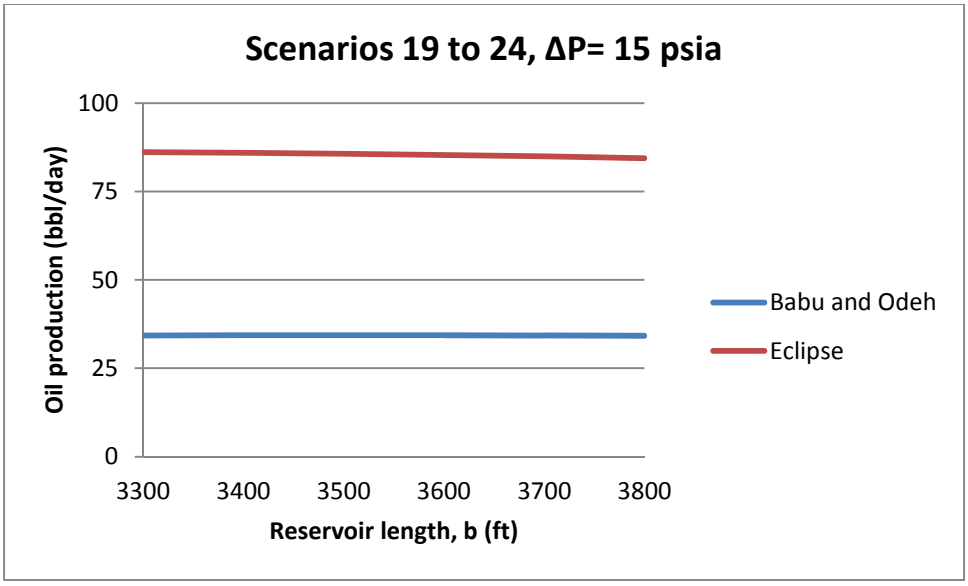

Figure G.7: Flow rates estimation for scenarios 19 to 24 with ΔP = 15 psi

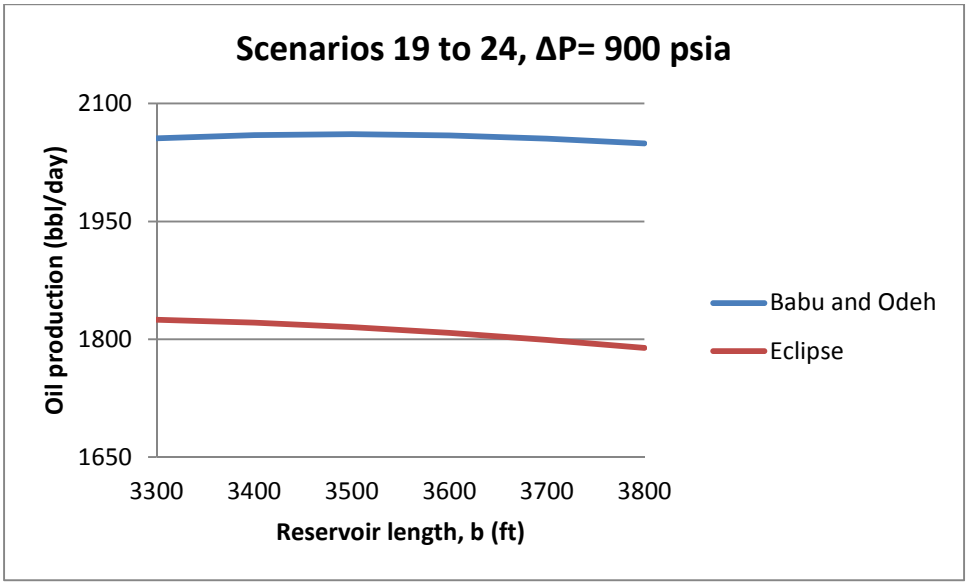

Figure G.8: Flow rates estimation for scenarios 19 to 24 with ΔP = 900 psi

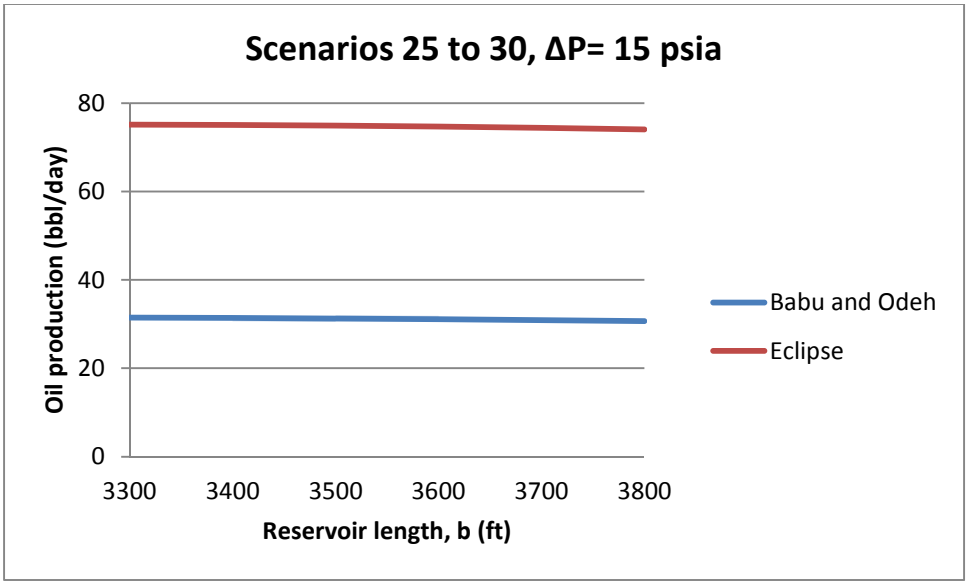

Figure G.9: Flow rates estimation for scenarios 25 to 30 with ΔP = 15 psi

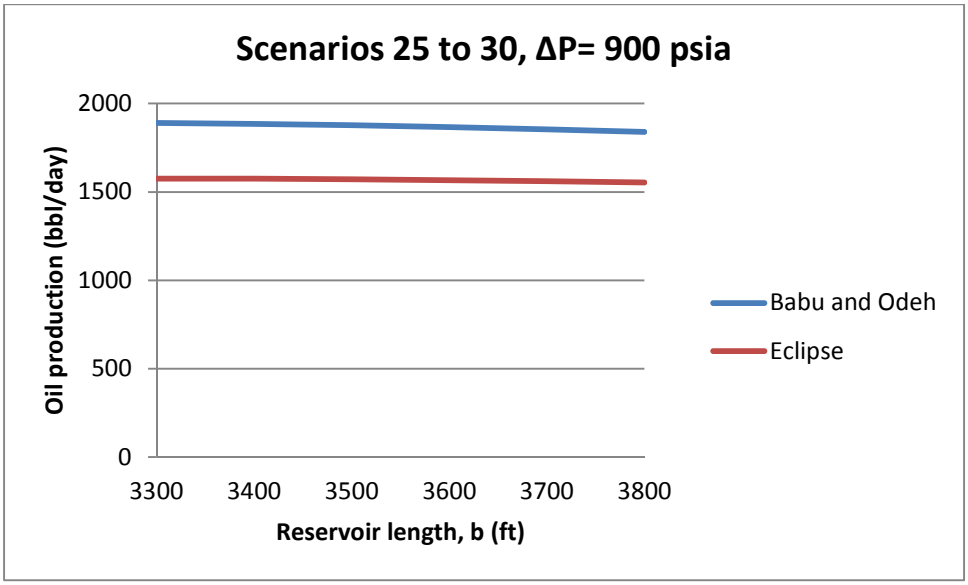

Figure G.10: Flow rates estimation for scenarios 25 to 30 with ΔP = 300 psi

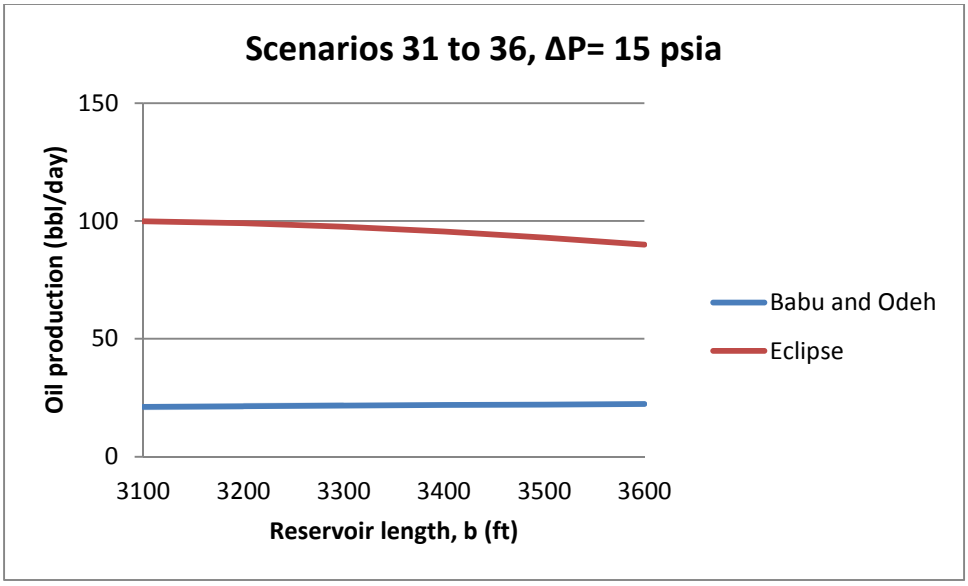

Figure G.11: Flow rates estimation for scenarios 31 to 36 with ΔP = 15 psi

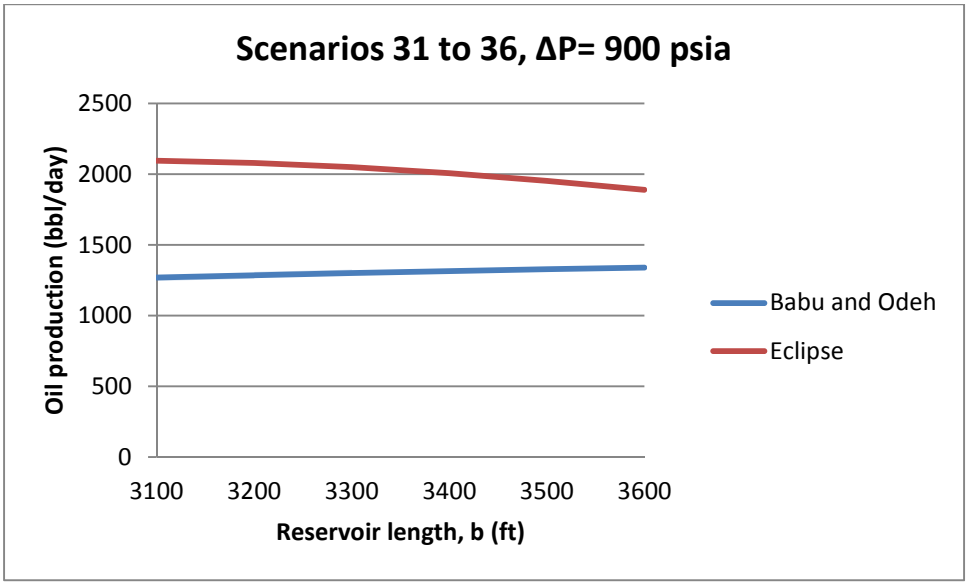

Figure G.12: Flow rates estimation for scenarios 31 to 36 with ΔP = 900 psi

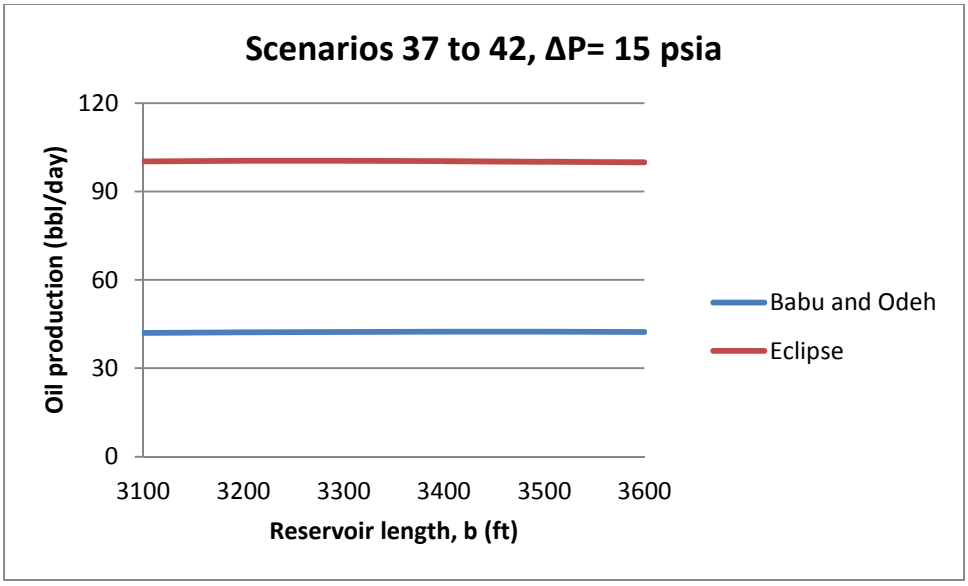

Figure G.13: Flow rates estimation for scenarios 73 to 42 with ΔP = 15 psi

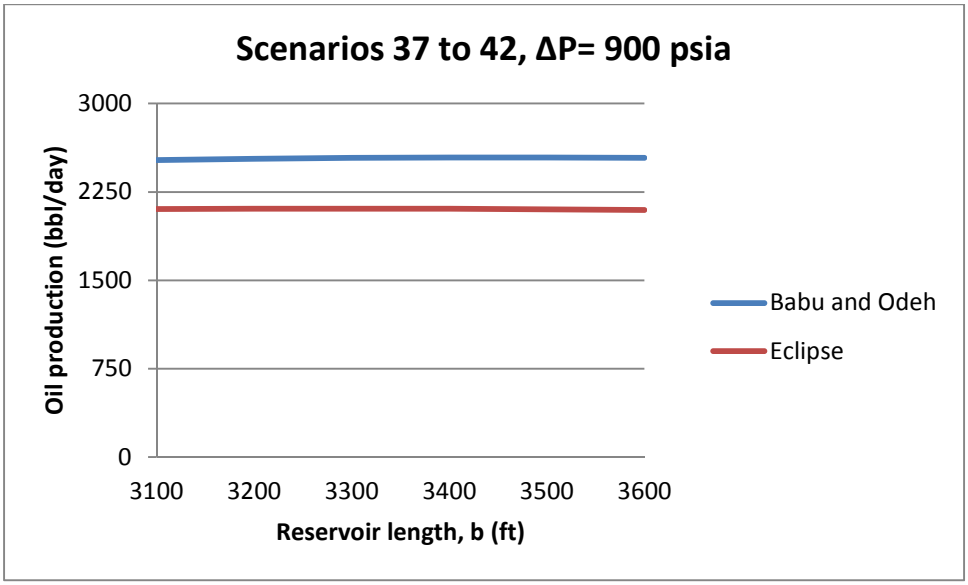

Figure G.14: Flow rates estimation for scenarios 37 to 42 with ΔP = 900 psi

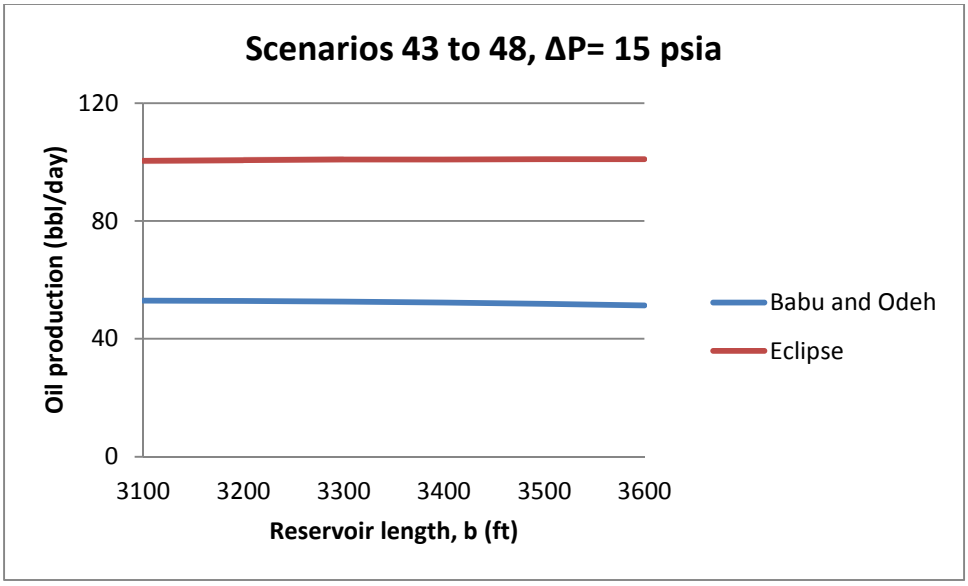

Figure G.15: Flow rates estimation for scenarios 43 to 48 with ΔP = 15 psi

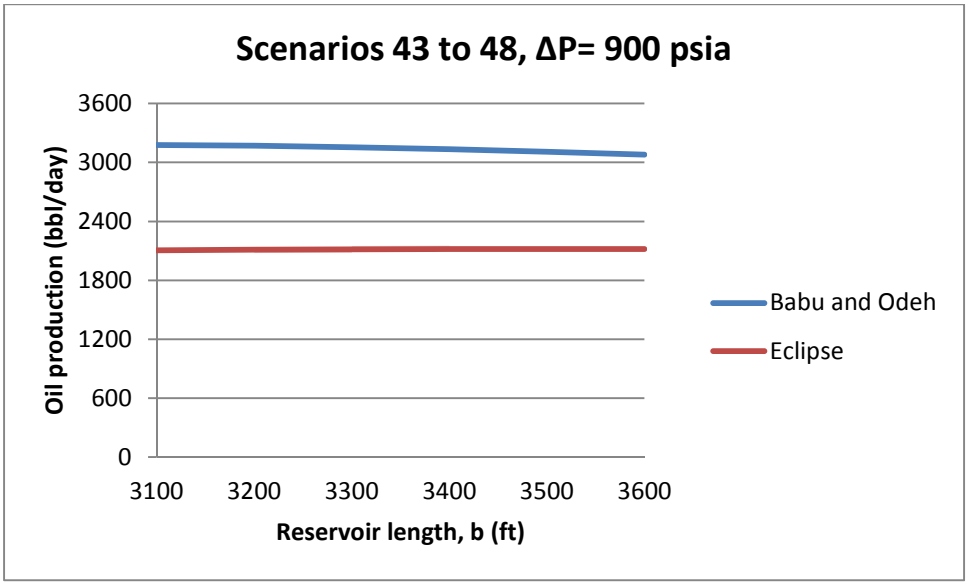

Figure G.16: Flow rates estimation for scenarios 43 to 48 with ΔP = 900 psi

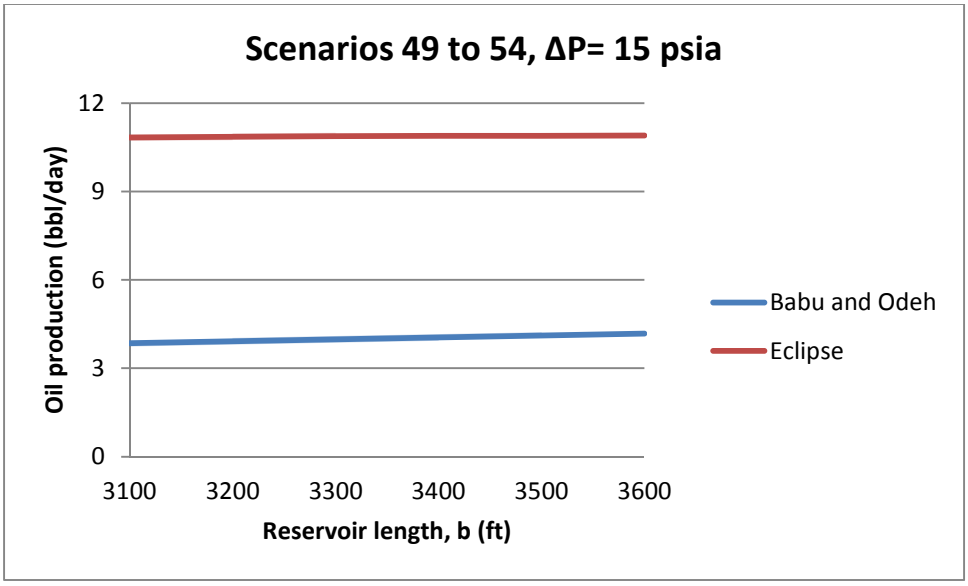

Figure G.17: Flow rates estimation for scenarios 49 to 54 with ΔP = 15 psi

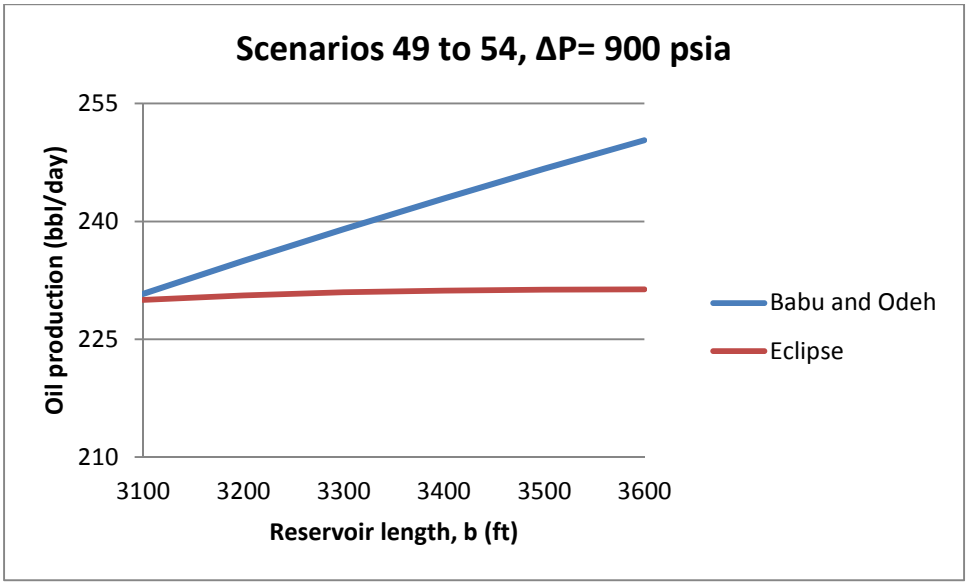

Figure G.18: Flow rates estimation for scenarios 49 to 54 with ΔP = 900 psi

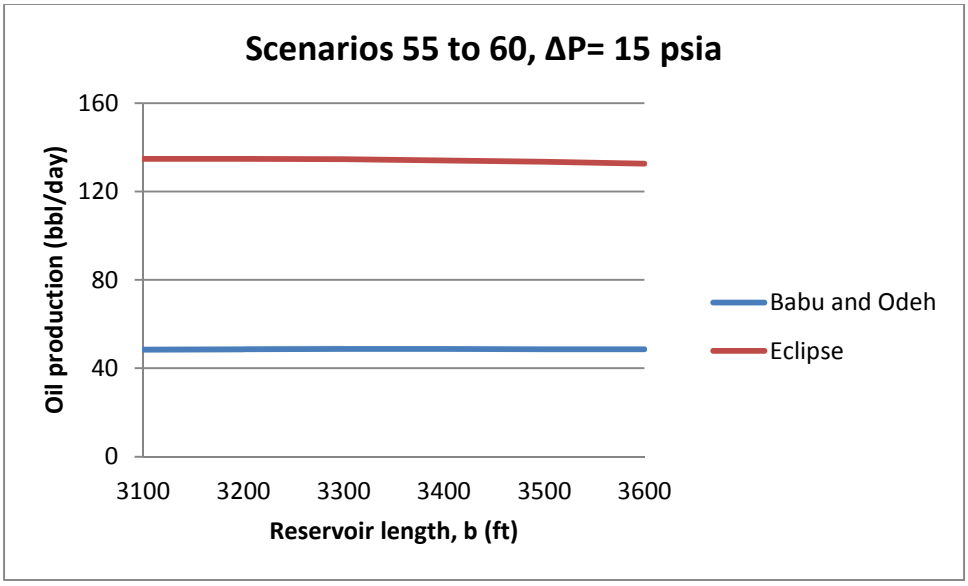

Figure G.19: Flow rates estimation for scenarios 55 to 60 with ΔP = 15 psi

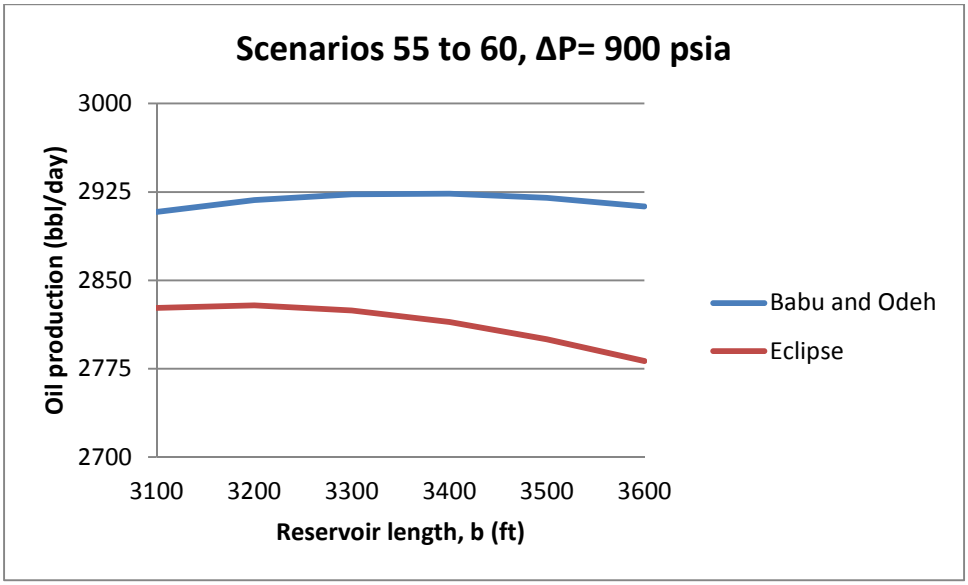

Figure G.20: Flow rates estimation for scenarios 55 to 60 with ΔP = 900 psi

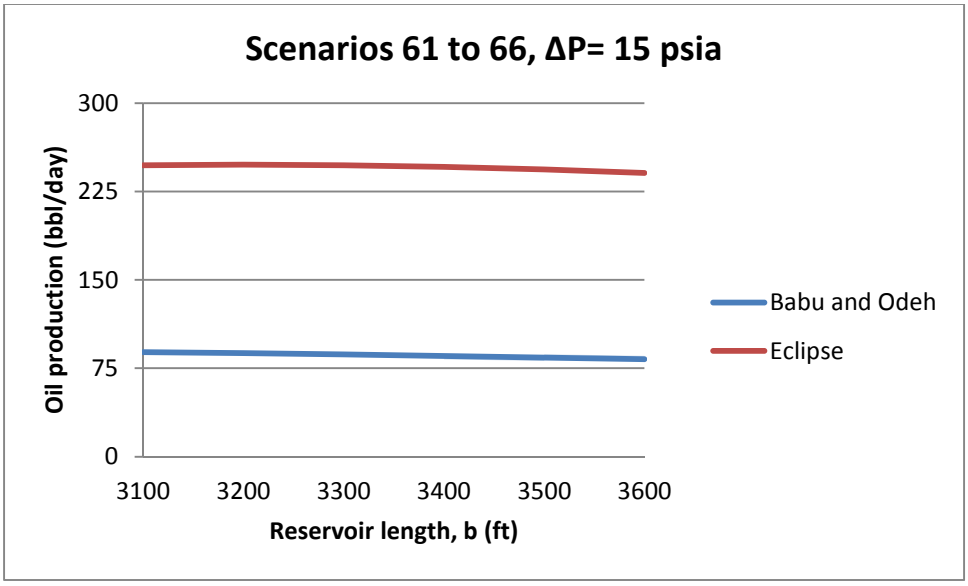

Figure G.21: Flow rates estimation for scenarios 61 to 66 with ΔP = 15 psi

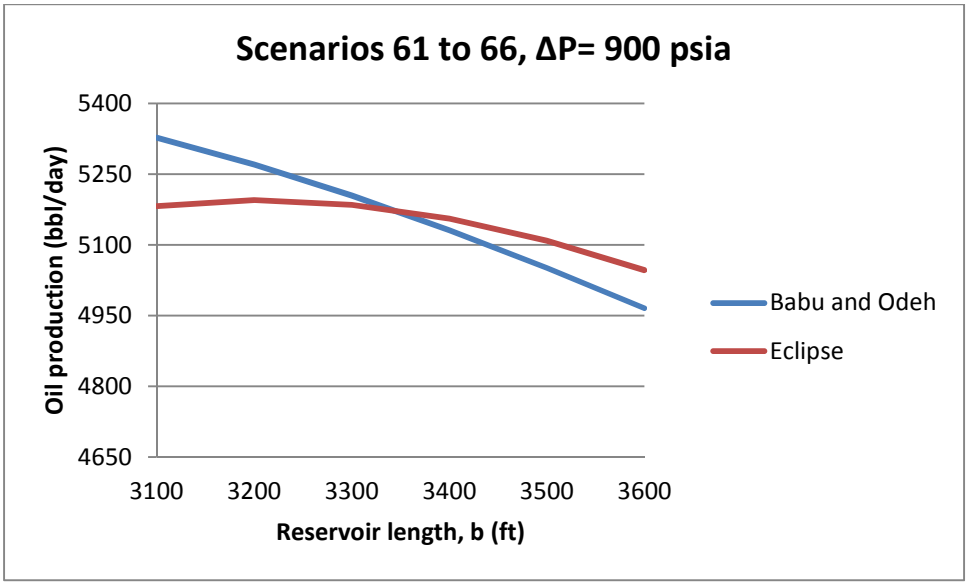

Figure G.22: Flow rates estimation for scenarios 61 to 66 with ΔP = 900 psi

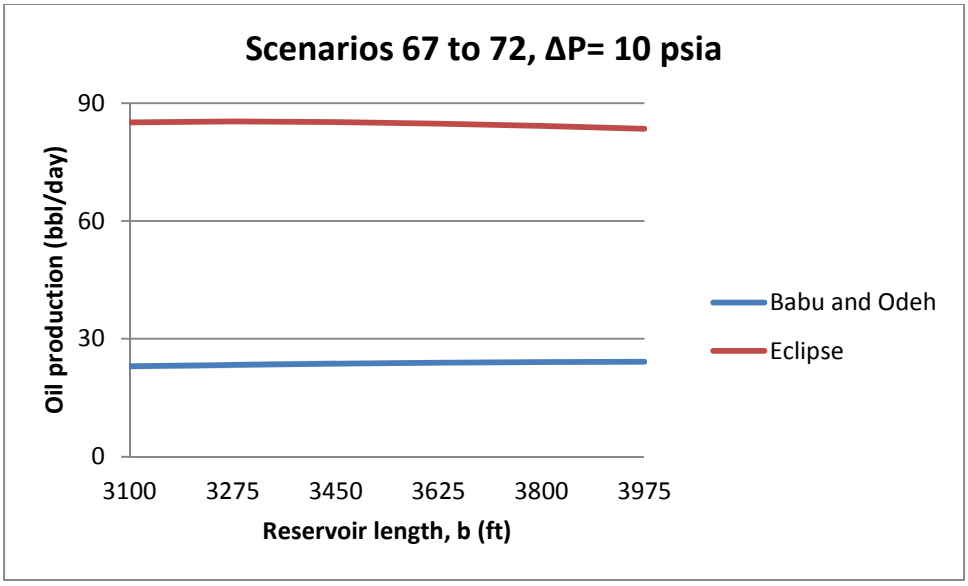

Figure G.23: Flow rates estimation for scenarios 67 to 72 with ΔP = 10 psi

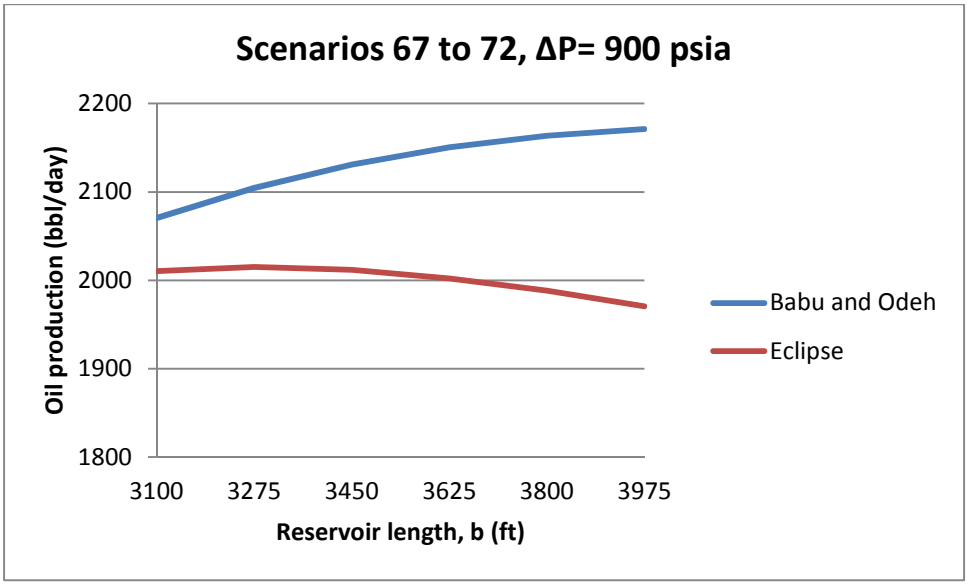

Figure G.24: Flow rates estimation for scenarios 67 to 72 with ΔP = 900 psi

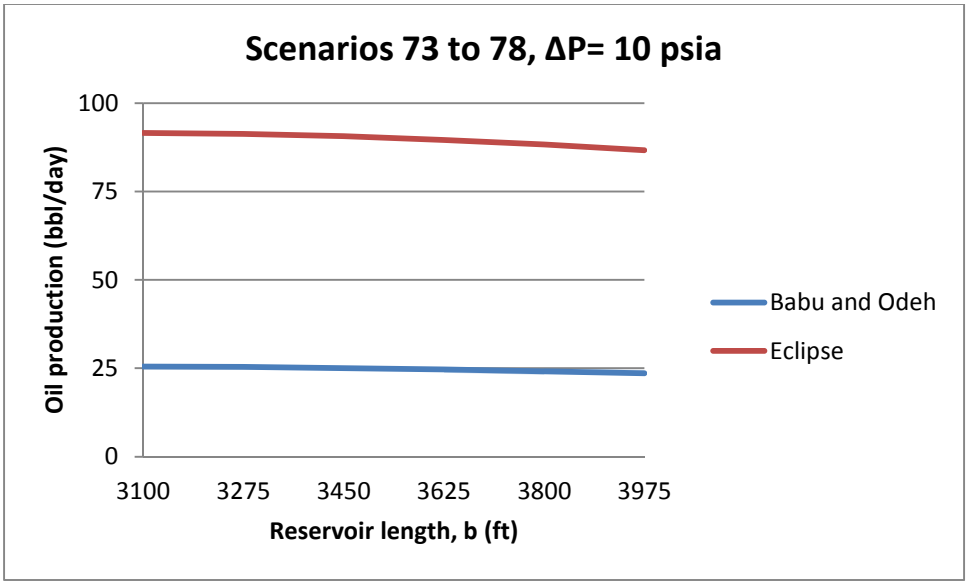

Figure G.25: Flow rates estimation for scenarios 73 to 78 with ΔP = 10 psi

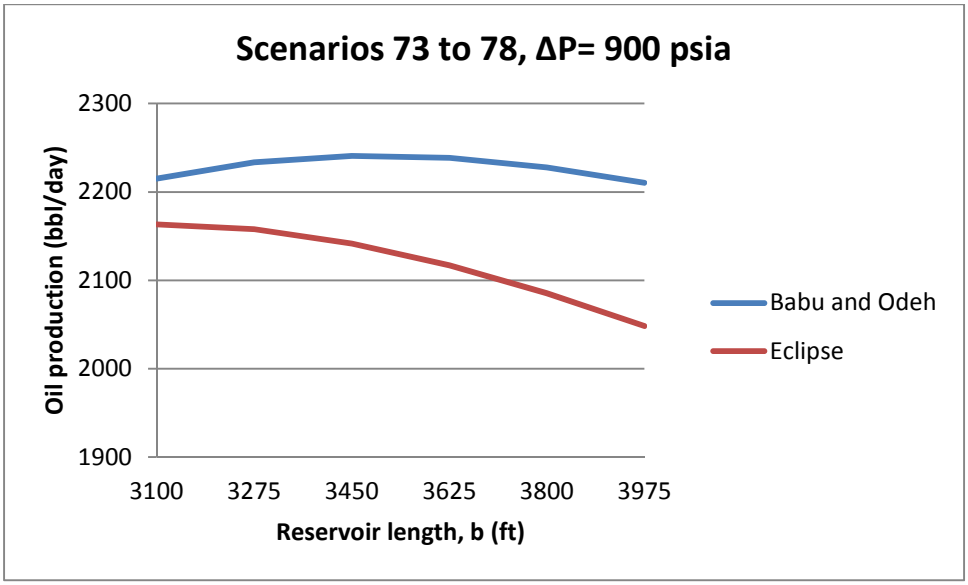

Figure G.26: Flow rates estimation for scenarios 73 to 78 with ΔP = 900 psi

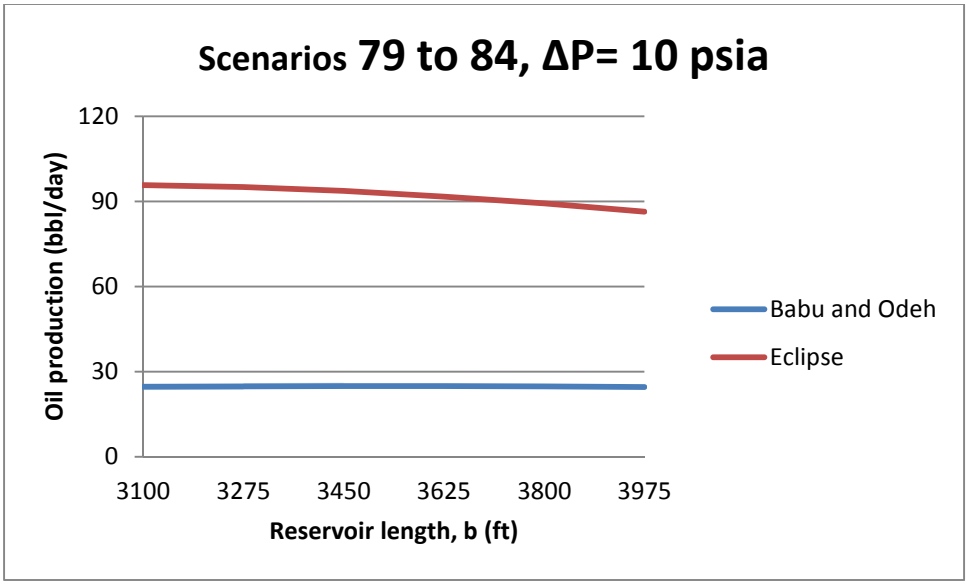

Figure G.27: Flow rates estimation for scenarios 79 to 84 with ΔP = 10 psi

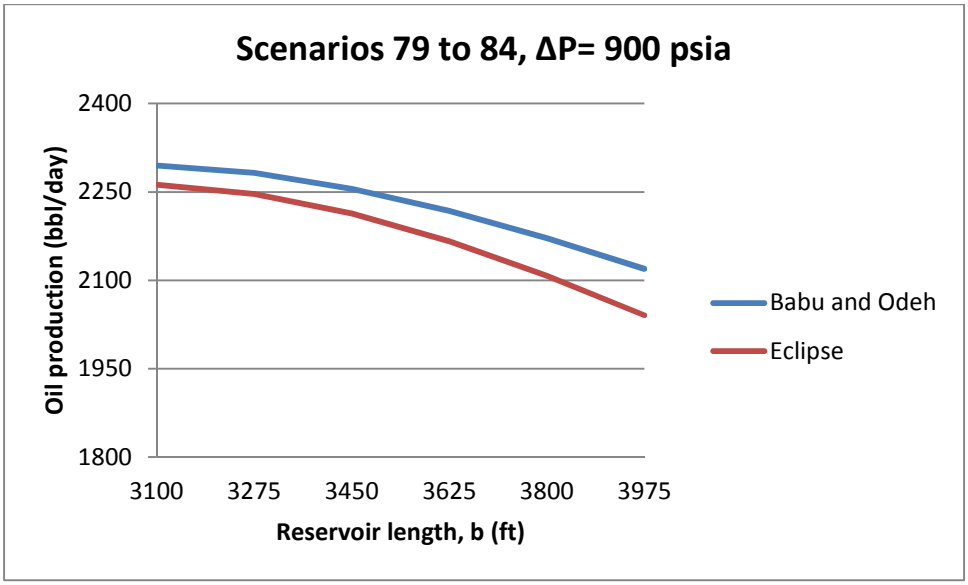

Figure G.28: Flow rates estimation for scenarios 79 to 84 with ΔP = 900 psi

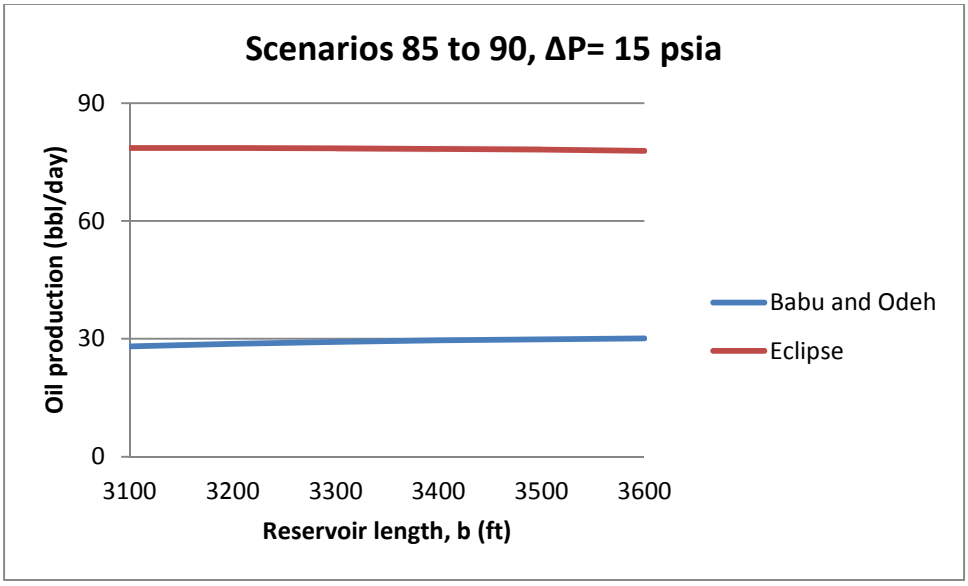

Figure G.29: Flow rates estimation for scenarios 85 to 90 with ΔP = 15 psi

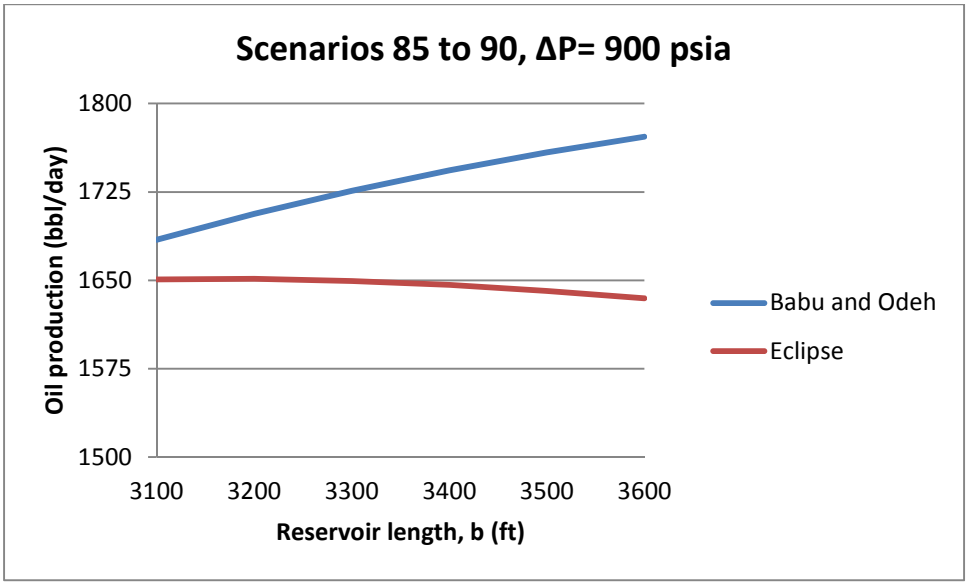

Figure G.30: Flow rates estimation for scenarios 85 to 90 with ΔP = 900 psi

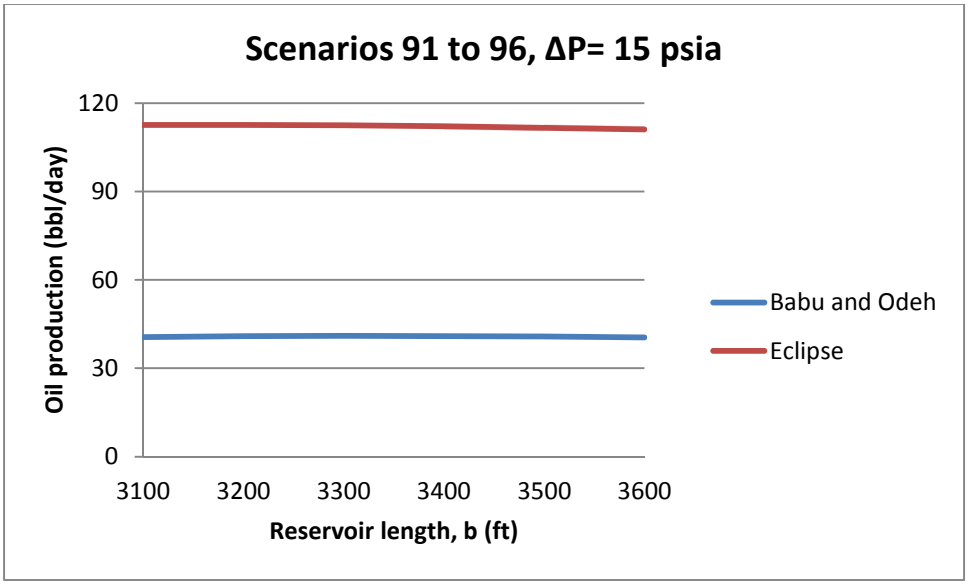

Figure G.31: Flow rates estimation for scenarios 91 to 96 with ΔP = 15 psi

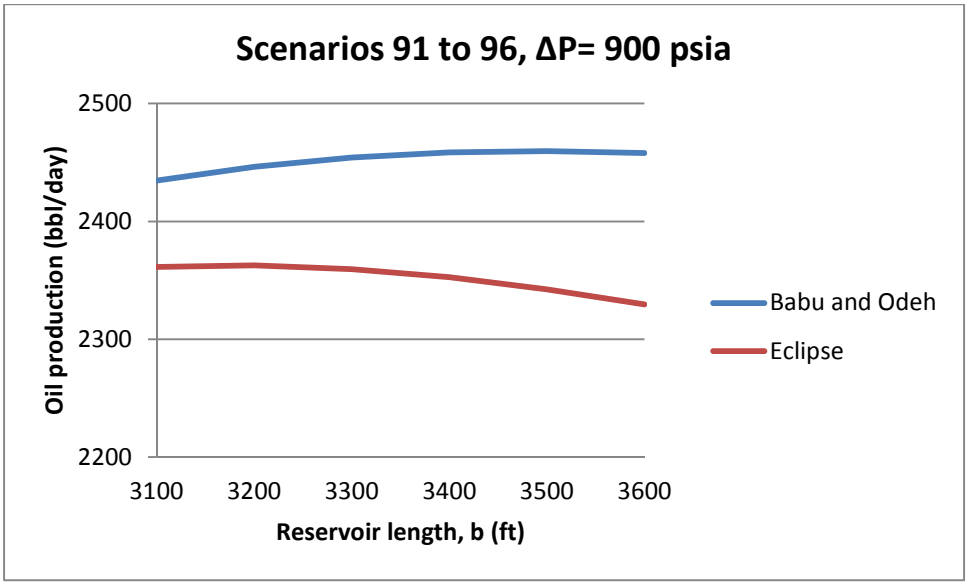

Figure G.32: Flow rates estimation for scenarios 91 to 96 with ΔP = 900 psi

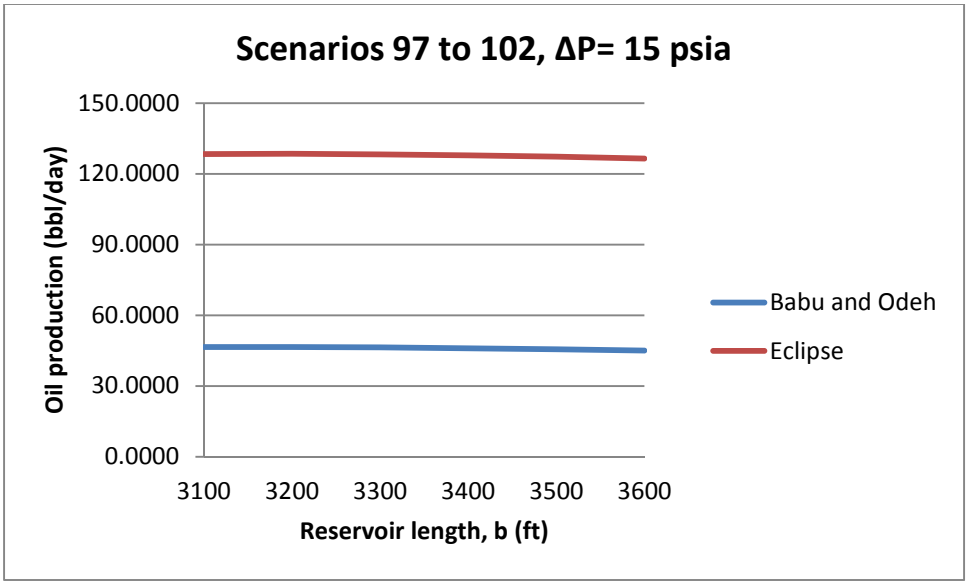

Figure G.33: Flow rates estimation for scenarios 97 to 102 with ΔP = 15 psi

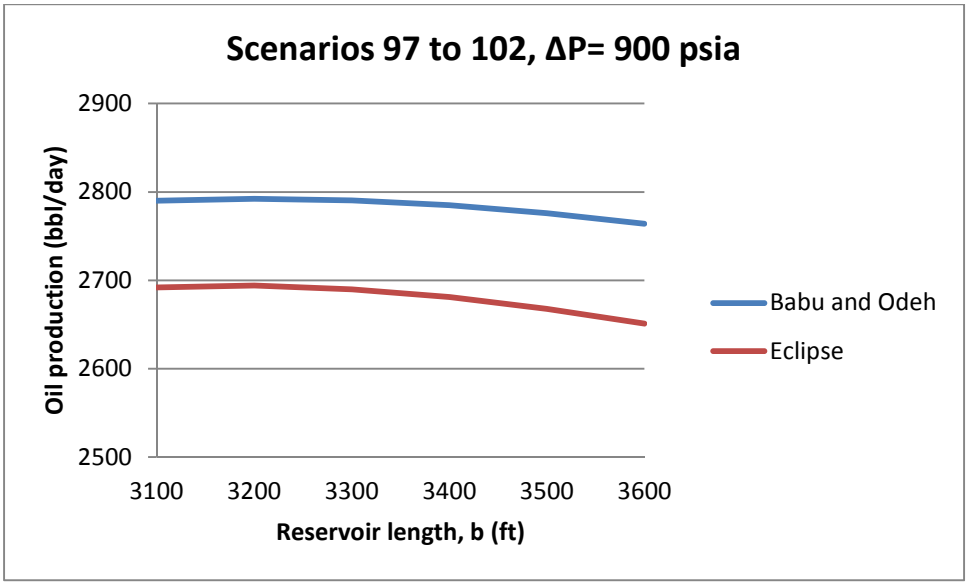

Figure G.34: Flow rates estimation for scenarios 97 to 102 with ΔP = 900 psi

APPENDIX H: SUMMARY OF SCENARIOS

This Appendix presents the table that summarizes the results obtained using B&O model and Eclipse, for all the scenarios simulated, and a figure that compares them.

The columns in table 1 depict:

- *Par*: parameter being analyzed.
- *Sc*: number assigned to scenario.
- *kx*: permeability in "x" direction (mD)
- *ky*: permeabity in "y" direction (mD)
- *kz*: permeabity in "y" direction (mD)
- *b*: reservoir length (ft)
- *a*: reservoir width (ft)
- *h*: reservoir height (ft)
- *s*: skin factor
- *PBH*: wellbore pressure (psia)
- *ΔP*: drawdown used (psia)
- *QBO*: flow rate predicted by B&O (bbl/day)
- *QEC*: flow rate predicted by Eclipse (bbl/day)
- *ΔQ*: Q EC-Q BO (bbl/day)
- *ΔQE*: ΔQ/Q EC
- *ratio*: Q EC/Q BO

- *Var B&O*: this value depicts the difference between the flow rate predicted by B&O in the corresponding scenario and the minimum flow rate predicted by B&O for the set of 6 scenarios (bbl/day)
- *Var Eclipse*: this value depicts the difference between the flow rate predicted by Eclipse in the corresponding scenario and the minimum flow rate predicted by Eclipse for the set of 6 scenarios (bbl/day)
- *Avg ratio*: average of the column ratio for each set of 6 scenarios
- *Q BO 900, Q EC 900, ΔQ 900, ΔQE 900, ratio 900, Var B&O 900, Var ECL 900* and *Avg ratio 900*: all these columns are the same as the previous ones, but using a drawdown of 900 psia.

The following parameters were not included in the table for simplicity, since they remain constant for all the scenarios considered:

- r_w: wellbore radius, 0.25 ft.
- L: wellbore length, 3,000 ft.
- B_o: oil formation volume factor, 1.1
- μ: oil viscosity, 1.05 cP
- ϕ: porosity, 25%

Par	Sc	kx	ky	kz	b	a	h	s	PBH	ΔP	QBO	QEC	ΔQ	ΔQE	ratio	VarB&O	VarEcl	AvgΔQE	Avgratio	QBO900	QEC900	ΔQ900	ΔQE900	ratio900	VarB&O900	VarEcl900	AvgΔQE900	Avgratio900
h	1	5	5	1	3300	1500	200	10	2000	80	200	223	23	10.5%	1.12	0.000	4.056	8.3%	1.09	2247	2080	-166	-8.0%	0.926	0.000	37.284	-10.6%	0.90
h	2	5	5	1	3400	1500	200	10	2000	80	201	223	21	9.6%	1.11	1.554	3.598			2264	2076	-188	-9.1%	0.917	17.485	33.023		
h	3	5	5	1	3500	1500	200	10	2000	80	203	222	19	8.7%	1.10	2.875	2.945			2279	2070	-209	-10.1%	0.908	32.345	26.933		
h	4	5	5	1	3600	1500	200	10	2000	80	204	221	17	7.9%	1.09	3.975	2.128			2291	2062	-229	-11.1%	0.900	44.714	19.276		
h	5	5	5	1	3700	1500	200	10	2000	80	205	220	15	7.0%	1.08	4.865	1.090			2301	2053	-248	-12.1%	0.892	54.727	10.231		
h	6	5	5	1	3800	1500	200	10	2000	80	205	219	14	6.3%	1.07	5.557	0.000			2309	2043	-266	-13.0%	0.885	62.519	0.000		
h	7	5	5	1	3300	1500	100	10	3000	10	23	106	83	78.3%	4.61	0.383	3.534	78.1%	4.57	2065	2037	-28	-1.4%	0.986	34.465	68.095	-2.2%	0.98
h	8	5	5	1	3400	1500	100	10	3000	10	23	105	83	78.3%	4.60	0.366	3.145			2064	2030	-34	-1.7%	0.984	32.977	60.653		
h	9	5	5	1	3500	1500	100	10	3000	10	23	105	82	78.2%	4.58	0.317	2.576			2060	2019	-40	-2.0%	0.980	28.508	49.691		
h	10	5	5	1	3600	1500	100	10	3000	10	23	104	81	78.1%	4.57	0.237	1.849			2052	2005	-47	-2.4%	0.977	21.341	35.673		
h	11	5	5	1	3700	1500	100	10	3000	10	23	103	81	78.0%	4.55	0.131	0.985			2043	1988	-54	-2.7%	0.973	11.751	18.994		
h	12	5	5	1	3800	1500	100	10	3000	10	23	102	80	77.9%	4.53	0.000	0.000			2031	1969	-62	-3.1%	0.970	0.000	0.000		
kx	13	10	5	1	3300	1500	150	10	3000	15	44	146	102	69.8%	3.32	0.000	5.604	68.6%	3.19	2644	3068	424	13.8%	1.160	0.000	118.404	10.2%	1.11
kx	14	10	5	1	3400	1500	150	10	3000	15	45	145	101	69.4%	3.26	0.465	4.873			2672	3053	380	12.5%	1.142	27.929	103.022		
kx	15	10	5	1	3500	1500	150	10	3000	15	45	144	99	68.9%	3.21	0.889	3.925			2698	3033	335	11.0%	1.124	53.332	82.992		
kx	16	10	5	1	3600	1500	150	10	3000	15	45	143	98	68.4%	3.16	1.272	2.783			2721	3009	288	9.6%	1.106	76.314	58.846		
kx	17	10	5	1	3700	1500	150	10	3000	15	46	142	96	67.8%	3.11	1.616	1.468			2741	2981	239	8.0%	1.087	96.976	31.035		
kx	18	10	5	1	3800	1500	150	10	3000	15	46	141	95	67.3%	3.05	1.924	0.000			2760	2950	190	6.4%	1.069	115.420	0.000		
kx	19	4	5	1	3300	1500	150	10	2000	15	34	86	52	60.2%	2.51	0.108	1.680	59.9%	2.49	2056	1825	-231	-12.7%	0.888	6.504	35.538	-13.7%	0.88
kx	20	4	5	1	3400	1500	150	10	2000	15	34	86	52	60.1%	2.50	0.177	1.510			2060	1821	-239	-13.1%	0.884	10.593	31.931		
kx	21	4	5	1	3500	1500	150	10	2000	15	34	86	51	59.9%	2.49	0.196	1.244			2061	1815	-246	-13.5%	0.881	11.755	26.349		
kx	22	4	5	1	3600	1500	150	10	2000	15	34	85	51	59.8%	2.49	0.170	0.897			2059	1808	-251	-13.9%	0.878	10.226	19.009		
kx	23	4	5	1	3700	1500	150	10	2000	15	34	85	51	59.7%	2.48	0.104	0.480			2055	1799	-256	-14.2%	0.875	6.233	10.162		
kx	24	4	5	1	3800	1500	150	10	2000	15	34	84	50	59.6%	2.47	0.000	0.000			2049	1789	-260	-14.5%	0.873	0.000	0.000		
kx	25	3	5	1	3300	1500	150	10	3000	15	31	75	44	58.1%	2.39	0.837	1.092	58.3%	2.40	1889	1576	-314	-19.9%	0.834	50.225	22.736	-19.3%	0.84
kx	26	3	5	1	3400	1500	150	10	3000	15	31	75	44	58.2%	2.39	0.757	1.011			1885	1574	-310	-19.7%	0.835	45.409	21.091		
kx	27	3	5	1	3500	1500	150	10	3000	15	31	75	44	58.2%	2.39	0.628	0.850			1877	1571	-306	-19.5%	0.837	37.671	17.750		
kx	28	3	5	1	3600	1500	150	10	3000	15	31	75	44	58.3%	2.40	0.455	0.621			1867	1566	-300	-19.2%	0.839	27.327	12.997		
kx	29	3	5	1	3700	1500	150	10	3000	15	31	74	43	58.5%	2.41	0.245	0.337			1854	1560	-294	-18.8%	0.842	14.675	7.026		
kx	30	3	5	1	3800	1500	150	10	3000	15	31	74	43	58.6%	2.42	0.000	0.000			1839	1553	-286	-18.4%	0.844	0.000	0.000		
ky	31	5	1	1	3100	1500	150	10	3000	15	21	100	79	78.8%	4.72	0.000	9.830	77.2%	4.41	1269	2096	827	39.4%	1.651	0.000	206.622	35.0%	1.54
ky	32	5	1	1	3200	1500	150	10	3000	15	21	99	78	78.4%	4.62	0.278	9.063			1286	2080	794	38.2%	1.618	16.699	190.784		
ky	33	5	1	1	3300	1500	150	10	3000	15	22	98	76	77.8%	4.50	0.534	7.643			1301	2050	749	36.5%	1.576	32.016	160.890		
ky	34	5	1	1	3400	1500	150	10	3000	15	22	96	74	77.1%	4.36	0.767	5.606			1315	2007	692	34.5%	1.526	46.037	117.988		
ky	35	5	1	1	3500	1500	150	10	3000	15	22	93	71	76.2%	4.20	0.981	3.024			1328	1953	625	32.0%	1.470	58.842	63.645		
ky	36	5	1	1	3600	1500	150	10	3000	15	22	90	68	75.2%	4.03	1.175	0.000			1339	1889	549	29.1%	1.410	70.509	0.000		
ky	37	5	8.5	1	3100	1500	150	10	3000	15	42	100	58	58.1%	2.39	0.000	0.338	57.8%	2.37	2520	2104	-415	-19.7%	0.835	0.000	6.720	-20.5%	0.83
ky	38	5	8.5	1	3200	1500	150	10	3000	15	42	100	58	58.0%	2.38	0.202	0.520			2532	2108	-424	-20.1%	0.832	12.100	10.005		
ky	39	5	8.5	1	3300	1500	150	10	3000	15	42	100	58	57.9%	2.37	0.330	0.513			2539	2108	-432	-20.5%	0.830	19.805	10.386		
ky	40	5	8.5	1	3400	1500	150	10	3000	15	42	100	58	57.8%	2.37	0.391	0.409			2543	2106	-437	-20.7%	0.828	23.433	8.610		
ky	41	5	8.5	1	3500	1500	150	10	3000	15	42	100	58	57.7%	2.36	0.388	0.237			2543	2103	-440	-20.9%	0.827	23.302	5.073		
ky	42	5	8.5	1	3600	1500	150	10	3000	15	42	100	58	57.6%	2.36	0.329	0.000			2539	2097	-442	-21.1%	0.826	19.724	0.000		
ky	43	5	20	1	3100	1500	150	10	3000	15	53	100	47	47.3%	1.90	1.614	0.000	48.1%	1.93	3177	2106	-1071	-50.9%	0.663	96.823	0.000	-48.4%	0.67
ky	44	5	20	1	3200	1500	150	10	3000	15	53	101	48	47.5%	1.91	1.490	0.269			3170	2112	-1058	-50.1%	0.666	89.413	5.892		
ky	45	5	20	1	3300	1500	150	10	3000	15	53	101	48	47.8%	1.92	1.255	0.438			3156	2116	-1040	-49.2%	0.670	75.273	9.419		
ky	46	5	20	1	3400	1500	150	10	3000	15	52	101	49	48.2%	1.93	0.919	0.527			3136	2117	-1018	-48.1%	0.675	55.169	11.258		
ky	47	5	20	1	3500	1500	150	10	3000	15	52	101	49	48.7%	1.95	0.497	0.560			3110	2118	-992	-46.8%	0.681	29.843	11.951		
ky	48	5	20	1	3600	1500	150	10	3000	15	51	101	50	49.1%	1.97	0.000	0.543			3080	2118	-963	-45.5%	0.687	0.000	11.653		

Table H.1 a: Summary of scenarios and results

Par	Sc	kx	ky	kz	b	a	h	s	PBH	ΔP	QBO	QEC	ΔQ	ΔQE	ratio	VarB&O	VarEcl	AvgΔQE	Avgratio	QBO900	QEC900	ΔQ900	ΔQE900	ratio900	VarB&O900	VarEcl900	AvgΔQE900	Avgratio900
kz	49	5	5	0.01	3100	1500	150	10	2000	15	4	11	7	64.5%	2.82	0.000	0.000	63.1%	2.71	231	230	-1	-0.4%	0.996	0.000	0.000	-4.3%	0.96
kz	50	5	5	0.01	3200	1500	150	10	2000	15	4	11	7	63.9%	2.77	0.070	0.028			235	231	-4	-1.9%	0.98	4.181	0.601		
kz	51	5	5	0.01	3300	1500	150	10	2000	15	4	11	7	63.4%	2.73	0.137	0.045			239	231	-8	-3.5%	0.97	8.220	0.972		
kz	52	5	5	0.01	3400	1500	150	10	2000	15	4	11	7	62.8%	2.69	0.202	0.055			243	231	-12	-5.1%	0.95	12.122	1.194		
kz	53	5	5	0.01	3500	1500	150	10	2000	15	4	11	7	62.3%	2.65	0.265	0.061			247	231	-15	-6.6%	0.94	15.889	1.318		
kz	54	5	5	0.01	3600	1500	150	10	2000	15	4	11	7	61.7%	2.61	0.325	0.063			250	231	-19	-8.2%	0.92	19.527	1.367		
kz	55	5	5	2	3100	1500	150	10	3000	15	48	135	86	64.0%	2.78	0.000	2.253	63.7%	2.76	2908	2827	-81	-2.9%	0.97	0.000	45.074	-3.7%	0.96
kz	56	5	5	2	3200	1500	150	10	3000	15	49	135	86	63.9%	2.77	0.166	2.303			2918	2829	-89	-3.2%	0.97	9.945	47.262		
kz	57	5	5	2	3300	1500	150	10	3000	15	49	135	86	63.8%	2.76	0.250	2.041			2923	2824	-99	-3.5%	0.97	14.979	42.832		
kz	58	5	5	2	3400	1500	150	10	3000	15	49	134	85	63.7%	2.75	0.258	1.564			2924	2814	-109	-3.9%	0.96	15.487	32.969		
kz	59	5	5	2	3500	1500	150	10	3000	15	49	133	85	63.5%	2.74	0.198	0.878			2920	2800	-120	-4.3%	0.96	11.855	18.486		
kz	60	5	5	2	3600	1500	150	10	3000	15	49	133	84	63.4%	2.73	0.074	0.000			2913	2782	-131	-4.7%	0.96	4.454	0.000		
kz	61	5	5	10	3100	1500	150	10	3000	15	89	247	158	64.1%	2.78	6.027	6.486	65.0%	2.86	5328	5182	-145	-2.8%	0.97	361.636	135.503	-0.2%	1.00
kz	62	5	5	10	3200	1500	150	10	3000	15	88	248	160	64.6%	2.82	5.081	7.070			5271	5195	-76	-1.5%	0.99	304.862	148.242		
kz	63	5	5	10	3300	1500	150	10	3000	15	87	247	161	64.9%	2.85	3.979	6.598			5205	5185	-20	-0.4%	1.00	238.743	138.307		
kz	64	5	5	10	3400	1500	150	10	3000	15	86	246	160	65.2%	2.88	2.749	5.186			5131	5156	25	0.5%	1.00	164.924	108.766		
kz	65	5	5	10	3500	1500	150	10	3000	15	84	244	160	65.5%	2.90	1.415	2.953			5051	5109	58	1.1%	1.01	84.898	61.935		
kz	66	5	5	10	3600	1500	150	10	3000	15	83	241	158	65.6%	2.91	0.000	0.000			4966	5047	81	1.6%	1.02	0.000	0.000		
a	67	5	5	1	3100	2000	150	10	3000	10	23	85	62	73.0%	3.70	0.000	1.673	72.0%	3.58	2070	2010	-60	-3.0%	0.97	0.000	39.662	-6.6%	0.94
a	68	5	5	1	3275	2000	150	10	3000	10	23	85	62	72.6%	3.65	0.378	1.884			2104	2015	-89	-4.4%	0.96	34.037	44.581		
a	69	5	5	1	3450	2000	150	10	3000	10	24	85	61	72.2%	3.60	0.672	1.734			2131	2012	-119	-5.9%	0.94	60.481	41.030		
a	70	5	5	1	3625	2000	150	10	3000	10	24	85	61	71.8%	3.55	0.889	1.331			2150	2002	-148	-7.4%	0.93	79.999	31.542		
a	71	5	5	1	3800	2000	150	10	3000	10	24	84	60	71.4%	3.50	1.036	0.741			2164	1988	-175	-8.8%	0.92	93.250	17.537		
a	72	5	5	1	3975	2000	150	10	3000	10	24	83	59	71.1%	3.46	1.121	0.000			2171	1971	-201	-10.2%	0.91	100.874	0.000		
a	73	5	5	1	3100	1200	150	10	3000	10	25	92	66	72.2%	3.59	1.950	4.847	72.5%	3.63	2215	2163	-52	-2.4%	0.98	4.763	114.870	-5.2%	0.95
a	74	5	5	1	3275	1200	150	10	3000	10	25	91	66	72.2%	3.60	1.808	4.625			2233	2158	-76	-3.5%	0.97	23.094	109.704		
a	75	5	5	1	3450	1200	150	10	3000	10	25	91	66	72.4%	3.62	1.510	3.933			2241	2142	-99	-4.6%	0.96	30.393	93.435		
a	76	5	5	1	3625	1200	150	10	3000	10	25	90	65	72.5%	3.64	1.091	2.892			2238	2117	-122	-5.7%	0.95	28.073	68.665		
a	77	5	5	1	3800	1200	150	10	3000	10	24	88	64	72.7%	3.66	0.579	1.560			2228	2085	-143	-6.8%	0.94	17.508	37.061		
a	78	5	5	1	3975	1200	150	10	3000	10	24	87	63	72.8%	3.68	0.000	0.000			2210	2048	-162	-7.9%	0.93	0.000	0.000		
a	79	5	5	1	3100	750	150	10	3000	10	25	96	71	74.3%	3.89	0.053	9.350	73.1%	3.72	2295	2262	-33	-1.4%	0.99	175.537	221.769	-2.4%	0.98
a	80	5	5	1	3275	750	150	10	3000	10	25	95	70	73.9%	3.83	0.257	8.676			2282	2246	-36	-1.6%	0.98	162.681	205.916		
a	81	5	5	1	3450	750	150	10	3000	10	25	94	69	73.4%	3.76	0.338	7.285			2255	2213	-42	-1.9%	0.98	135.924	172.896		
a	82	5	5	1	3625	750	150	10	3000	10	25	92	67	72.9%	3.69	0.312	5.295			2218	2166	-51	-2.4%	0.98	98.187	125.685		
a	83	5	5	1	3800	750	150	10	3000	10	25	89	64	72.3%	3.60	0.195	2.825			2172	2108	-64	-3.0%	0.97	52.113	67.055		
a	84	5	5	1	3975	750	150	10	3000	10	25	86	62	71.6%	3.52	0.000	0.000			2119	2041	-79	-3.9%	0.96	0.000	0.000		
s	85	5	5	1	3100	1500	150	15	3000	15	28	79	51	64.3%	2.80	0.000	0.756	62.7%	2.68	1684	1651	-34	-2.0%	0.98	0.000	15.910	-5.2%	0.95
s	86	5	5	1	3200	1500	150	15	3000	15	29	79	50	63.5%	2.74	0.616	0.779			1706	1651	-55	-3.3%	0.97	21.985	16.458		
s	87	5	5	1	3300	1500	150	15	3000	15	29	79	49	62.8%	2.69	1.116	0.698			1726	1649	-76	-4.6%	0.96	41.644	14.727		
s	88	5	5	1	3400	1500	150	15	3000	15	30	78	49	62.3%	2.65	1.508	0.532			1743	1646	-97	-5.9%	0.94	59.057	11.235		
s	89	5	5	1	3500	1500	150	15	3000	15	30	78	48	61.8%	2.62	1.800	0.296			1759	1641	-118	-7.2%	0.93	74.309	6.257		
s	90	5	5	1	3600	1500	150	15	3000	15	30	78	48	61.4%	2.59	2.001	0.000			1772	1635	-137	-8.4%	0.92	87.488	0.000		
s	91	5	5	1	3100	1500	150	8	3000	15	41	113	72	64.0%	2.77	0.077	1.523	63.6%	2.75	2435	2361	-73	-3.1%	0.97	0.000	31.768	-4.3%	0.96
s	92	5	5	1	3200	1500	150	8	3000	15	41	113	72	63.7%	2.76	0.372	1.585			2446	2363	-84	-3.5%	0.97	11.503	33.247		
s	93	5	5	1	3300	1500	150	8	3000	15	41	112	72	63.6%	2.74	0.489	1.429			2454	2359	-95	-4.0%	0.96	19.328	29.967		
s	94	5	5	1	3400	1500	150	8	3000	15	41	112	71	63.5%	2.74	0.452	1.095			2458	2353	-106	-4.5%	0.96	23.738	22.990		
s	95	5	5	1	3500	1500	150	8	3000	15	41	112	71	63.5%	2.74	0.282	0.612			2460	2342	-117	-5.0%	0.95	24.992	12.859		
s	96	5	5	1	3600	1500	150	8	3000	15	41	111	71	63.5%	2.74	0.000	0.000			2458	2330	-129	-5.5%	0.95	23.345	0.000		
s	97	5	5	1	3100	1500	150	6	3000	15	46	128	82	63.8%	2.76	1.541	1.954	64.0%	2.78	2790	2692	-98	-3.6%	0.96	25.916	40.754	-3.9%	0.96
s	98	5	5	1	3200	1500	150	6	3000	15	47	129	82	63.8%	2.76	1.563	2.052			2792	2694	-98	-3.6%	0.96	28.233	42.834		
s	99	5	5	1	3300	1500	150	6	3000	15	46	128	82	63.9%	2.77	1.389	1.855			2790	2690	-101	-3.7%	0.96	26.430	38.806		
s	100	5	5	1	3400	1500	150	6	3000	15	46	128	82	64.0%	2.78	1.052	1.425			2785	2681	-104	-3.9%	0.96	20.885	29.853		
s	101	5	5	1	3500	1500	150	6	3000	15	46	127	82	64.2%	2.79	0.580	0.798			2776	2668	-108	-4.1%	0.96	11.959	16.732		
s	102	5	5	1	3600	1500	150	6	3000	15	45	126	82	64.5%	2.81	0.000	0.000			2764	2651	-113	-4.3%	0.96	0.000	0.000		

Table H.1 b: Summary of scenarios and results